Sheffield Hallam University

Biomechanical adaptations in the acceleration phase of bend sprinting

JUDSON, Laura Jade

Available from the Sheffield Hallam University Research Archive (SHURA) at:

http://shura.shu.ac.uk/26726/

A Sheffield Hallam University thesis

This thesis is protected by copyright which belongs to the author.

The content must not be changed in any way or sold commercially in any format or medium without the formal permission of the author.

When referring to this work, full bibliographic details including the author, title, awarding institution and date of the thesis must be given.

Please visit http://shura.shu.ac.uk/26726/ and http://shura.shu.ac.uk/information.html for further details about copyright and re-use permissions.

Biomechanical adaptations in the acceleration phase of bend sprinting

Laura Jade Judson
Sheffield Hallam University

A thesis submitted in partial fulfilment of the requirement of Sheffield Hallam University for the degree of Doctor of Philosophy

September, 2019

I hereby declare that:

1. I have been enrolled for another award of the University, or other academic or professional organisation, whilst undertaking my research degree. I was an enrolled student for the following award:

   Name of award: Postgraduate certificate in teaching and learning in Higher Education
   Awarding body: Sheffield Hallam University

2. None of the material contained in the thesis has been used in any other submission for an academic award.
3. I am aware of and understand the University's policy on plagiarism and certify that this thesis is my own work. The use of all published or other sources of material consulted have been properly and fully acknowledged.
4. The work undertaken towards the thesis has been conducted in accordance with the SHU Principles of Integrity in Research and the SHU Research Ethics Policy.

5. The word count of the thesis is 43,244.

Name	*Laura Jade Judson*
Award	*PhD*
Date of Submission	*September, 2019*
Faculty	*Health and wellbeing*
Director(s) of Studies	*Professor Jon Wheat*

FOR GK,

For teaching me always to try my best and that life is better with chips x

Abstract

During bend sprinting athletes are unable to reach the same maximal speeds achieved on the straight. Since over half of the race distance is run on a curved portion of track, this has implications for race performance. This thesis aims to understand the biomechanical aspects of technique and performance in the acceleration phase of bend sprinting.

Chapter 3: The accuracy of two reduced marker sets (lower limb and lower limb and trunk) were evaluated in comparison to a full-body marker set in the calculation of the centre of mass location and associated variables (velocity, touchdown distance and turn of centre of mass). Intraclass correlation coefficients demonstrated excellent agreement between all marker sets. However, the lower limb and trunk model was favoured and recommended for future use due to the marginally better agreement observed and the requirement for only four additional markers compared with the lower limb model.

Chapter 4: The within- and between-day reliability of a lower limb and trunk marker set was established during bend sprinting. The results demonstrated that, where possible, data for each participant should be collected in the same session to increase reliability and reduce the required minimum detectable difference. The minimum detectable difference was used in subsequent studies to aid in the interpretation of results.

Chapter 5: This marker set was used to identify the biomechanical adaptations of the lower limb during the acceleration phase of bend sprinting with a 36.5 m radius (lane one). Whilst the left limb demonstrated a greater peak hip adduction, peak hip internal rotation and peak ankle eversion on the bend compared with the straight, the right limb was characterised by an increase in peak hip abduction. In addition, with regard to spatio-temporal variables, there was a reduction in left step frequency and touchdown distance.

Chapter 6: The use of statistical parametric mapping revealed a lower propulsive force at 38 - 44 % of stance on the bend than straight. In the left limb, this coincided with the use of the oblique axis for push-off at the metatarsophalangeal joint. In addition, mediolateral force was higher on the bend than the straight for the majority of the stance phase (3-96%).

Chapter 7: No changes in extensor moment were observed at the hip and knee joints. Large effect sizes suggest a trend towards an increase in left step peak ankle plantar flexor moment. This increased plantar flexor moment may be due to a greater need for stabilisation as a consequence of non-sagittal plane adaptations of the lower limb.

Publications

Journal manuscripts:

Judson, L.J., Churchill, S. M., Barnes, A., Stone, J, A., Brookes, I., & Wheat, J. (2018). Measurement of bend sprinting kinematics with three-dimensional motion capture: a test-retest reliability study. *Sports Biomechanics, 1-17.* doi: 10.1080/14763141.2018.1515979

*Judson, L.J., Churchill, S. M., Barnes, A., Stone, J, A., Brookes, I., & Wheat, J. (2019).*Horizontal force production and multi-segment foot kinematics during the acceleration phase of bend sprinting. *Scandinavian Journal of Medicine & Science in Sport.* doi.org/10.1111/sms.13486

Judson, L.J., Churchill, S. M., Barnes, A., Stone, J, A., Brookes, I., & Wheat, J. (2019). Kinematic modifications of the lower limb during the acceleration phase of bend sprinting. *Journal of Sports Science.* doi: 10.1080/02640414.2019.1699006

Judson, L.J., Churchill, S. M., Barnes, A., Stone, J, A. & Wheat, J. (in press). Joint moments, power and energy in the acceleration phase of bend sprinting. *Journal of Biomechanics.*

Conference presentations:

Judson, L.J., Churchill, S. M., Barnes, A., Stone, J, A., & Wheat, J. (2017). Simplified marker sets for the calculation of centre of mass duration during bend sprinting. *Paper presented at the 36th Conference of the International Society of Biomechanics in Sports (ISBS);* Cologne, Germany.

Judson, L.J., Churchill, S. M., Barnes, A., Stone, J, A., & Wheat, J. (2018). Metatarsophalangeal joint push-off axis during sprinting on the bend and straight. *Poster presentation at the BASES Biomechanics Interest Group,* Salford University, UK.

Judson, L. J, Churchill, S. M., Barnes, A., Stone, J. A., & Wheat, J. (2018). Metatarsophalangeal joint push-off axis and horizontal force production during sprinting on the bend and straight. *Oral presentation at the BASES Annual Conference, Harrogate.*

Judson, L. J., Churchill, S. M., Barnes, A., Stone, J, A., & Wheat, J. (2019). Lower extremity joint moments during the acceleration phase of bend sprinting. *Presented at the European College of Sports Science (ECSS) Congress,* Prague 2019.

Acknowledgements

There are several people to whom I would like to express my thanks. Firstly to my supervisory team Professor Jon Wheat, Dr Sarah Churchill, Dr Andrew Barnes and Dr Joseph Stone, thank you for all your time and input on both a professional and personal level. I am full of gratitude and admiration for you all. In particular, thank you to Jon for never making me feel like an idiot. To Sarah for all the sprint expertise and the introduction to soft spaces, and Andy and Joe for all the support in the form of cake and booze. Also, thank you to Rea for all the pastoral care!

Thank you to the Sports Science Technical Team, Ian, Brent, Katy and Richard for all your time, patience and hard work. I am thankful to receive your support, input and willingness to keep trying until we made things work. A huge thank you to the athletes who gave up their time to participate, and to all the student research assistants who made the data collections a success - especially Ben Strafford, Tommy Munday, Ariel Pinto Torres and Chris Jenks.

To my past supervisors, Janet and Sarah. Thank you for trusting in my potential and allowing me to learn under your guidance. I am forever grateful for your time and ongoing mentorship.

To all my mates for being there to share love, hugs, booze, music and food. You are all amazing and especially, Pete, Phil, Shorty, Emma, Susie, Matt, Laura B, Becky T, Slipper and Becky P for being so thoughtful and reassuring and always bringing me laughter. To all my canine companions (Buddy, Jesse, Luna, Bob, Ekko, Hugo and Fraser) for the walks and cuddles that have been so good for the soul.

To the Monkeys, Trev and Grandma Lucy, for all your support and for bringing me into the family. Especially Stef for your time and patience in all the maths tutorials.

To Linda and Janet for being such lovely human beings and to Eleanor and Uncle Brian for all your support.

Most importantly, thank you to my Mam and Jimmy, for everything.

Contents

1. Thesis Introduction 18

1.1. Aims and objectives 21

2. Literature review 23

2.1. Research overview 23

2.2. Spatio-temporal parameters of bend sprinting 24

2.3. Kinematics in bend sprinting 27

2.4. Kinetics of maximal speed bend sprinting 32

2.5. Acceleration phase kinematics 35

2.6. Acceleration phase kinetics 37

2.7. Joint moments in sprinting 40

2.8. Methodological considerations 45

2.8.1. Data collection with high speed video 46

2.8.2. Data collection with optoelectronic cameras 46

2.8.3. Choice of marker set 47

2.8.4. Modelling the multi-segment foot 49

2.8.5. Inertial models 51

2.8.6. Measuring kinetics 52

2.8.7. Filtering 56

2.9. Summary 58

3. Simplified marker sets for the calculation of the centre of mass location during bend sprinting 61

3.1. Introduction 61

3.2. Methods 62

3.2.1. Participants 62

3.2.2. Experimental set-up 63

3.2.3. Protocol 65

3.2.4. Data Processing 65

3.2.5. Calculation of variables 66

3.2.6. Statistical analysis 67

3.3. Results 67

3.4. Discussion 72

3.5. Conclusion 74

4. Measurement of bend sprinting kinematics with three-dimensional motion capture: a test-retest study 76

4.1. Introduction 76

4.2. Methods 79

4.2.1. Participants 79

4.2.2. Equipment 80

4.2.3. Test-retest protocol 91

4.2.4. Data processing 91

4.2.5. Calculation of variables 92

4.2.6. Reliability measures 94

4.3. Results 95

4.4. Discussion 101

4.5. Conclusion 105

5. The effect of the bend on technique and performance in the acceleration phase of sprinting 108

5.1. Introduction 108

5.2. Methods 111

5.2.1. Participants 111

5.2.3. Protocol 113

5.2.4. Data processing 114

5.2.5. Statistical analysis 117

5.3. Results 118

5.3.1. Spatio-temporal variables 118

5.3.2. Joint kinematics 119

5.4. Discussion 123

5.5. Conclusion 128

6. Force production and kinetics of the acceleration phase during bend sprinting 131

6.1. Introduction 131

6.2. Methods 133

6.2.1. Participants 133

6.2.2. Experimental set-up 134

6.2.3. Protocol 135

6.2.4. Data processing 136

6.2.5. Statistical analysis 139

6.3. Results 141

6.4. Discussion 147

6.5. Conclusion 153

7. Joint moments, power and energy in bend sprinting 156

7.1. Introduction 156

7.2. Methods 159

7.2.1. Participants 159

7.2.3. Protocol 161

7.2.4. Data processing 162

7.2.5. Statistical analysis 166

7.3. Results 166

7.3.1. Joint moments 166

7.3.2. Joint power and energy 173

7.4. Discussion 181

7.5. Conclusion 186

8. Overall discussion 189

8.1. Review of previous chapters 189

8.2. Implications for performance 192

8.3. Implications for injury 194

8.4. Limitations 196

8.5. Future work 200

8.6. Conclusion 201

9. References 203

Appendix A.Comparison of key kinematic variables calculated from force plate and marker identification of touch down. 221

Appendix B.Additional force trials to demonstrate repeatability. 222

Appendix C.Recorded step numbers for force trials. 223

Appendix D.Additional joint moment trials to demonstrate repeatability. 224

Appendix E.Example consent form. 225

List of figures

Figure 3.2.2.1 Plan view of test set-up (not to scale) 63
Figure 3.2.2.2 Full-body marker set. 64
Figure 3.3.1 Comparison of the difference between whole-body CoM velocity and CoM representations 68
Figure 3.3.2 Bland Altman plots for right step velocity 69
Figure 3.3.3 Bland Altman plots for left step velocity 69
Figure 3.3.4 Bland Altman plots for right step touchdown distance 70
Figure 3.3.5 Bland Altman plots for left step touchdown distance 70
Figure 3.3.6 Bland Altman plots for right step turn of CoM 71
Figure 3.3.7 Bland Altman plots for left step turn of CoM 71
Figure 4.2.2.1 Plan view of test set-up (not to scale) 81
Figure 4.2.2.2 Custom built block to enable consistent placement of calcaneus markers 82
Figure 4.2.2.2 Lower limb and trunk marker set anatomical locations. 83
Figure 4.2.2.3 Multi-segment foot model marker placement and segment division.. 83
Figure 4.2.2.4 Rearfoot segment definition. 84
Figure 4.2.2.5 Forefoot segment definition. 85
Figure 4.2.2.6 Toebox segment definition. 86
Figure 4.2.2.7 Shank segment definition. 87
Figure 4.2.2.8 Thigh segment definition. 88
Figure 4.2.2.9 Pelvis segment definition. 89
Figure 4.2.2.10 Trunk segment definition. 90
Figure 4.2.5.1 Calculation of directional step length 94
Figure 5.2.2.1 Plan view of experimental set-up (not to scale). 113
Figure 6.2.2.1 Plan view of experimental set-up (not to scale). 134
Figure 6.2.4.1 Right foot representation of the transverse and oblique axes of the foot. 139
Figure 6.3.1 Group mean resultant force. 141
Figure 6.3.2 Group mean vertical force. 141
Figure 6.3.3 Group mean anteroposterior force. 142
Figure 6.3.4 Group mean mediolateral force 144

Figure 6.3.5 Mean centre of pressure mediolateral position 147
Figure 7.2.1.1 Plan view of experimental set-up (not to scale)..... 161
Figure 7.3.1.1 Hip joint angle, joint moment and joint power..... 169
Figure 7.3.1.2 Knee joint angle, joint moment and joint power. 170
Figure 7.3.1.3 Ankle joint angle, joint moment and joint power..... 171
Figure 7.3.1.4 Midfoot and MTP joint angle, joint moment and joint power 172

List of tables

Table 3.3.1 Mean values ± SD, mean difference, limits of agreement and ICC values. 72
Table 4.3.1 Left step spatio-temporal variables. 97
Table 4.3.2 Right step spatio-temporal variables. 98
Table 4.3.3 Left step joint kinematics. 99
Table 4.3.4 Right step joint kinematics. 100
Table 6.3.1 Group mean values (± standard deviation), effect sizes (% difference) force variables of the left and right step.. 145
Table 6.3.2 Group mean values (± standard deviation) of symmetry angle (θ_{SYM})..146
Table 7.3.2.1 Peak joint moments for hip and knee joints. 175
Table 7.3.2.2 Peak joint moments for ankle, midfoot and MTP joints. 176
Table 7.3.2.3 Peak power values for the hip and knee joints. 177
Table 7.3.2.4 Peak power for the ankle, midfoot and MTP joints. 178
Table 7.3.2.5 Energy generation and absorption at the hip and knee joints. 179
Table 7.3.2.6 Energy generation and absorption at the ankle, midfoot and MTP joints. 180

Abbreviations

0D	Discrete
1D	One-dimensional
2D	Two-dimensional
3D	Three-dimensional
ANOVA	Analysis of variance
CAST	Calibrated anatomical system technique
CI	Confidence intervals
CoM	Centre of mass
CoP	Centre of pressure
CT	Computed tomography
GCS	Global coordinate system
ICC	Intraclass correlation coefficient
ISB	International Society of Biomechanics
LCS	Local coordinate system
LL	Lower limb
LLT	Lower limb and trunk
MDD	Minimal detectable difference
MTH1	First metatarsal head
MTH2	Second metatarsal head
MTH5	Fifth metatarsal head
MTP	Metatarsophalangeal
SEM	Standard error of measurement
SPM	Statistical parametric mapping

Chapter One: THESIS INTRODUCTION

1. Thesis Introduction

The rectangular running tracks in Ancient Greek stadia and the nature of the 'there and back' sprint events meant it was neither possible nor required to run on a bend. Coinciding with the introduction of the oval running track at Panathinaiko Stadium (Athens, 1896), the 400 m has been an ever-present feature at the modern Olympic Games. The 200 m event made its first appearance at the Paris 1900 Olympic games. Unlike the 100 m race that takes place entirely on the straight, the 200 m and 400 m races include a portion on the bend that accounts for approximately 58% of the total distance covered (Meinel, 2008). The longer distance run on the bend during the 200 m, and 400 m races suggests that performance on the bend makes a substantial contribution to overall race performance. More recently, events such as the Great City Games provide a unique opportunity to compare athletes' performance across the same distance on the bend and the straight. The current male record for the 200 m straight is held by Tyson Gay at 19.41 s (Manchester, 2010) – 0.17 s faster than his personal best on the bend (19.58 s, New York, 2009). The difference between first and second place at the London (2012) Olympics in the men's 200 m was 0.12 s, demonstrating the effect small improvements on the bend can have on race performance. These figures provide some limited anecdotal evidence that sprinting on the bend is detrimental to overall race time.

The mechanics of human and animal motion intrigued scientists long before the inception of the modern Olympics. Aristotle's *De Motu Animalium* (On the movement of animals, Aristotle & Barnes, 1984) is potentially one of the first recordings to consider the general principles of motion in animals. From approximately 1489, Leonardo da Vinci meticulously observed the human body. The process was not just a means to create his famous anatomical drawings, but more to

discover, understand and document anatomical structures and their relation to human movement. Technological advances have not only confirmed the inconceivable accuracy of da Vinci's work but also aided the progress of human motion analysis.

Early studies of human movement were performed using observations from the human eye (Weber, 1836). Whilst this was a welcome contribution to the body of literature, further progress was halted until the introduction of innovations such as the use of several cameras with electro-magnet shutters (Muybridge, 1887) and manually advanced, hand-cranked film (Fenn, 1931). Now commonplace, cinematographically collected data became fully established in sports performance research after the publication of Thomas Cureton's 1939 guide '*Elementary Principles and Techniques of Cinematographic Analysis as Aids in Athletic Research'* (Cureton Jr, 1939).

Motion capture using optoelectronic systems is now considered the gold standard (Hood, McBain, Portas, & Spears, 2012). Optoelectronic systems use the location of markers placed on bony landmarks to reconstruct three-dimensional (3D) body segments and have been utilised to answer a variety of sports-related research questions (e.g., Alt, Heinrich, Funken, & Potthast, 2015; Vanrenterghem, Gormley, Robinson, & Lees, 2010). More recently, proposals have been put forward for methods of markerless motion capture (Choppin & Wheat, 2013; Mündermann, Corazza, & Andriacchi, 2006), demonstrating further advances in methods of human motion analysis.

Current biomechanical sprint research largely concentrates upon on the mechanics of straight-line sprinting. Consequently, the biomechanical demands of the 100 m are well understood (e.g., Girard, Brocherie, Tomazin, Farooq, & Morin, 2016; Krell & Stefanyshyn, 2006; Krzysztof & Mero, 2013; Morin et al., 2012). At present, the same cannot be said for bend sprinting. Whilst there is a growing body of literature

focussed upon the maximal speed phase of bend sprinting (e.g., Alt et al., 2015; Churchill, Salo, & Trewartha, 2015), the acceleration phase is yet to receive sufficient attention. This is despite the fact that maximal velocity is dependent upon the ability to accelerate. Given the importance of bend sprinting in events such as the 200 and 400 m, further research is required to increase understanding of bend sprinting mechanics. Advancing knowledge in this field would enable the development of strategies to aid race performance and tactics alongside strength and conditioning programmes to prevent injury and improve performance.

A recent review of plantaris injuries in elite British track and field athletes over four years demonstrated a high incidence of right-sided plantaris injuries in bend sprinters (Pollock, Dijkstra, Calder, & Chakraverty, 2016). Of the 19 injuries reported in bend sprinters, 15 were right-sided (Pollock et al., 2016). In addition, most athletes who presented with a plantaris injury also suffered from Achilles tendinopathy (Pollock et al., 2016). Moreover, asymmetric differences in the strength of hindfoot invertor and evertor muscle groups in indoor athletes have also been reported (Beukeboom, Birmingham, Forwell, & Ohrling, 2000). Therefore, bend sprinting may be associated with high injury incidence and muscular strength imbalance. The evidence presented regarding injury prevalence in bend sprinting athletes provides a rationale for further investigation of lower limb function during bend sprinting, which may provide important insights for the development of injury prevention strategies.

1.1. Aims and objectives

The aim of this programme of research was to understand the biomechanical aspects of technique and performance in the acceleration phase of sprinting on the bend compared with the straight.

The objectives were:

1 Determine the accuracy of a reduced marker set for CoM calculations compared with a full-body marker set (Chapter 3)

2 Determine the within- and between-day reliability of bend sprinting using 3D optoelectronic motion capture with a lower limb and trunk marker set (Chapter 4).

3 Evaluate the effect of the bend on lower limb kinematic parameters of technique and spatio-temporal variables during the acceleration phase (Chapter 5).

4 Evaluate the effect of the bend on the kinetic parameters of technique and performance during the acceleration phase (Chapter 6).

5 Evaluate the effect of the bend on joint moments and joint kinetics during the acceleration phase (Chapter 7).

Chapter Two: LITERATURE REVIEW

2. Literature review

2.1. Research overview

A reduction in velocity during bend sprinting has been observed, for example; 7.70 m/s (straight) to 5.66 m/s (6 m radius, Chang & Kram, 2007); 9.86 m/s (left step, straight) to 9.40 m/s (left step, 37.72 m radius, Churchill et al., 2015). Thus it is apparent that bend sprinting is detrimental to maximum sprint speed. At the London 2017 World Championships, the difference between first and second place in the women's 200 m final was 0.03 s. Therefore, even small decreases in velocity on the bend can have a big impact on overall race performance. Of the studies available that have examined bend sprinting, most have been in the form of two-dimensional (2D) analyses (Ryan & Harrison, 2003; Stoner & Ben-Sira, 1979). In addition, some analyses have relied upon televised footage (Mann & Herman, 1985), which is often problematic due to the inability to verify calibration methods and camera quality. Finally, for research where to the evaluated radii (e.g., 1-6 m, Chang and Kram, 2007; 5 m, Smith, Dyson, Hale, and Janaway, 2006) and surfaces (e.g., grass, Smith et al., 2006) are not representative of those found in bend sprinting with elite athletes, it is not possible to apply these results to the athletic population.

Mathematical models which have investigated bend sprinting performance support the reported reduction in velocity during bend sprinting (e.g., Greene, 1985; Usherwood and Wilson, 2006; Ward-Smith and Radford, 2002). Mathematical models are typically based on assumptions, such as the constant limb force hypothesis which assumes maximum resultant force will be the same in both bend and straight-line sprinting (Usherwood & Wilson, 2006). However, empirical research demonstrates this might not be entirely valid during bend sprinting, where asymmetrical limb function results in a decreased force production during the left step on the bend

compared with the straight (Churchill, Trewartha, Bezodis, & Salo, 2016). Recent studies have chosen to utilise 3D methods of analysis and findings remain consistent regarding the reduction in velocity found on the bend (e.g., Churchill et al., 2015; Churchill et al., 2016). This reduction is suggested as a result of asymmetric kinematic differences and how these differences consequently affect force production (Alt et al., 2015; Churchill et al., 2015).

The following sub-sections will present an overview of previous anti-clockwise bend sprinting research (that is the direction of competitive athletics), exploring the available evidence regarding the kinematic and kinetic adaptations that occur during maximal and sub-maximal velocity bend sprinting. In addition, since the current evidence base surrounding the acceleration phase on the bend is limited, the literature review will discuss the biomechanical variables associated with straight-line acceleration performance to identify suitable parameters for comparison. Similarly, literature investigating joint moments, power and energy during straight-line sprinting is reviewed to provide the basis for evaluation during bend sprinting. Finally, issues regarding the collection and analysis of data during bend sprinting are addressed to aid in the research design.

2.2. Spatio-temporal parameters of bend sprinting

Step length and step frequency determine velocity (Hay, 1993), and thus have been prominent measures of evaluation of technique in bend sprinting investigations. During bend sprinting, several authors have reported a shorter step length compared with the straight at maximum velocity (Chang & Kram, 2007; Churchill et al., 2015; Churchill et al., 2016; Ishimura, Tsukada, & Sakurai, 2013; Ryan & Harrison, 2003). However, Ryan and Harrison (2003) neglected to differentiate between the left and right step. Whilst this may be appropriate at smaller radii (1-6 m) where a significant

reduction in both left and right step length has been observed (Chang & Kram, 2007), at larger radii (e.g., 37.72 m), the reduction was present in the right step only (Churchill et al., 2015; Churchill et al., 2016; Ishimura et al., 2013). Therefore, during bend sprinting at a radius representative of competitive athletics performance, combining measures for the left and right limbs potentially masks asymmetry between limbs.

There are further inconsistencies evident in the reported results with regard to step frequency. Whilst both Churchill et al. (2015) and Ishimura et al. (2013) reported reductions in left step frequency on the bend compared to the straight, Alt et al. (2015), who evaluated a constant sub-maximum velocity between conditions, found step length and step frequency were not affected by the bend. These results are supported by Chang and Kram (2007), who also observed no change in step frequency whilst sprinting at smaller radii. In addition, flight time was found to have a reduction in the right step on the bend compared with the straight by Churchill et al. (2015), Churchill et al. (2016), and Ishimura et al. (2013), yet Alt et al. (2015) reported no difference. These results suggest adaptations such as a decrease in step length and step frequency may be velocity specific.

The literature with regard to ground contact time appears more consistent. For example, Alt et al. (2015) reported a 2.5% increase in left ground contact time on the bend (107.5 ms) compared with the straight (104.9 ms). This increase is consistent with other research (Chang & Kram, 2007; Churchill et al., 2015; Churchill et al., 2016; Ishimura & Sakurai, 2010; Ishimura et al., 2013; Ryan & Harrison, 2003; Smith et al., 2006). Since the longer left step contact time has been observed within the varying protocols used, it is possible that, unlike differences in step length and frequency that appear velocity dependent, an increased ground contact time is a bend specific modulation. Large effect sizes for left contact time (d = 2.97, bend left: 0.116

s, straight left: 0.105 s and d = 1.39, bend left: 0.112 s, straight left: 0.102 s, Churchill et al., 2015, and Ishimura et al., 2013 respectively), add further support to the potential importance of left step contact time during bend sprinting. Moreover, an asymmetry between limbs was reported during bend sprinting, with the left contact time being longer than the right (Alt et al., 2015; Churchill et al., 2015; Churchill et al., 2016; Ishimura & Sakurai, 2010).

Touchdown distance (defined as the 'horizontal distance from the head of the second metatarsal of the stance foot to the centre of mass [CoM]', Hunter, Marshall, & McNair, 2004a, p852) has been suggested as having an important relationship with 200 m sprint performance (Mann & Herman, 1985). Moreover, a shorter touchdown distance has also been associated with a shorter ground contact time (Hunter, Marshall, & McNair, 2004b) which Weyand, Sandell, Prime, and Bundle (2010) demonstrated is associated with faster speeds. Furthermore, Hay (1993) proposed a smaller touchdown distance may be related to a decrease in braking force. However, only Churchill et al. (2015), Churchill, Trewartha, and Salo (2018) and Ishimura and Sakurai (2016) have examined touchdown distance during bend sprinting. Coinciding with the longer contact times reported Churchill et al. (2015), touchdown distance was greater in the left step compared to the right step on the bend (Churchill et al., 2015; Churchill et al., 2018; Ishimura & Sakurai, 2016). These asymmetries further suggest the left and right limb may perform different functions during bend sprinting. Churchill et al. (2016) turn of CoM results suggests more turning (mean difference: 1.6º) was achieved during the left foot contact in comparison to the right. Ishimura and Sakurai (2016) somewhat dispute this, with findings that indicate that the running direction was changed more during the right step. However, Ishimura and Sakurai (2016) used

a different calculation method, and so direct comparisons between the two studies may not be appropriate.

In summary, bend sprinting has an impact on some performance descriptors. There is compelling evidence to suggest that an increased contact time (particularly with the left foot) is one of the key adaptations occurring as a consequence of the bend. This longer contact time is thought to be associated with a decrease in step frequency, which consequently results in decreased velocity on the bend compared with the straight (Churchill et al., 2015). However, differences between protocols make comparisons between studies problematic and conclusions would benefit from further supporting research.

2.3. Kinematics in bend sprinting

Kinematic analysis of technique during bend sprinting is, to some extent, contradictory. For example, Alt et al. (2015) evaluated the effect of the bend on three joints (hip, knee, and ankle) and observed no changes in the sagittal plane. However, findings from Churchill et al. (2015) contradict this. For example, an increase in left hip peak extension angle was found when compared with the right hip on the bend (Churchill et al., 2015). As such, there is a lack of consistency surrounding what the kinematic adaptations during bend sprinting are and in which plane they occur. However, the contrasting methods used between studies make comparisons problematic. Whilst Alt et al. (2015) used optoelectronic cameras to evaluate sub-maximal effort sprinting (left step: 9.26 m/s, right step: 9.39 m/s), Churchill et al. (2015) measured maximal velocity (left step: 9.40 m/s, right step: 9.34 m/s) with high-speed video cameras. The radii evaluated also differed from lane one (36.5 m) by Alt et al. (2015) and lane two (37.72 m) by Churchill et al. (2015).

Findings from Alt et al. (2015) regarding the knee joint are currently the only published insights to the 3D function of the knee during bend sprinting. An increase in internal rotation of the right knee was reported in comparison to the left (mean difference 4.0°; Alt et al., 2015). The internal rotation at the right knee was combined with a high external rotation of the right ankle (mean difference 4.9°, Alt et al., 2015). Alt et al. (2015) concluded the left and right limbs have different functional roles during bend sprinting, with the right limb described as implementing a rotational strategy with transverse plane modulations which served to control the horizontal plane motion. However, Alt et al. (2015) did not present any supporting reliability data, and transverse plane variables have previously been reported as having lower reliability during running analyses (Alenezi, Herrington, Jones, & Jones, 2016; Ferber, McClay Davis, Williams, & Laughton, 2002). Therefore, it is difficult to determine whether the observed differences are due to changes in the experimental condition, as opposed to errors in the experimental protocol or natural variance in technique.

Nevertheless, the findings are consistent regarding a greater left hip adduction during sprinting on the bend than straight (Alt, Heinrich, Funken, & Potthast, 2015; Churchill, Salo, & Trewartha, 2015). Alt et al. (2015) observed the left limb was characterised by an increase in hip adduction and external rotation which, combined with an increase in left ankle eversion during bend sprinting, is thought to contribute towards a stabilising function during sub-maximal velocity bend sprinting. The increase in left ankle eversion of 10.1° reported by Alt et al. (2015) is close to 13° which Clarke, Frederick, and Hamill (1984) suggested as excessive and, if reached repeatedly, may result in injury. Thus emphasising the importance of understanding the kinematic adaptations that occur at the foot and ankle joints as a result of bend sprinting. Moreover, Luo and Stefanyshyn (2012a) introduced wedged footwear to

align the left foot in a more neutral position during bend sprinting with a 2.5 m radius. A 4.3% increase in sprint performance was observed, which coincided with a 4.2° reduction in ankle eversion (Luo & Stefanyshyn, 2012a). The non-sagittal plane adaptations reported by Alt et al. (2015), alongside the increase in performance when such adaptations are alleviated (Luo & Stefanyshyn, 2012a), support the suggestion that sprint performance on the bend is limited by a need to change direction and stabilise the lower limb in the transverse and frontal planes (Chang & Kram, 2007).

In addition, van Ingen Schenau, Bobbert, and Rozendal (1987) described using the Geometrical Constraints theory how horizontal velocity is dependent on two factors: segmental angular velocity and segment orientation. It is thought that segments possess greater horizontal velocity when closest to a vertical orientation and so when segments are aligned more vertically, they are better able to contribute to the horizontal translation of whole-body CoM (van Ingen Schenau et al., 1987). Therefore, geometrical constraints are important when considering the performance of an essentially translational task, i.e., to shift a body from one point in space to another. Jacobs and van Ingen Schenau (1992, p. 954) described how, during the first steps of sprinting, the motor system aims to 'control the transformation of joint angular accelerations into an increase in velocity of the body centre of gravity in the horizontal direction'. During the stance phase of bend sprinting, the foot remains in a fixed position and the shank rotates anteriorly about the foot. Therefore, adaptations such as increased hip adduction may result in a deviation away from the more optimal vertical segmental alignment and consequently have a detrimental effect on that segments ability to contribute to the horizontal translation of the CoM. Further understanding of these limiting mechanisms may have important implications for both performance and injury prevention strategies.

Chan and Rudins (1994) described how, when the foot is in a fixed position (such as the stance phase during sprinting), motion at the foot and ankle passes proximally as part of a closed kinematic chain to the tibia, fibula, and femur. Therefore, adaptations at the hip and ankle during sprinting are likely a consequence of motion at the foot. The metatarsophalangeal joint (MTP) has been highlighted as making an important contribution to performance in straight-line sprinting (Krell & Stefanyshyn, 2006; Smith, Lake, & Lees, 2014). Krell and Stefanyshyn (2006) investigated the relationship between 100 m sprint performance and MTP joint function, demonstrating that faster male sprinters elicited higher maximal rates of MTP extension. However, it is not possible to review the role of the foot in bend sprinting further; since analyses using a multi-segment foot model during bend sprinting are currently missing from the literature. Therefore, it is not known whether the MTP joint makes a similar contribution to performance during bend sprinting to that demonstrated on the straight (Krell & Stefanyshyn, 2006; Smith et al., 2014).

Bojsen-Moller (1979) described the two possible push-off axes at the foot; transverse and oblique and suggested propulsive capacity is superior when push-off occurs with the transverse axis (see Figure 6.2.4.1). Churchill et al. (2016) postulated that the potential use of different push off axes by the MTP joint might have important implications in force production during bend sprinting. The greater inward lead found during the left stance phase (Churchill et al., 2015) might result in the left foot contact being more lateral, resulting in the use of the less effective oblique axis during the push-off phase (Churchill et al., 2016). Therefore, research into the kinematic function of the lower limb and multi-segment foot during bend sprinting is warranted.

It is evident the biomechanical demands of the lower limb during bend sprinting are different to straight-line sprinting (Alt et al., 2015; Churchill et al., 2015;

Churchill et al., 2016; Ishimura & Sakurai, 2010; Ishimura & Sakurai, 2016; Ishimura et al., 2013). Whilst an insight into the consequential adaptations of the lower limb that occur as a result of bend sprinting has been presented, there is a lack of supporting literature regarding individual joints, which weakens the strength of conclusions. Moreover, information regarding how the limb functions collectively is also required. In addition, the function of the multi-segment foot has not yet been investigated.

Mann and Herman (1985) proposed that the arms do not have a significant role in straight-line sprint performance. Subsequently, upper body kinematics has received little attention in the scientific literature. However, it is thought body lateral lean may be responsible for inducing the asymmetrical changes in spatio-temporal variables and lower limb kinematics previously discussed. Churchill et al. (2015) have included analysis of whole-body variables; body sagittal and lateral lean. For body sagittal lean, the range of motion was greater on the left step on the bend (57.2°) compared with the left step on the straight (51.1°), and the right step on the bend (52.9°). Body sagittal lean range of motion is thought to be associated with an increase in contact time during straight-line sprinting (Hunter et al., 2004b). Therefore, a greater body sagittal lean range of motion may be detrimental to sprint performance.

Churchill et al. (2015) also reported body lateral lean at touchdown and take-off was greater in both the left and right step on the bend compared with the straight. However, this is a necessary consequence of the requirement to produce centripetal force in order to maintain a curved path and continuously change direction whilst bend sprinting (Hamill, Murphy, & Sussman, 1987). Therefore, whilst the joints of the upper body may not substantially influence performance, body lateral lean might be a key characteristic of bend sprinting and should be included in future analyses.

2.4. Kinetics of maximal speed bend sprinting

Kinematic adaptations occurring during bend sprinting, such as changes in joint configuration, may alter force production capacity. Force production ability has previously been shown to be related to straight-line sprint performance (Weyand et al., 2010; Weyand, Sternlight, Bellizzi, & Wright, 2000) and therefore highlights the importance of gaining an in-depth understanding of the kinetic patterns present in bend sprinting.

While several authors have considered the effect of the bend on force production during sprinting (Chang & Kram, 2007; Luo & Stefanyshyn, 2012a, 2012b; Smith et al., 2006), only one has done so in conditions representative of elite athletics performance (Churchill et al., 2016). Peak resultant and vertical force was lower for the left step on the bend (3.61 ± 0.45 BW) compared with the straight at maximal velocity (3.82 ± 0.53 BW; Churchill et al., 2016), a finding that supports previous research at smaller radii (Chang & Kram, 2007; Smith et al., 2006). Findings from Churchill et al. (2016) are in contrast to results from theoretical modelling that propose the 'constant limb hypothesis' (Usherwood & Wilson, 2006). Based upon empirical research from Weyand et al. (2000), Usherwood and Wilson (2006) assumed athletes produce the same maximum resultant force when sprinting on both the bend and straight. However, it was suggested that, during bend sprinting, an increase in ground contact time is necessary to achieve the same amount of maximum force as produced on the straight (Usherwood & Wilson, 2006). Longer contact times were observed empirically for the left step at maximal (Churchill et al., 2015; Churchill et al., 2016) and sub-maximal velocities (Alt et al., 2015) during sprinting on the bend compared with the straight.

Luo and Stefanyshyn (2012b) evaluated ground reaction forces during a control condition and externally weighted sprinting condition (wearing a modified life jacket containing a total mass of 12.4 kg) at a 2.5 m radius and the findings further dispute the constant limb force concept (Usherwood & Wilson, 2006). Peak left resultant ground reaction force increased in the weighted condition compared to the control (Luo & Stefanyshyn, 2012b). If, as Usherwood and Wilson (2006) proposed, the limb was operating at a maximum limit, the force generated would remain the same regardless of condition. Thus, these results provide evidence that maximal force is not achieved during bend sprinting at smaller radii. Moreover, although not statistically significant, peak resultant force during the right step increased from 3.66 ± 0.29 BW on the straight, to 4.19 ± 1.29 BW on the bend (Churchill et al., 2016). The results from Ishimura and Sakurai (2016) support this finding, reporting an increase in vertical force in the right step compared to the left on the bend when derived using the impulse-momentum relationship. Again, much like conclusions from Luo and Stefanyshyn (2012b), the increase in peak resultant force provides further evidence against the constant limb force hypothesis. Luo and Stefanyshyn (2012b) postulated that maximum force generation capacity might be reduced by alterations in joint configurations. Kinematic adaptations such as an inward lean of the trunk (Churchill et al., 2015; Ishimura & Sakurai, 2010), increased hip adduction (Alt et al., 2015; Churchill et al., 2015) and increased ankle eversion (Alt et al., 2015) could potentially support this claim. Moreover, the possible change in MTP joint axis use for push-off would also add strength to this argument. Hence, the importance of the investigation of simultaneous kinematic and kinetic data is clear.

With regard to mediolateral forces on the bend, some inconsistencies are present between findings. For example, although research tends to agree that

mediolateral forces are greater on the bend compared with the straight (Chang & Kram, 2007; Churchill et al., 2016; Smith et al., 2006), findings regarding between limb differences are less certain. Churchill et al. (2016) reported the left limb produced greater peak inward force (relative to the bend) at maximal velocity (supported by Viellehner, Heinrich, Funken, Alt, and Potthast (2016) at sub-maximal velocity), whereas others reported greater medial forces in the right limb (Chang & Kram, 2007; Smith et al., 2006). Again, it is expected that differences in radii are most likely responsible for these differing outcomes. However, further research would be beneficial in providing supporting data to strengthen conclusions at radii representative of a competitive athletics environment. Running at tight radii possibly shares more similarities with an open cutting manoeuvre (Rand & Ohtsuki, 2000), as opposed to sprinting at larger radii such as those found on a typical outdoor running track. Therefore, more work is required to assess force production during representative radii of sprint performance on a bend to increase understanding of the role of mediolateral force in sprint performance.

In summary, there is strong evidence that force production adaptations occur during bend sprinting (Chang & Kram, 2007; Churchill et al., 2016; Viellehner et al., 2016). However, there are some contradictory results observed amongst studies. In particular, the force production function of the left and right lower limbs remains unclear. Additionally, although Viellehner et al. (2016) and Luo and Stefanyshyn (2012a) provide some insight into the mechanisms responsible for limiting bend sprinting performance, their research is not in conditions representative of elite bend sprinting. Further research is warranted to simultaneously evaluate kinematic and kinetic adaptation that occur during bend sprinting and clarify the asymmetry between lower limbs.

2.5. Acceleration phase kinematics

Existing research has focussed almost wholly on the maximal velocity phase of bend sprinting, which does not reflect the full requirements of sporting performance in events such as the 200 m. In straight-line sprinting, the acceleration phase (approximately 0 - 30 m, Mero, 1988) has been found to make an essential contribution to overall sprint performance (Delecluse et al., 1995; Mero, 1988). Yet the impact of the bend on the acceleration phase is still largely unknown.

Owing to the step-to-step changes in touchdown kinematics observed at different stages of acceleration, it is too simplistic to consider acceleration as a single phase. As such, authors have sub-divided the acceleration phase of straight-line sprinting into two phases: initial acceleration and the transition phase (Delecluse et al., 1995). The initial acceleration phase is defined as the block phase along with the first two steps and the transition phase occurs from the third step to the point at which the athlete reaches 80% of their maximum velocity (Delecluse et al., 1995). The fundamental principles of straight-line sprinting are governed by Newton's laws of motion (Morin et al., 2015), which dictate that acceleration is directly proportional to the net force, in the same direction as the net force. Thus, as demonstrated experimentally by Rabita et al. (2015), straight-line sprint acceleration is dependent on the ability to generate anterior force.

However, during bend sprinting at maximal speed, the need to achieve up to 4° change of direction during ground contact (Churchill et al., 2016) changes the mechanical demands of the task and requires generation of the necessary centripetal force (a force that acts on a body moving in a circular path and is directed towards the centre around which the body is moving) in order to accelerate towards the centre of the curve. Thus, body lateral lean is required to counteract the rotational torque in the

mediolateral direction and achieve the change in direction required to stay in lane and follow the curve of the athletics track. The magnitude of centripetal force produced is proportional to the square of velocity and therefore greater centripetal force is required as the athlete reaches faster velocities.

There have been attempts to evaluate performance in the acceleration phase of bend sprinting. Stoner and Ben-Sira (1979) observed a trend for a slower (approximately 0.02 s) time to 12 m on the bend than the straight. However, no statistically significant differences were reported. There was a significant reduction in step length in both the left and right step (Stoner & Ben-Sira, 1979), coinciding with a significant reduction in left step velocity (Stoner & Ben-Sira, 1979). In contrast to the strong outcomes reported during the maximal velocity (30 - 40 m) phase (e.g., Alt et al., 2015; Churchill et al., 2015; Ryan & Harrison, 2003), Stoner and Ben-Sira (1979) did not find a difference in contact time between the bend and the straight. However, it is not clear whether this was genuinely unaffected or a consequence of the sampling rate (148 Hz) used. For example, Churchill et al. (2015) found a significantly greater left contact time compared to the right with a mean difference of 0.007s, whereas a sampling rate of 148 Hz provides a time resolution of 0.0068. Hence, a faster sampling rate (≥ 200 Hz) with improved time resolution is appropriate for future research to ensure differences are detected. Further research is necessary to provide clarity surrounding performance descriptors such as contact time, whilst also identifying the kinematic mechanisms responsible for such changes and increasing the available supporting research for the previously reported differences in step length and step frequency (Stoner & Ben-Sira, 1979).

Research during straight-line acceleration links rapid hip extension to a greater propulsive impulse (Hunter, Marshall, & McNair, 2005). The knowledge that the

movement patterns of the hip are altered during maximal bend sprinting (i.e., increased adduction, Alt et al., 2015; Churchill et al., 2015) questions whether this high hip extension angular velocity is still influential in force production on the bend. During bend sprinting, it is possible adaptations such as the greater left step hip adduction and body lateral lean observed at maximal speed on the bend (Churchill et al., 2015) restrict the ability to produce a high hip extension angular velocity. Therefore, research is required to establish whether the kinematic adaptations found at maximal speed on the bend are present during the acceleration phase and, if so, what impact these adaptations have on the force production capabilities of the lower limbs. Furthermore, these forces may impact upon the internal forces of the lower limb, therefore increasing the risk of injury.

2.6. Acceleration phase kinetics

The evaluation of kinetic and kinematic functions of the lower limb is crucial in furthering understanding of whether acceleration performance is limited by the bend. As Clark and Weyand (2015) stated, the forces produced are a consequence of a complex segmental arrangement of the limb. Therefore, there could be concomitant changes in force production. Moreover, evidence suggests there are differences in force production during acceleration and maximal speed straight-line sprinting (Morin et al., 2015; Rabita et al., 2015; Yu et al., 2016), and it is not known whether the mechanics of acceleration on the bend can be characterised in the same way.

Previous research into the kinetics of bend sprinting has shown changes in vertical and resultant force during maximal sprinting (Churchill et al., 2016). However, straight-line acceleration research suggests that the direction and orientation of force may be more important than resultant magnitude (Morin et al., 2012; Morin, Edouard, & Samozino, 2011; Rabita et al., 2015). When several sprints were used to reconstruct

the entire 40 m acceleration phase, neither resultant ground reaction force or its vertical component were correlated to sprint acceleration performance (Rabita et al., 2015). It was, however, found that mean anteroposterior force was strongly correlated to 40 m maximal speed. These findings (supported by others such as Morin et al., 2011) demonstrate the biomechanical demands of acceleration performance are different to those associated with maximal velocity, which relies on the production of vertical ground reaction force (Morin et al., 2012; Morin et al., 2011; Weyand et al., 2000). This view is further reinforced by Morin et al. (2015), which found mean velocity over 40 m was significantly correlated with net horizontal impulse and propulsive impulse, whereas vertical and braking impulse was not. Correlations were only observed in the 0 - 20 m sections, and not 20 - 40 m, suggesting the production of horizontal impulse (and specifically propulsive impulse) in the first 20 m determines acceleration performance (Morin et al., 2015).

With the findings of Rabita et al. (2015) in mind, it seems the use of resultant ground reaction force in evaluating technique in force production during the acceleration phase is limited. Researchers have proposed the use of 'ratio of force' - a concept borrowed from cycling (for additional information, please see: Bini, Hume, Croft, Cowan, & Kilding, 2013) as a meaningful measure in the evaluation of acceleration performance (Morin et al., 2011; Morin et al., 2012; Rabita et al., 2015). This parameter combines both the force applied by the athlete and their ability to apply this force effectively in the forward direction. Mean ratio of force was found to be one of the mechanical variables most highly correlated with 40 m performance in comparison to other variables such as average vertical force and average horizontal force (Rabita et al., 2015). However, impulse was not included in this analysis (Rabita

et al., 2015), despite propulsive impulse being identified as a key performance indicator by Morin et al. (2015).

The index of force application technique, which evaluates a runner's ability to maintain a high ratio of force at increasing speeds across the acceleration phase (Morin et al., 2011), has also been established as being significantly related to 100 m performance (Morin et al., 2011). However, owing to the requirement of several force plates to acquire measurements over a period of time, index of force application cannot be measured with most experimental set-ups, hence limiting its wider applicability to most research settings. The concept of orientation of force rather than magnitude may have importance in understanding bend sprinting. Although Rabita et al. (2015) concluded mediolateral forces were negligible throughout straight-line sprinting, Churchill et al. (2016) highlighted their potential importance during maximal velocity bend sprinting. The greater mediolateral forces may impact upon the ratio of force and thus acceleration performance during bend sprinting. However, owing to the continual change in direction that occurs during bend sprinting, an adapted version of ratio of force may be required. Research evaluating the force production capacity and ratio of force during bend sprinting is therefore required.

Whilst the aforementioned studies (Morin et al., 2012; Morin et al., 2011; Morin et al., 2015; Rabita et al., 2015) have contributed to a greatly increased understanding of sprint acceleration, their reliance on the reduction of one-dimensional (1D) waveforms to discrete (0D) variables is a persistent limitation. Although the introduction of ratio of force is a move away from the traditional analysis of peak and mean forces, it remains somewhat problematic since it is presented as a single, mean 0D value which therefore does not permit analysis of the entire waveform. Statistical parametric mapping (SPM) presents an opportunity to overcome these limitations and

analyse sprint performance across the whole stance phase, providing insight that may have previously been lost with the reductionist approach of 0D analysis. Colyer, Nagahara, and Salo (2018) were able to use SPM to investigate relationships between force production across the stance phase and straight-line sprint performance from acceleration to maximal speed. Uniquely, the use of fifty-four force plates enabled the analysis of consecutive steps over 52 m. Using linear regressions, it was established that better performances were associated with the production of higher horizontal force production in the mid-late propulsive phase (58-92% of stance in the second step; 55 - 85% of stance in the eighth step). As the athletes progressed through the sprint, these associations appeared earlier in the ground contact phase, occurring predominantly in the braking phase of stance (19 - 64% for the nineteenth step). These results highlight not only the importance of horizontal force production for acceleration but additionally the phase during stance where this contribution is most crucial. Thus, implementing SPM as an analysis technique to evaluate acceleration performance during bend sprinting may hold important insights.

2.7. Joint moments in sprinting

Evaluation of joint moments through the calculation of inverse dynamics can provide insight into the underlying causes of motion and the musculoskeletal demand associated with performing a particular skill (Brazil et al., 2017). As Zajac, Neptune, and Kautz (2002) described, moments generated at the lower extremity joints are one of the main sources for the development of the ground reaction force required for sprinting. Thus, information regarding these moments during bend sprinting could identify the limiting factor to sprint performance on the bend. Chang and Kram (2007) have suggested that, during bend sprinting, the muscles of the lower limb are restricted in their ability to produce force in the sagittal plane owing to adaptations in the frontal

and transverse planes (such as hip adduction and ankle eversion). Analysis of joint moments would provide empirical evidence to support or otherwise refute this theory, whilst also supporting our understanding of injury mechanisms.

During straight-line acceleration, it has been established that extension moments generated at the ankle joint during the stance phase are mostly responsible for GRF development (Dorn, Schache, & Pandy, 2012). However, at speeds above 7 m/s, this strategy is thought to shift, and muscles of the hip and knee joint contribute to increased speed through a greater acceleration of hip and knee joints during the swing phase, thus increasing stride frequency. Therefore, it is likely the application of moments at these joints may restrict the limb force generation. Although changes in lower limb joint kinematics have been reported during bend sprinting (Alt et al., 2015), it is not known if or how these adaptations impact on internal joint moments and thus, force production ability. Burnie et al. (2017) reported that elite coaches believed the transfer of strength training to sports performance was dependent on maintaining coordination and sports-specific movement patterns throughout periods of strength training. Therefore, confirmation of the functioning mechanisms in place during bend sprinting and the resulting joint moments may increase the specificity of strength and conditioning programmes and consequently improve the transfer of training to performance.

The current evidence base regarding joint moments and bend sprinting is limited. Heinrich, Alt, Funken, Brueggemann, and Potthast (2015) examined muscle energies of the lower limb establishing that, during sprinting on the bend compared with the straight, the ankle was the largest energy absorber and generator in the sagittal plane, whereas the hip joint was largest in the frontal and transverse planes. These findings suggest the left hip is highly loaded during bend sprinting. Furthermore, it

appears the roles of the left and right hip joints are asymmetrical. In addition, Viellehner et al. (2016) found an increase in left peak hip and knee adduction moment during constant sub-maximal effort bend sprinting at 9.38 m/s, when compared with the straight. The presence of greater peak external rotation moments at the left hip and knee compared with the right further supports the previous findings from Heinrich et al. (2015) demonstrating different functions of the left and right limb on the bend. Although insightful, the experimental protocols used may not be applicable to bend sprinting performance due to the matched velocity conditions that are not representative of athletic performance conditions. Hence, an investigation of joint moments with a protocol more closely replicating competitive bend sprinting would provide further valuable insights.

During straight-line sprinting, the important role of the ankle joint in contributing to sprint performance in the acceleration phase has been highlighted. For example, Debaere, Delecluse, Aerenhouts, Hagman, and Jonkers (2015) simulated individual muscle forces and established the ankle joint of the stance leg made the greatest contribution to CoM propulsion in all athletes, accounting for 67.1% and 92.9% of propulsion in the first and second stance phase, respectively. Similarly, the plantar flexors of the ankle (gastrocnemius and soleus) were found to contribute the most to propulsion at a muscular level (Debaere et al., 2015). The hip and knee joints were found to have a supporting role in the propulsion of CoM (Debaere et al., 2015). Brazil et al. (2017) supported this, reporting ankle dominance in energy generation of the first stance. However, it is possible that the high ankle eversion and hip adduction found during bend sprinting (Alt et al., 2015, Churchill et al., 2015) places the limb in a complex position and consequently prevents the limb from generating the necessary extension moments demonstrated on the straight.

A proximal-distal sequencing of peak joint powers has been observed during the first stance phase of straight-line sprinting (Brazil et al., 2017; Charalambous et al., 2012). This sequential pattern was also reported by Johnson and Buckley (2001) when investigating muscle power patterns during the acceleration phase of straight-line sprinting. Biarticular muscles are believed to contribute towards the transfer of power from proximal to distal joints (Jacobs, Bobbert, & van Ingen Schenau, 1996). Consequently, smaller muscles of the foot and ankle can achieve a high power output, and thus generate a large ground reaction force due to work done by larger, monoarticular hip muscles. It is possible that kinematic adaptations found during bend sprinting may disrupt this sequencing, resulting in a decrease in sprint performance.

Luo and Stefanyshyn (2012a) introduced a wedged footwear condition during bend sprinting with a 2.5 m radius, inducing a 4° decrease in left step ankle eversion compared with the control condition. The wedged footwear resulted in a 4.3% increase in sprint speed and an 18.8% increase in peak ankle plantar flexion moment generation. These results provide some indication of the importance of joint moment generation at the ankle joint and its relationship with sprint speed on the bend. However, the radius used by Luo and Stefanyshyn (2012a) is smaller than those used during athletics, meaning these results cannot be generalised to an athletics environment. Therefore, further research utilising a representative radius in the context of sprint performance is warranted.

Whilst evidence suggests joint moments of the ankle joint are influential in sprint acceleration, a common limitation of the existing literature is that most inverse dynamics analyses fail to include the MTP joint. This is despite Bezodis, Salo, and Trewartha (2012) showing inclusion of the MTP joint is necessary for the accurate

calculation of joint moments in sprinting. Stefanyshyn and Nigg (1997) showed peak resultant MTP moments of up to 120 Nm during sprinting, with the MTP joint accounting for approximately 32% of the total energy absorbed at the stance leg. Moreover, the MTP joint did not generate energy at take-off (Stefanyshyn & Nigg, 1997). Stefanyshyn and Nigg (1997) results highlighted the potentially important contribution of the MTP joint in sprinting and led Bezodis et al. (2012) to calculate joint moments, power and work during accelerated sprinting (15 m) using three different models to examine the influence of including the MTP joint in these calculations. The thigh and shank were modelled consistently, and three different foot representations were used: ankle to distal hallux, ankle to MTP and a two-segment foot with a rearfoot (ankle to MTP) and forefoot (MTP to distal hallux) segment. A within-participant analysis of three participants revealed a significant effect of the choice of foot model on peak resultant moment, peak power and net work at the knee and ankle joints. There was a significantly greater peak ankle joint moment when the MTP joint was not included, which can be attributed to the linked-segment nature of inverse dynamics. Bezodis et al. (2012) also described a general non-significant increase in peak hip extensor moments when the foot was represented as a single segment.

Further work by Bezodis, Salo, and Trewartha (2014) found a resultant MTP joint plantar flexor moment throughout stance, with the MTP joint also being a net absorber of energy. Thus supporting the previous work of Stefanyshyn and Nigg (1997) and Smith, Lake, Lees, and Worsfold (2012) and demonstrating the importance of including the MTP joint in sprint analyses. Whilst including the MTP joint in sprint analyses is an improvement on single-segment representations, Bezodis et al. (2012) rightfully acknowledge this remains a simplification of the complex foot anatomy.

It has been demonstrated that extension joint moments make a substantial contribution to straight-line sprint performance in the acceleration phase, particularly at the ankle (Debaere et al., 2015). There is also a sequential transfer of power elicited from the hip joint enabling a higher power output at the smaller, more distal joints of the foot and ankle (Brazil et al., 2017; Charalambous et al., 2012; Jacobs et al., 1996; Johnson & Buckley 2001). However, changes in the segmental arrangement of the limb during bend sprinting could impact on both the ability to produce these moments and the proximal-distal transfer of power. Therefore, an investigation of joint moments and the associated power and energy is required in conditions representative of a competitive athletics environment.

2.8. Methodological considerations

Collecting data in a competition is the optimum method of data collection since it enables the measurement of representative performance behaviours. Unfortunately, this is not always possible due to restrictions regarding athlete access, collaborative opportunities, obstructions within stadia and the often invasive nature of data collection methods that can require the attachment of markers to the athlete. Although some researchers have opted to use television broadcasts in their analyses (e.g., Salo, Bezodis, Batterham, & Kerwin, 2011), the quality of the camera settings cannot be verified. Furthermore, analysis of repeated measures under the same experimental conditions is not possible during a competitive setting. Researchers must instead promote ecological validity and replicate a competitive environment through a representative research design. Achieving a representative design most often requires a compromise of some sort owing to the measurement technique employed. All methods of data collection have individual merit, alongside some limitations which will be discussed within this chapter. It is necessary to consider these limitations,

alongside the ecological validity and representativeness of the research, and select the most appropriate method of data collection to best answer the research question within these constraints.

2.8.1. Data collection with high speed video

Previous bend sprinting research has used high speed video cameras in the collection of data (e.g. Churchill et al., 2015; Churchill et al., 2018). These methods are considered beneficial due to their unobtrusive nature. For example, it is possible to collect data without the application of markers which therefore maintains the representativeness of protocols. However, without the use of markers, it is not possible to determine the amount of flexion/extension, abduction/adduction or internal/external rotation that exists at a joint with the calculation of 3D vector angles. Instead, orientation angles, developed by Yeadon (1990) are required, which require the known location of three points on each segment. However, as described by Churchill et al. (2015), this is not possible for all joints of the lower limb due to a lack of independent points for segment definition. The inability to calculate joint angles at all joints presents a substantial limitation to this measurement technique, particularly at the ankle joint where Alt et al. (2015) reported significant adaptions during sprinting on the bend.

2.8.2. Data collection with optoelectronic cameras

Optoelectronic cameras are considered the gold standard of motion capture due to the high validity and reliability values associated with this technique (Hood et al., 2012). They record the location of retro-reflective or active markers, which are used to reconstruct the geometry of bones and joint axes using standardised algorithms (Hood et al., 2012). The use of bone pins is considered the most accurate method of data collection of this type (Hood et al., 2012). However, this is mostly unfeasible for

several reasons, not least the highly invasive and impractical procedure that may impede natural movement. The most common solution is to place spherical, retro-reflective markers directly on the skin over bony landmarks thought to represent the underlying anatomical structures. However, there are some limitations associated with this method, notably, the unknown error from skin artefact. Marker placement and attachment techniques can minimise skin movement artefact (Manal, McClay, Stanhope, Richards, & Galinat, 2000). A cluster of skin-mounted markers was reported as the most inaccurate method due to the independent movement of the markers in relation to each other (Manal et al., 2000). The use of cluster markers attached to a rigid board and then applied to the segment using tape or a hook and loop attachment has been promoted as a viable solution to this problem with increased accuracy over a cluster of skin-mounted markers (Manal et al., 2000). However, even this optimal solution provides individual rotational deviations of ± 2° (mediolateral axis) and ± 4º (longitudinal axis, Manal et al., 2000). Furthermore, some researchers suggest this method may not only increase the amount of time required to apply the marker set, but the tight strapping may provide an alternative stimulus to the participant that may disrupt natural movement (Mündermann et al., 2006). The Vicon Plug-in Gait (PiG) marker set (Davis, Õunpuu, Tyburski, & Gage, 1991), provides an opportunity to solve this problem as it is promoted as a minimal marker set, utilising just one marker per segment to define the third dimension of rotation, therefore negating the previous issues highlighted. The use of a single marker per segment rather than a cluster does, however, increase the likelihood of marker drop-out during the data collection process.

2.8.3. Choice of marker set

Keeping the limitations associated with the application of markers in mind, alongside the constraints of the research environment, a key consideration when

working with optoelectronic systems is the choice of marker set (Milner, 2008). There are several, well-established marker sets in existence which have subtle variations in marker placement, for example, the six degrees-of-freedom (Collins, Ghoussayni, Ewins, & Kent, 2009), and the conventional gait models such as Vicon PiG (Davis et al., 1991) or Helen Hayes (Baker, 2006). The conventional gait models were introduced as minimalistic options to account for the small number of low-resolution cameras originally used in clinical laboratories (discussed in Baker, 2006). These models are hierarchical and require detection of the proximal segment before the distal segment can be calculated. In contrast, the six degrees-of-freedom marker set was introduced using anatomical landmarks following ISB (International Society of Biomechanics) recommendations (Wu et al., 2002) which enable the independent tracking of each segment (Collins et al., 2009). However, some of the anatomical landmarks are located medially (Wu et al., 2002), which not only introduces problems in terms of marker detection but also may increase the risk of marker dropout or obstruction with the opposing limb due to the technique used in bend sprinting. The conventional gait models are often favoured for their simplicity and have demonstrated high repeatability and comparable outcomes in the calculation of gait variables to five of the most common marker sets including conventional and six degrees-of-freedom models (Ferrari et al., 2008; Collins et al., 2009; Żuk & Pezowicz, 2015). Most bend sprinting research making use of optoelectronic techniques have failed to provide explicit information on the location of markers used (Alt et al., 2015; Heinrich et al., 2015; Ishimura & Sakurai, 2010; Ishimura et al., 2013), and so it is often difficult to determine which models have been used in past analyses. Furthermore, current reliability assessments of kinematic variables with optoelectronic systems are limited to walking gait (Bishop, Paul, & Thewlis, 2012; Deschamps et al., 2012) and running

(Milner & Brindle, 2016) that is not representative of the higher velocities found in sprinting. Therefore, information regarding the reliability of variables measured during sprinting is scarce, and those in existence have focussed on parameters of technique such as step length and step frequency (Hunter et al., 2004a; Standing & Mauler, 2017).

Software such as Visual 3D enables the user to make adaptations to marker sets as necessary. These might include: the CODA pelvis option to comply with ISB recommendations (Wu et al., 2002), calculating the ankle joint centre from the mid-point of the medial and lateral malleoli to mitigate against the accumulation of errors found in PiG (Nair, Gibbs, Arnold, Abboud, & Wang, 2010), and the inclusion of a multi-segment foot to enable measurement of more detailed movements such as inversion and eversion (Milner, 2008). Therefore, the researcher must choose the marker set that best meets their requirements taking into consideration the research question and available equipment/space.

2.8.4. Modelling the multi-segment foot

Most conventional models consider the foot as a singular, rigid body which can sometimes be considered appropriate depending on the research question. However, although sprint research including a multi-segment foot model is limited, the MTP joint has been shown to make a substantial contribution to sprint performance (Krell & Stefanyshyn, 2006), whilst its inclusion in analyses also affects the accuracy of joint moment data (Bezodis et al., 2012). Therefore, a more in-depth evaluation of sprinting using a multi-segment foot model is required. There have been several foot models introduced and validated through research (Rankine, Long, Canseco, & Harris, 2008; Stebbins, Harrington, Thompson, Zavatsky, & Theologis, 2006), although a criticism might be that they are unnecessarily complex due to an abundance of markers. The

model used by Smith et al. (2012) can measure the movement of the forefoot, rearfoot and toebox without an overabundance of markers. In addition, it appears this marker set is one of few to be used in a sprint setting (e.g., Smith et al., 2012; Smith et al., 2014). Therefore, its continued use would contribute towards the standardisation of research protocols and enable comparison between studies.

Other than the choice of marker sets available, modelling the multi-segment foot presents further challenges. One example is the use of markers placed on top of footwear at locations thought to represent bony landmarks. These markers are then used to measure the underlying movement of the foot. The accuracy of marker placement of this kind is often brought into question (e.g., Stacoff, Reinschmidt & Stüssi, 1992) and there have been attempts in the literature to overcome this persistent limitation. The use of specially designed sandals during gait studies has allowed marker placement directly onto the skin (Barnes, Wheat, & Milner, 2010). However, their use is not appropriate for sprinting where sprint spikes should be worn to maintain the representativeness of the protocol. Some have achieved marker to skin placement by making small incisions into the footwear (Smith et al., 2014), although this method compromises the integrity of the shoe and the representativeness of this method is questionable. Fortunately, sprint spikes are lightweight and worn tight-fitting so palpating bony landmarks through the shoe is not challenging to an infeasible extent. Furthermore, recent work from McDonald, Honert, Cook, and Zelik (2019) demonstrated no statistically significant effect on net ankle joint power across the stance phase of walking (0.8 - 1.6 m/s) and running (2.6 - 3.0 m/s) when comparing skin vs. shoe-mounted calcaneal markers with the use of SPM. With the various available options, the identification of a suitable marker set for use in the analysis of bend sprinting is desirable.

2.8.5. Inertial models

CoM calculations are required for the analysis of bend sprinting performance. For the calculation of CoM, segment mass and moment of inertia are needed. Determination of these properties requires inertial properties of body segments. It is not possible to directly measure these quantities without difficulties such as the time-consuming process of taking multiple measurements (Hanavan, 1964) or radiation exposure associated with Gamma Mass scanning (Zatsiorsky, 1983). Therefore, inertial properties are most often estimated with the use of regression equations based on anthropometric measurements, which are comparatively simplistic and easier to apply. However, these models are deficient in several areas; the small and uniform populations used, and the possible inaccuracies associated with the application of cadaver data to living humans being the main concerns (Winter, 2009). Despite these drawbacks, their use is prominent and generally considered acceptable and used throughout the sprint literature (e.g., Churchill et al., 2015; Churchill et al., 2016). Zatsiorsky, Seluyanov, and Chugunova (1990) used gamma scanning techniques to obtain data from 115 physically fit participants - much greater than most cadaver studies which are typically in the range of 8-13 (e.g., Dempster and Gaughran, 1967). In addition, the population of physically fit adults are more representative of those typically used in biomechanical research of sports performance. The Zatsiorsky et al. (1990) parameters were adjusted by de Leva (1996), making the reference landmarks in line with those more commonly used in biomechanics. In sprint research, further adjustments are often made to account for the mass of a sprinting shoe to each foot (Hunter et al., 2004b). The mass of the foot (including sprint spike) requires distribution amongst the multi-segment foot. There does not seem to be an accepted standard for this segmentation within the literature, with methods including the use of

computed tomography (CT) scans (Saraswat, Andersen, & MacWilliams, 2010; Saraswat, MacWilliams, Davis, & D'Astous, 2014); distribution based on the relative forefoot:rearfoot length (Bezodis et al., 2012; Bruening, Cooney, & Buczek, 2012) and arbitrary use of 50:50 for forefoot:rearfoot (Dixon, Böhm, & Döderlein, 2012). Whilst the use of CT scans is the most accurate method, they require expensive and specialised equipment that is not available in most laboratories.

The choice of inertial properties influences the calculation of joint moments with inverse dynamics. For example, Rao, Amarantini, Berton, and Favier (2006) compared lower limb inverse dynamics computations from six body segment parameter models. During the stance phase at 'fast' cadence, the highest percentage of variation between models was 19% for flexion/extension at the hip (Rao et al., 2006); although values were much lower for the knee and ankle joints. This presents an issue with regard to the foot as there are currently no guidelines for the estimation of body segment parameters of the multi-segment and as such, they are largely based on assumption. A number of different methods have been used within the gait community, with the most common being the use of CT scans (Saraswat et al., 2010; Saraswat et al., 2014) or the application of body segment parameter estimates for a single segment foot (Deschamps et al., 2017; Dixon et al., 2012). However, owing to the small mass of the foot, any influence of body segment parameter values is likely to have a minimal effect on the calculation of inverse dynamics. Rather, it is generally accepted that joint moments at the foot are almost entirely a product of the ground reaction force and the associated moment arm (Bruening & Takahashi, 2018).

2.8.6. Measuring kinetics

Ground reaction force can be measured with the use of force plates which can be synchronised with a motion capture system to enable simultaneous data collection.

The accuracy of these systems is generally accepted as very high. However, it is dependent on several factors; for example, crosstalk, cable interference, mounting technique and force detection threshold (Lees & Lake, 2008). With regard to experimental procedures, one of the main concerns is 'targeting' of the force plate by the athlete, where the athlete deliberately tries to strike the force plate, which can lead to adaptations in normal movement patterns (Sanderson, Franks & Elliot, 1993) and consequently affects the ecological validity of the protocol. Every effort must, therefore, be made to reduce the likelihood of this occurring. The optimum solution would be to have a number of adjacent force plates, therefore improving the possibility of a clean strike. Although there have been some studies that have utilised a series of force plates 52 m in length (Colyer et al., 2018), in most laboratories, this is not possible, and targeting must be addressed using different techniques. Monitoring and adjusting the start position of the athlete is a solution most often employed in sprint studies (Bezodis, Kerwin, & Salo, 2008; Churchill et al., 2016).

In the calculation of joint moments, it is generally considered that ground reaction forces are error-free (Camomilla et al., 2017). However, when using a multi-segment foot, each segment in contact with the ground requires an individual ground reaction force vector (Saraswat et al., 2010). Bruening and Takahashi (2018) established that the most accurate way to partition ground reaction forces amongst the multi-segment foot is with the use of a pressure mat, although even with this method sagittal plane peak moment and power were slightly overestimated by 10% and 9%, respectively. The measurement of plantar pressure to distribute vertical ground reaction force across segments of the foot has been implemented in a number of gait analyses (Deschamps et al., 2017; MacWilliams, Cowley, & Nicholson, 2003; Saraswat et al., 2010; Saraswat et al., 2014). However, the use of pressure insoles is

not always possible and may further reduce the representativeness of sprint protocols. Furthermore, the proportionality assumption (Saraswat et al., 2014) used to distribute shear forces (which pressure insole systems do not measure) may not be appropriate for use during bend sprinting where mediolateral forces are much greater than those found during straight-line sprinting (Churchill et al., 2016).

To avoid the problems associated with the distribution of ground reaction force, analysis after heel raise (at which point contact occurs mostly in the forefoot) has been implemented within the literature where pressure insoles have not been available (Dixon et al., 2012). However, this method restricts inverse dynamics analysis to the latter part of the stance phase and so is not a favourable alternative. Therefore, the 'Centre of Pressure Cross' method described by Bruening and Takahashi (2018) is often used, whereby the anteroposterior location of the centre of pressure is used to allocate ground reaction force to a segment. This method does have its limitations, notably the overestimation of joint moments at the MTP joint by approximately 17% (Bruening & Takahashi, 2018). Despite this, several sprint analyses have chosen to implement this method, whereby the MTP joint moment was considered negligible until the ground reaction force acted distal to the joint (Smith et al., 2014; Smith et al., 2012; Stefanyshyn & Nigg, 1997). This method was also used by Bezodis et al. (2012) and Bezodis et al. (2014) who investigated joint moments during the first stance phase of straight-line sprinting. However, Bezodis et al. (2012) identified, through the qualitative assessment of previous work, that foot contact occurred with the forefoot only during the first stance phase and so partition of ground reaction forces amongst the multi-segment foot was not necessary. Although, this may not be the case when the athlete has progressed further along the sprint distance.

As Schache and Baker (2007) described, the net activity in muscle groups (and hence which group is dominant) is represented by joint moments. Therefore, the reference frame chosen should best represent the relative activity of different muscle groups (Schache & Baker, 2007). Schache and Baker (2007) presented joint moment profiles calculated in different reference frames (laboratory, proximal segment, distal segment and joint coordinate system). Significant differences were observed between reference frames, particularly in the transverse plane (Schache & Baker, 2007). Although the author's note these differences are not representative of errors between conditions, Schache and Baker (2007) go on to advocate the use of the joint coordinate system reference frame. Their reasoning behind selecting the joint coordinate system reference frame as the most appropriate is based upon the definition of different muscle groups as the rotation the muscles would produce if the moment were the only force applied to the joint (Schache & Baker, 2007). The joint coordinate system is recommended by the ISB as a standard convention for describing rotations about a joint (Wu et al., 2002; Wu et al., 2005). Therefore, to achieve correspondence between joint angles and joint moments, it seems logical that the joint moment thought to create that rotation should also be expressed in the joint coordinate system (Schache and Baker, 2007). Kristianslund, Krosshaug, Mok, McLean, and van den Bogert (2014) and Desroches, Cheze, and Dumas (2010) also support the use of the joint coordinate system reference frame, with the latter suggesting expressing both joint angles and moments in the same coordinate system might provide an improved biomechanical insight. Use of a non-orthogonal reference frame may warrant concern since, due to crosstalk, the sum of the squares of the three components will always be greater than the square of the total moment. However, as Schache and Baker (2007) state, the actions of different muscle groups cannot be allocated to acting purely about a single

axis. Therefore, it was felt the joint coordinate system was the most appropriate reference frame for the representation of joint moments.

2.8.7. Filtering

There are inevitably some errors associated with all measurement techniques, which may exist as a consequence of skin movement artefact or factors such as electrical interference. These errors become increasingly problematic when using differentiation techniques such as those used to calculate velocities and accelerations (Winter, 2009) and so are typically removed using data smoothing techniques before analysis takes place. These techniques work by identifying and removing elements of 'noise' that occur at a frequency range different from the actual signal (Robertson, Caldwell, Hamill, Kamen, & Whittlesey, 2013). Of those in existence, polynomial fitting, spline fitting and digital filtering appear the most commonly used in current sprint literature (e.g., Churchill et al., 2015; Churchill et al., 2016; Johnson & Buckley, 2001; Hunter et al., 2004a).

Polynomial smoothing fits a shape that is assumed to represent the 'best fit' of the data. Whilst it is advantageous in that it allows the interpolation of points at different time points alongside the calculation of derivatives with ease, their use can distort the true shape of a signal (Robertson et al., 2013). In addition, Winter (2009) suggests that the use of polynomials may be more appropriate in non-repetitive movements. Splines are a modification of polynomials that work on smaller sections of the curve and because of this, are more adaptable to changes in curvature. They also share the advantage of making derivatives easier to obtain. However, as Robertson et al. (2013) highlight, the points of inflexion used to determine individual sections of the curve are influenced by the noise within the signal which the filter is attempting to remove.

Digital filtering takes a different approach to remove noise from the signal. It instead removes noise by focussing on differences between the frequency content of the signal and noise. Since the use of a digital filter introduces a phase lag, a second filter must be applied in the opposite direction. The choice of cut-off frequency can affect the resulting signal and whilst several methods exist to determine this cut-off point, Winter (2009) suggests that a residual analysis is the most appropriate. It is important to note that this applies to displacement data only and the fact that different markers are likely to have different optimum frequencies exists as a further limitation to this selection method. It has been suggested that when differentiation is required, much higher cut-off frequencies are needed than those suggested as a result of a residual analysis (Yu, Gabriel, Noble, & An, 1999).

Another important consideration when using digital filters is 'endpoint error' which refers to the distortion that these types of filter can often introduce at the start and end of a signal. Whilst this can be avoided through the collection of additional frames of data, doing so is not always possible, so techniques such as 'padding' or 'reflection' are often used during the filtering process. In an investigation of the effectiveness of these techniques in reducing endpoint error, it was found that the reflection of data points produced results similar to those found with the addition of real data points (Smith, 1989).

Furthermore, Bezodis, Salo, and Trewartha (2013) highlighted the importance of selecting an appropriate cut-off frequency when calculating joint moments. In an analysis of kinetic and kinematic data with four different cut-off frequencies (10, 25, 50 and 100 Hz) and ten combinations where the kinetic data cut-off frequency was equal to or exceeding the kinematic input data. The choice of cut-off frequency combination influenced the magnitude of peak knee extensor moment during the first

5% of stance, with greater peaks introduced when the kinetic cut-off frequency exceeded that of the kinematic data (Bezodis et al., 2013). These impact peaks were close to non-existent when the cut-off frequencies were matched (Bezodis et al., 2013). Thus, the application of identical cut-off frequencies for kinetic and kinematic data is recommended to avoid these fluctuations at impact.

2.9. Summary

There is a growing body of research examining the biomechanical differences between sprinting on the bend and straight. Increased hip adduction and longer contact time in the left step appear key characteristics of bend sprinting performance at maximal and sub-maximal speeds (Alt et al., 2015; Churchill et al., 2015). These adaptations have been associated with an increase in body lateral lean (Churchill et al., 2015), a consequence of the additional requirement of producing centripetal force during bend sprinting. Furthermore, a high left step ankle eversion at sub-maximal speed (Alt et al., 2015) and a smaller radius (Luo & Stefanyshyn, 2012a) have been observed. However, the ankle and multi-segment foot are yet to be investigated in conditions representative of elite athletics competition despite their importance being demonstrated during straight-line sprinting (Bezodis et al., 2008; Bezodis, Trewartha, & Salo, 2015; Bezodis, Salo, & Trewartha, 2014; Brazil et al., 2017; Charalambous et al., 2012; Debaere et al., 2015; Krell & Stefanyshyn, 2006; Smith et al., 2014).

Although it is clear athletes are unable to reach the same maximal speeds on the bend and straight (Churchill et al., 2015; Churchill et al., 2016), the number of studies evaluating the acceleration phase of bend sprinting is limited. Therefore, it remains unclear if the bend has the same effect on acceleration performance. Ratio of force analysis encapsulates the technical ability of sprinters by assessing the way force is applied to the ground (Morin et al., 2011). A higher ratio of force, achieved through

the production of high amounts of anteroposterior force, has been associated with acceleration performance in straight-line sprinting (Morin et al., 2011; Rabita et al., 2015). However, during bend sprinting at maximal speed, an increase in mediolateral force has been observed (Churchill et al., 2016), which might impact upon the technical ability of sprinters. Therefore, analysis of force production during the acceleration phase of bend sprinting might provide important insights and aid understanding of performance.

Furthermore, it is likely that joint kinetics hold some insights into the mechanisms of bend sprinting performance. However, joint moments and power have yet to be investigated under conditions replicating a competitive athletic environment. A review of the methodological considerations pertinent to addressing the research question has also been presented. It is essential that the representativeness of the experimental protocol is maintained throughout and optimum solutions to the issues raised are sought from the literature. Taking into consideration the constraints of the research environment, the most appropriate solution should be implemented throughout the programme of research.

Chapter 3: SIMPLIFIED MARKER SETS FOR THE CALCULATION OF CENTRE OF MASS LOCATION DURING BEND SPRINTING

THE WORK FROM THIS CHAPTER FORMED THE BASIS OF THE FOLLOWING PEER-REVIEWED CONFERENCE ABSTRACT:

Judson, L. J., Churchill, S. M., Barnes, A., Stone, J. A., & Wheat, J. (2017). Simplified marker sets for the calculation of centre of mass duration during bend sprinting. *Paper presented at the 35th Conference of the International Society of Biomechanics in Sports (ISBS);* Cologne, Germany.

3. Simplified marker sets for the calculation of the centre of mass location during bend sprinting

3.1. Introduction

Analysis of the position, trajectory and velocity of the CoM is common within bend sprinting research (Alt et al., 2015; Churchill et al., 2015; Churchill et al., 2016; Churchill et al., 2018; Ishimura & Sakurai, 2016). In addition, key variables such as touchdown distance and turn of CoM during ground contact require knowledge of the location of CoM for calculation (Churchill et al., 2015; Churchill et al., 2016). Furthermore, during bend sprinting the kinematic adaptations that occur are multi-dimensional, occurring in all three planes (Alt et al., 2015; Churchill et al., 2015; Churchill et al., 2016). Therefore, evaluation of bend sprinting necessitates the use of 3D data collection methods.

With the use of a full-body marker set, 3D methods such as optoelectronic motion capture allow calculation of CoM position. Segment inertial parameters (derived from anthropometric studies, e.g. de Leva, 1996; Dempster & Gaughran, 1967; Zatsiorsky, 1983) are used to estimate the whole-body CoM location based on the distribution of mass within the multi-segment model. However, there are difficulties with optoelectronic data collections that have complex lower limb marker sets (e.g., a multi-segment foot model) with a required minimum of three markers for each segment. The ability to achieve an appropriate frame rate, resolution and capture volume to aid marker detection is both determined and restricted, due to the number of cameras and laboratory space available. Additional factors such as the time-consuming application of markers, and increased interference with the athlete causing a potential decrease in ecological validity, make the collection of data with a simple model, using the fewest possible markers (e.g., lower limb only), preferable to

using a full-body marker set. Furthermore, kinematic analysis of the arms is rarely performed due to the implication that the arms do not have a significant impact on sprint performance (Mann & Herman, 1985). Finally, the capture volume must be defined as a square or rectangular shape with most motion capture systems. This is problematic due to the curved nature of bend sprinting, which therefore requires a long and wide capture volume, resulting in essentially 'wasted' space within the capture volume. A reduced marker set would enable a capture volume lower in height and longer in length enabling more steps to be calculated, increased resolution and reducing the risk of marker drop-out. Therefore, the ability to calculate the required variables (including CoM location) using a simplified marker set would be desirable. The purpose of this study was to ascertain to what extent the simplification of a kinematic marker set is appropriate for the accurate calculation of CoM during bend sprinting.

3.2. Methods

3.2.1. Participants

Following ethical approval from the Sheffield Hallam University Local Research Ethics Committee, seven sprinters (five males; mean age 20 ± 1.11 years; body mass 70.37 ± 4.88 kg; stature 1.79 ± 0.48 m and two females; mean age 22 ± 3.50 years; body mass 58.85 ± 1.35 kg; stature 1.66 ± 0.40 cm) volunteered for the study. The inclusion criteria required athletes to have competitive experience of bend sprinting (200 and/or 400 m). Mean personal best times were 22.90 ± 0.85 s (range: 22.00 - 24.10 s; 200 m, five males) and 64.00 ± 0.00 s (400 m, two females). All participants provided written informed consent prior to data collection.

3.2.2. Experimental set-up

Kinematic data were collected using a 12-camera optoelectronic motion capture system (10 x model Raptor and 2 x model Eagle, Motion Analysis Corporation, Santa Rosa, CA, USA) operating at 240 Hz. A right-handed global coordinate system was defined using a rigid L-frame with four markers of known locations. A three marker wand of 500 mm was used within the calibration volume to scale the individual camera views. The capture volume (7 m long, 1.5 m wide and 2 m high) was located tangentially to the apex of the curve to record data at the 38 - 45 m section of the 60 m sprints where athletes are likely to be at maximum speed (Krzysztof & Mero, 2013, Figure 3.2.2.1).

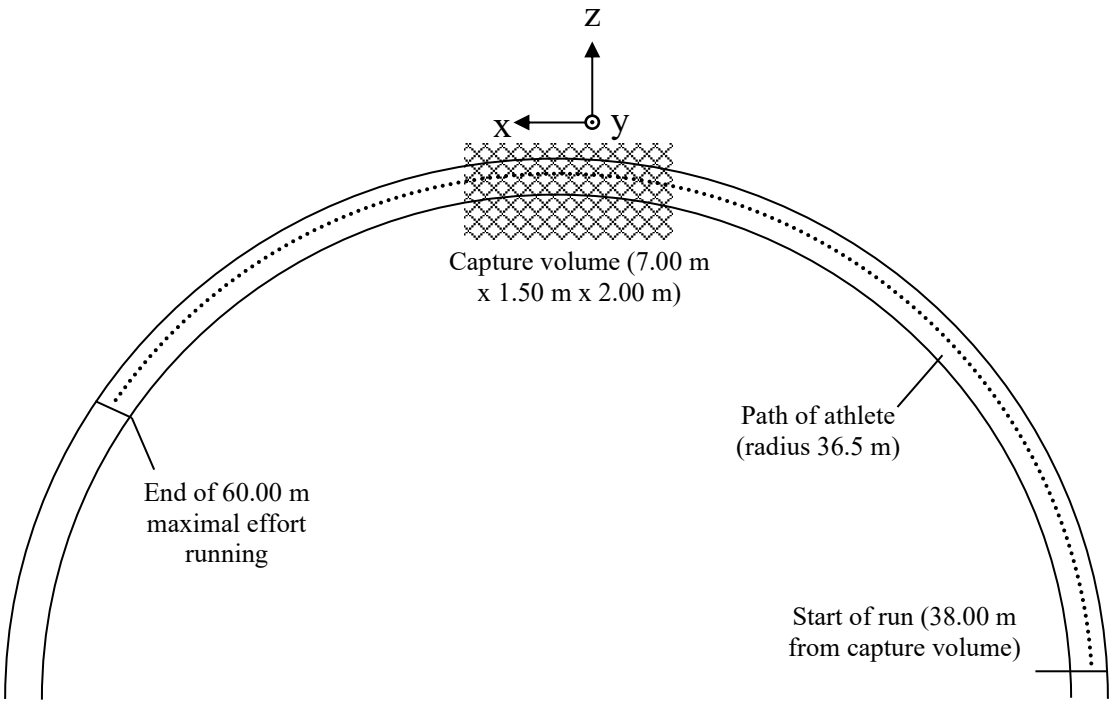

Figure 3.2.2.1 Plan view of test set-up (not to scale)

A full-body marker set (59 markers) modified from Davis et al. (1991) was used to model 13 segments (head, upper arms, lower arms, torso, pelvis, thighs, shanks and feet). Retro-reflective spherical markers (12.7 mm) were placed on both sides of the body on the following anatomical landmarks: head, acromioclavicular joint, upper

arm, lateral humeral epicondyle, medial humeral epicondyle, forearm, ulnar styloid, radial styloid, C7, T10, jugular notch, xiphoid process, anterior superior iliac spine (ASIS), posterior superior iliac spine (PSIS), greater trochanter, medial femoral epicondyle, lateral femoral epicondyle, thigh, tibia, medial malleolus, lateral malleolus, posterior calcaneus, medial calcaneus, lateral calcaneus, 1st and 5th metatarsal base, 1st, 2nd and 5th metatarsal head and head of the 2nd toe. The results of this chapter will inform the identification of a marker set for use throughout the remainder of the thesis. Therefore, full details of the marker set (including segment definitions) chosen for use with subsequent studies can be found in Section 4.2.2. A static trial was completed prior to data collection, with the participant in the anatomic position for three seconds.

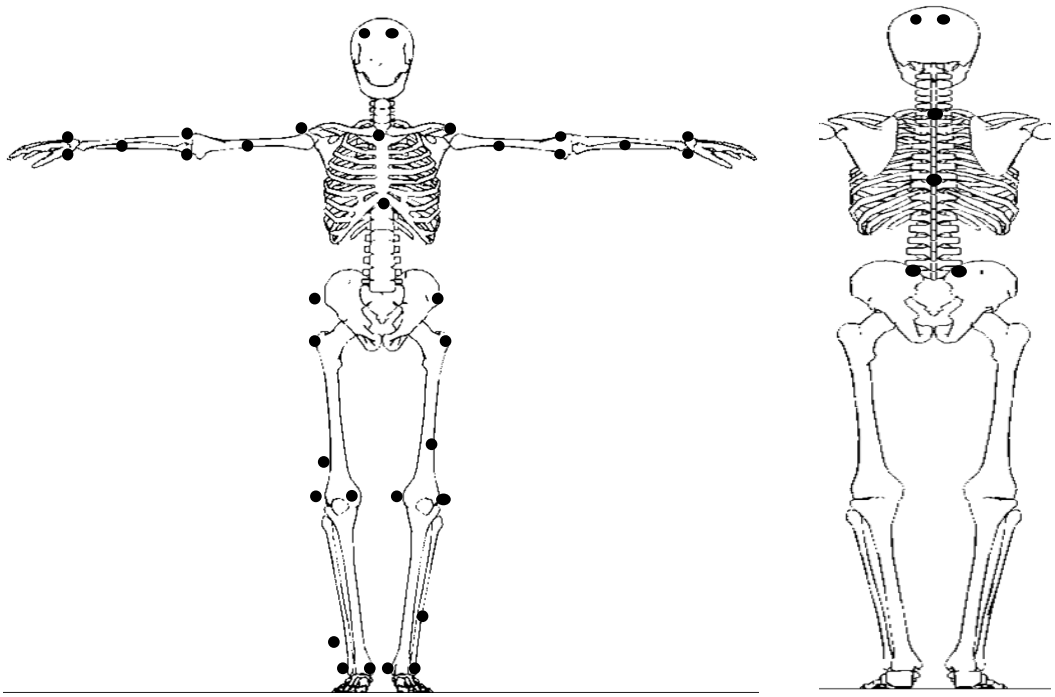

Figure 3.2.2.2 Full-body marker set. Markers were placed on the following anatomical landmarks on both sides of the body: head, (front left, front right, rear left, rear right) acromioclavicular joint, upper arm, lateral humeral epicondyle, medial humeral epicondyle, forearm, ulnar styloid, radial styloid, C7, T10, jugular notch, xiphoid process, anterior superior iliac spine (ASIS), posterior superior iliac spine (PSIS), greater trochanter, medial femoral epicondyle, lateral femoral epicondyle, thigh, tibia, medial malleolus, lateral malleolus. The multi-segment foot (not shown) was modelled using markers placed on: posterior calcaneus, medial calcaneus, lateral calcaneus, 1st and 5th metatarsal base, 1st, 2nd and 5th metatarsal head and head of the 2nd toe.

3.2.3. Protocol

Data were collected on a flat standard indoor track surface with a reconstructed bend, replicating lane 1 (radius 36.5 m) of a standard 400 m running track (IAAF, 2008). It was necessary to reconstruct the bend indoors to enable use of the optoelectronic cameras. In addition, a standard 200 m indoor track is banked and has a radius ranging from 15 - 17 m (IAAF, 2008) and has not been used competitively in World Championships since 2004. Thus, a reconstructed bend replicating a standard outdoor track was required. The bend was reconstructed using cones placed 4 m apart, with a lane width of 1.2 m. Following a typical competition warm up, participants performed five trials at maximal effort for 60 m, starting with the use of starting blocks. Participants were topless (or wearing just a sports bra for female athletes) and wore form fitting shorts, allowing the majority of markers to be placed directly onto the skin. Approximately eight minutes were allowed between trials to allow recovery and avoid the onset of fatigue (Churchill et al., 2015).

3.2.4. Data Processing

Cortex (version 5.3, Motion Analysis Corporation, Santa Rosa, CA, USA) was used to track and export raw 3D coordinate data. Automatic gap filling was performed using a cubic spline where gaps were <10 frames. Raw marker positions were filtered at 18 Hz (chosen with the use of residual analysis, Winter, 2009) using a low-pass, fourth-order recursive Butterworth filter. Segments, local coordinate systems (LCS) and joint centres were defined and constructed in Visual 3D (version 4, C-Motion, Rockville, MD, USA). There are numerous models available for the prediction of inertial characteristics which enable CoM calculation, the merits of which have been discussed in section 2.8.1. The de Leva (1996) adjusted parameters were considered the most appropriate due to the combination of a large sample of recreationally fit

adults being most representative of the athletic population within the present programme of research and, the reference landmarks corresponding to those used within biomechanical analyses of sports performance. Therefore, body segment parameters were estimated from de Leva (1996) and adjusted to allow the addition of 0.2 kg to each foot which represents the mass of a spiked shoe (Hunter et al., 2004b).

Two further simplified models were defined following methods of Vanrenterghem et al. (2010). Firstly, a CoM representation was calculated with lower limb and trunk segments (LLT) including pelvis, thighs, shanks, feet and thorax (total markers: 42). Following this, the trunk segment was then excluded, and CoM calculated based upon lower limbs (LL) segmental position only (total markers: 38). CoM trajectories across two steps (one left, one right) were calculated with each of the three models and the mean calculated across all participants. Take-off and touchdown events were identified using the position of the marker coordinates for 5th metatarsal head (MTH5) in the static trial as a threshold following Bezodis, Thomson, Gittoes, and Kerwin (2007).

3.2.5. Calculation of variables

Variables requiring the calculation of the CoM that are important within the previous bend sprinting literature were calculated (Alt et al., 2015; Churchill et al., 2015; Churchill et al., 2016; Churchill et al., 2018). Horizontal velocity for each CoM representation was calculated in Matlab (v2015b, Mathworks, Natick, USA) using a finite difference algorithm (Winter, 2009). Velocity data were analysed for the duration of the left and right steps and normalised to 101 data points to represent 100% of the gait cycle. Left and right steps were defined by the foot that initiated the step.

Touchdown distance, defined as the horizontal displacement between the CoM and second MTP joint, was calculated in line with methods from Churchill et al.

(2015). An instantaneous progression vector for the CoM (calculated from the horizontal position of the CoM one frame before the instant of interest to the horizontal position of the CoM one frame after the instant of interest, then divided by its norm to create a unit vector) and a horizontal vector from the CoM to the 2nd metatarsal head of the touchdown limb were created. A scalar projection of this vector onto the instantaneous progression vector gave touchdown distance. For all trials the middle step was used to calculate turn of CoM, this resulted in 16 trials for the right step and 19 for the left step. Turn of CoM (the amount the athlete turns 'into' the bend during ground contact; Churchill et al., 2016) was calculated using the angle between CoM progression vectors during the flight phase before and after the ground contact of interest.

3.2.6. Statistical analysis

Descriptive statistics (mean and standard deviation) were calculated. In addition, Bland-Altman plots with 95% limits of agreement were used to evaluate the agreement between models for all variables. Intraclass correlations (ICC), model (3, 1) were used to further assess agreement according to the criteria set by Cicchetti (1994), where > 0.75 *excellent* agreement.

3.3. Results

Mean velocity for the whole-body model for all participants was 8.14 ± 0.74 m/s (right step) and 8.12 ± 0.73 m/s (left step, Table 3.3.1). Deviations from whole-body model CoM across mean velocity profiles for all participants during the left and right step are shown in Figure 3.3.. Visual inspection of these curves suggests that representation of the CoM with both LLT and LL models provide a close (0.00 – 0.10 m/s) approximation when compared to the whole-body model CoM velocity, with LLT providing a more accurate representation throughout the entire step.

Observations from Bland-Altman plots (Figures 3.3.3 - 3.3.8) and the small mean difference found suggest no evidence of systematic bias in the CoM representations with LLT and LL when compared to whole-body CoM. The mean difference for mean step velocity in the LLT condition was 0.0207 ± 0.0643 m/s for the right step and 0.0037 ± 0.0808 m/s for the left step. The mean difference increased to 0.0524 ± 0.0860 m (right step) and 0.0375 ± 0.0661 m (left step) during the LL condition.

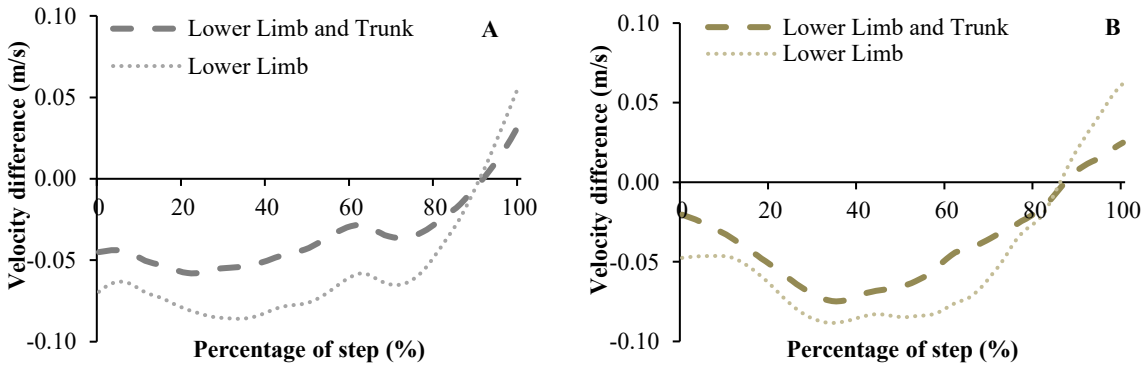

Figure 3.3.1 Comparison of the difference between whole-body CoM velocity and CoM representations, zero indicates no deviation from whole-body model CoM during a step. Mean velocity profiles for (A) the right step and (B) the left step.

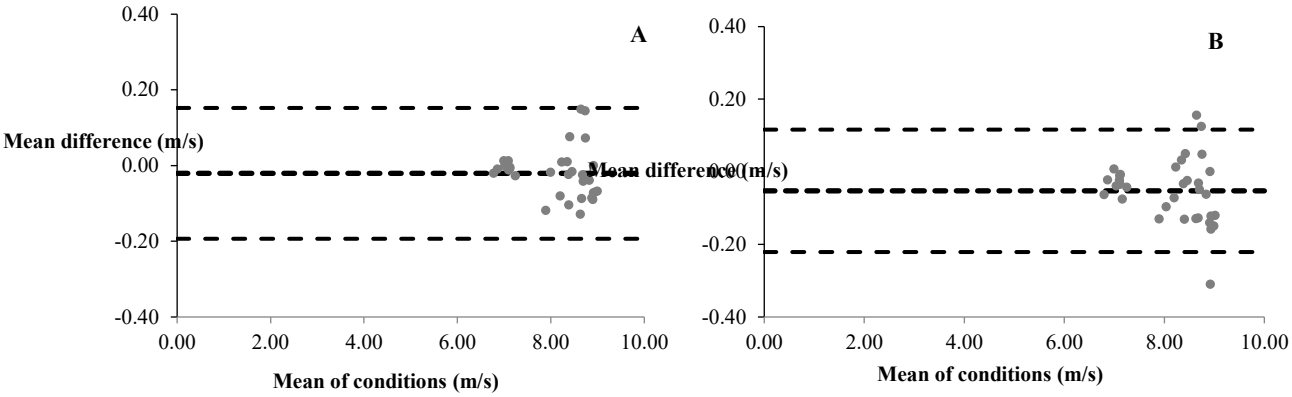

Figure 3.3.2 Bland Altman plots for right step velocity for (A) LLT and (B) LL, where the dashed line represents the upper and lower limits of agreement (mean difference ± 1.96 x standard deviation), and the bold dashed line represents the mean difference.

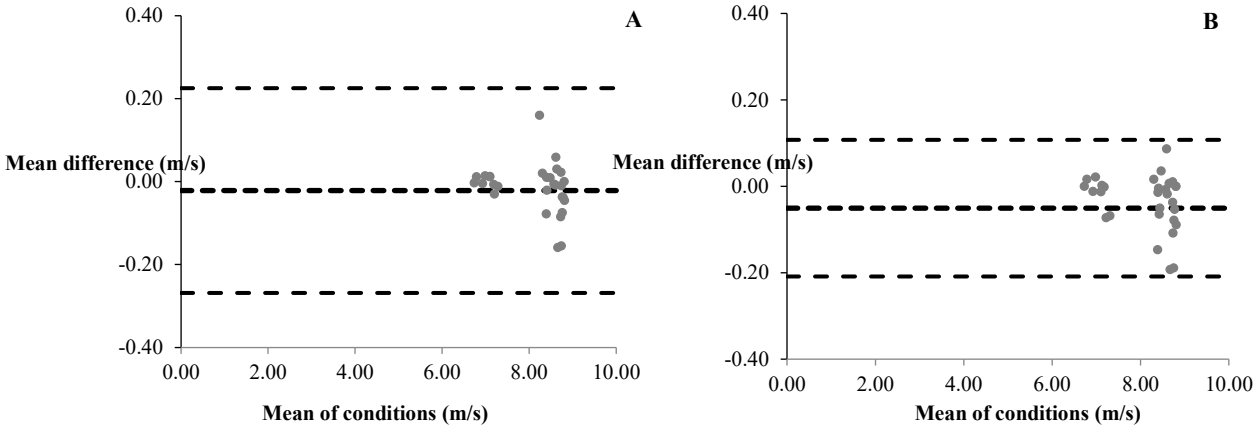

Figure 3.3.3 Bland Altman plots for left step velocity for (A) LLT and (B) LL, where the dashed line represents the upper and lower limits of agreement (mean difference ± 1.96 x standard deviation), and the bold dashed line represents the mean difference.

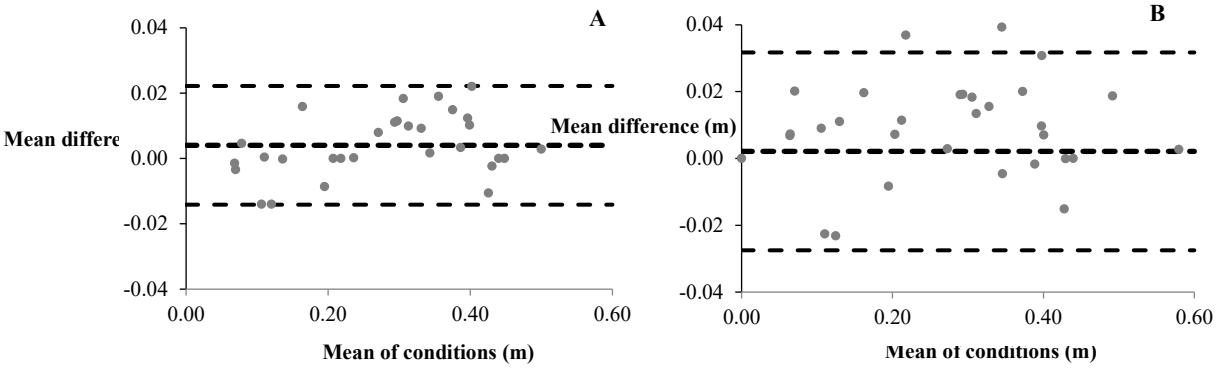

Figure 3.3.4 Bland Altman plots for right step touchdown distance for (A) LLT and (B) LL, where the dashed line represents the upper and lower limits of agreement (mean difference ± 1.96 x standard deviation), and the bold dashed line represents the mean difference.

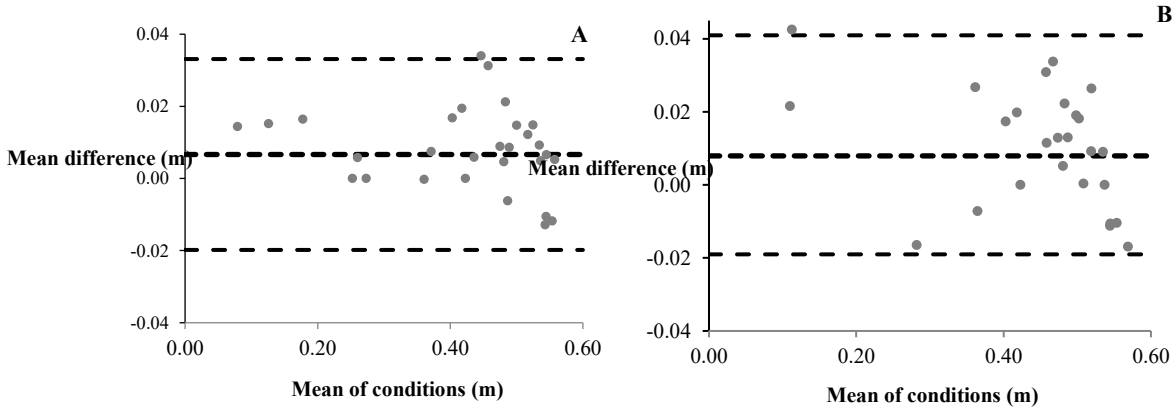

Figure 3.3.5 Bland Altman plots for left step touchdown distance for (A) LLT and (B) LL, where the dashed line represents the upper and lower limits of agreement (mean difference ± 1.96 x standard deviation), and the bold dashed line represents the mean difference.

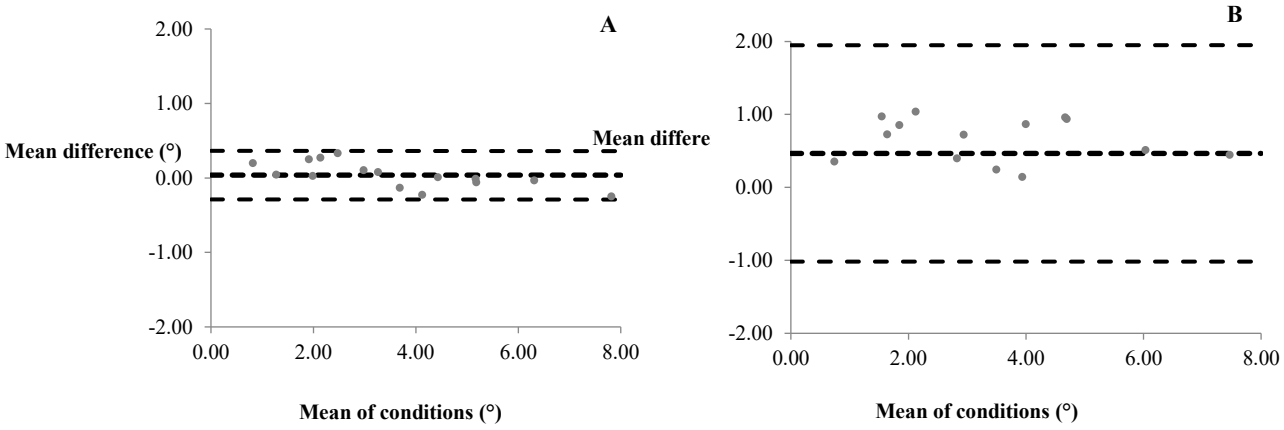

Figure 3.3.6 Bland Altman plots for right step turn of CoM for (A) LLT and (B) LL, where the dashed line represents the upper and lower limits of agreement (mean difference ± 1.96 x standard deviation), and the bold dashed line represents the mean difference.

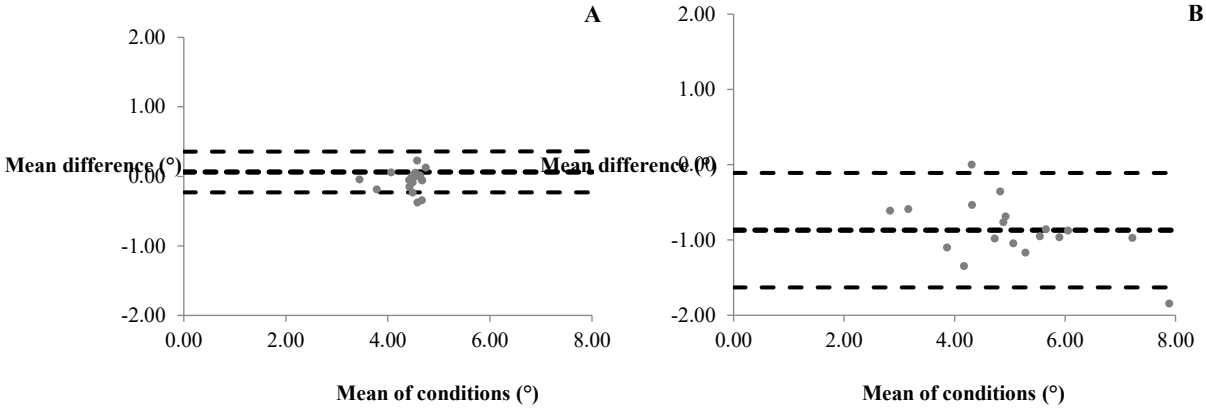

Figure 3.3.7 Bland Altman plots for left step turn of CoM for (A) LLT and (B) LL, where the dashed line represents the upper and lower limits of agreement (mean difference ± 1.96 x standard deviation), and the bold dashed line represents the mean difference.

Table 3.3.1 Mean values ± SD, mean difference, limits of agreement and ICC values for the left and right step during bend sprinting.

	Mean step velocity (m/s)		**Touchdown distance (m)**		**Turn of CoM (°)**	
	Right	*Left*	*Right*	*Left*	*Right*	*Left*
Whole-body Mean ± standard deviation	8.14 ± 0.74	8.12 ± 0.73	0.28 ± 0.13	0.43 ± 0.13	3.59 ± 1.83	4.60 ± 1.13
LLT Mean ± standard deviation	8.16 ± 0.75	8.13 ± 0.74	0.28 ± 0.13	0.42 ± 0.13	3.55 ± 1.95	4.66 ± 1.16
LL Mean ± standard deviation	8.18 ± 0.76	8.14 ± 0.74	0.28 ± 0.14	0.43 ± 0.12	3.13 ± 1.78	5.47 ± 1.34
Mean difference (Whole-body – LLT)	0.0207	0.0037	0.0040	0.0066	0.0381	0.0402
Mean difference (Whole-body – LL)	0.0524	0.0375	0.0100	0.0010	0.4659	0.8696
Upper Limits of Agreement (Whole-body – LLT)	0.14	0.16	0.02	0.03	0.11	0.33
Lower Limits of Agreement (Whole-body – LLT)	0.11	0.15	-0.01	-0.02	-0.04	-0.25
Upper Limits of Agreement (Whole-body – LL)	0.12	0.09	0.04	0.09	1.95	1.63
Lower Limits of Agreement (Whole-body – LL)	0.22	0.16	-0.02	-0.09	-1.02	0.11
ICC (Whole-body – LLT)	0.998	0.997	0.998	0.995	0.998	0.995
ICC (Whole-body – LL)	0.996	0.998	0.995	0.900	0.942	0.873

Discussion

This study aimed to determine the accuracy of simplified marker sets in the calculation of the location of the CoM and associated variables during bend sprinting. For mean velocity, ICCs suggest an excellent level of agreement between the whole-body model and simplified LLT and LL representations providing support for the use of an LLT model to measure mean velocity. However, wide (≥ 0.09 m/s) limits of agreement were also observed. The high limits of agreement could be related to the high standard deviation shown between trials which are likely a consequence of the differing maximal velocities achieved by participants. Both between- and within-participant differences are accounted for in the calculation of the ICCs (Hopkins, 2000; Weir, 2005). ICC results for LLT and LL models for all variables were above excellent suggesting these between participant differences did not affect the data.

Mean difference for touchdown distance in the LLT condition (< 0.0066 m) in both the left and right step, indicate the method provides near equivalent results, supported by narrow limits of agreement and all trials falling within these limits. The mean difference of touchdown distance was also low for the LL condition. The limits of agreement for the LLT condition are similar to the 1.11 limits of agreement ratio for touchdown distance reported as part of a reliability assessment of sprint variables (Hunter et al., 2004a). The mean difference was <1° across all models for the turn of CoM. ICC results for turn of CoM again demonstrated excellent agreement between the whole-body and LLT methods (0.995-0.998). Whilst both models showed very good agreement, the whole-body condition with the LLT condition being marginally better.

The results of the present study are in line with the conclusions of Vanrenterghem et al. (2010) who found a better agreement in the LLT model compared to the LL model in the analysis of lateral cutting movements. Thus, whilst both CoM representations provide a close approximation of whole-body CoM, LLT is a more accurate solution. Since the use of LLT requires only a small number (four) of additional markers, its use should be favoured over LL. The LLT marker set is comprised of 17 fewer markers than the whole-body marker set. Thus, its use can decrease the amount of time required in the application of markers and the data cleansing process whilst also increasing the representativeness of the protocol by reducing the amount of intrusion the athlete experiences. In addition, the use of a LLT marker set negates issues with data collection owing to the athlete's height which, with taller athletes, can require a change in experimental set-up to ensure detection of head markers. Extending the height of the capture volume reduces the resolution within the capture volume and increases the likelihood of drop-out of lower limb markers.

3.4. Conclusion

The aim of this study was to establish whether the CoM and associated variables required for the analysis of performance during bend sprinting could be estimated from a simplified marker set. The LLT model was deemed to provide good agreement with whole-body CoM. It is thought the benefits associated with utilising this simplified model outweigh the small differences reported. Therefore, use of an LLT marker set is suggested as an appropriate alternative to a full-body marker set in kinematic studies of bend sprinting. The test re-test reliability of bend sprinting with the LLT marker set will be established in Chapter 4.

Chapter Four: MEASUREMENT OF BEND SPRINTING KINEMATICS WITH THREE-DIMENSIONAL MOTION CAPTURE: A TEST-RETEST RELIABILITY STUDY

THE WORK FROM THIS CHAPTER FORMED THE BASIS OF THE FOLLOWING PEER-REVIEWED JOURNAL ARTICLE:

Judson, L. J., Churchill, S. M., Barnes, A., Stone, J. A., Brookes, I. & Wheat, J. (2018). Measurement of bend sprinting kinematics with three-dimensional motion capture: a test-retest reliability study. *Sports Biomechanics, 1-17.* doi: 10.1080/14763141.2018.1515979

4. Measurement of bend sprinting kinematics with three-dimensional motion capture: a test-retest study

4.1. Introduction

Sprint velocity decreases on the bend in comparison to the straight (Chang & Kram, 2007; Churchill et al., 2015; Churchill et al., 2016). This reduction is suggested to be related to the additional need to generate centripetal force (Chang & Kram, 2007; Usherwood & Wilson, 2006). Unlike the 100 m race that occurs entirely on the straight, the 200 m and 400 m races include a portion on the bend that accounts for approximately 58% of the total distance covered (Meinel, 2008). Therefore, performance on the bend makes a substantial contribution to overall race performance.

Whilst there has been some consideration of the reliability of sprint related performance variables within the literature (most notably, Hunter et al., 2004a; Salo & Grimshaw, 1998; Standing & Maulder, 2017), the analysis of performance descriptors has been the main focus. For example, Hunter et al. (2004a) evaluated the within-day reliability of 26 kinematic and seven kinetic variables. It was concluded that reliability could be improved with the use of an average score of multiple trials as opposed to a single measure. Even for variables demonstrating low reliability (such as touchdown distance), averaging across multiple trials was an appropriate method of improving reliability. Substantial adaptations in joint kinematics have been reported during bend sprinting in comparison to straight-line sprinting (e.g., Alt et al., 2015; Churchill et al., 2015), without supporting reliability data it is difficult to determine whether these changes have been influenced by variation in task execution, equipment calibration, random error or protocol design.

To evaluate performance on the bend, the analysis of spatio-temporal, kinematic and kinetic variables is required. Owing to its high reliability and validity,

data collection with optoelectronic systems is considered the gold standard of kinematic measurement techniques (Hood et al., 2012). Despite this, few bend sprinting studies have used optoelectronic cameras to investigate kinematic variables (for exceptions see: Alt et al., 2015; Ishimura & Sakurai, 2010; Ishimura & Sakurai, 2016; Ishimura et al., 2013). A key consideration when working with 3D motion capture is the choice of marker set (Milner, 2008, section 2.8.3). However, in studies that have used 3D motion capture, most fail to provide explicit information on the location of markers used (Alt et al., 2015; Ishimura & Sakurai, 2010; Ishimura & Sakurai, 2016; Ishimura et al., 2013). Furthermore, there is a lack of published evidence regarding the reliability of such models in conditions representative of elite bend sprinting (i.e., radius, velocity and surface), since the majority of research focuses on straight-line walking (e.g., Bishop, Paul, & Thewlis, 2013; Deschamps et al., 2012; Milner & Brindle, 2016) or running (e.g., Alenezi et al., 2016; Ferber et al., 2002; Milner & Brindle, 2016). These studies have typically reported lower reliability in the frontal and transverse planes. Therefore, this is an expected outcome regardless of speed. However, bend sprinting occurs at much a higher velocity (e.g., 9.86 m/s, Churchill et al., 2015) than walking (e.g. 1.25 m/s, Milner & Brindle, 2016) or running (e.g., 3.65 m/s, Ferber et al., 2002). These higher velocities produced during sprinting are likely to affect the reliability of a marker set, for example, through an increase in skin movement artefact. Thus, it is not appropriate to assume the same reliability as for walking or running actions. Due to the issues highlighted (see section 2.8.3), selecting a marker set for use in bend sprinting is problematic. Knowledge of reliability data enables researchers to determine the meaningfulness of reported differences between conditions and conclude, with confidence, that the effects are due to the independent variable and not the method of data collection, or any other form of

random variation (Hopkins, 2000). A standardised marker set with supporting reliability data would be a valuable tool for use in future bend sprinting research. It is important to examine both between- and within-day reliability. Whilst within-day reliability is affected by task execution, random error and skin movement artefact, additional factors such as system calibration and marker application may affect between-day measurements. Although the use of ICCs is supported for establishing the level of reliability, it is further recommended that ICCs should not be used as a sole measure (Atkinson & Nevill, 1998). Therefore, ICCs are often combined with the standard error of measurement (SEM) which provides a measure of absolute reliability and allows results to be extrapolated to other populations and measurement tools since it is expressed in the actual units of measurement (Atkinson & Nevill, 1998). Furthermore, there is a lack of agreement or clarity regarding what is considered an 'acceptable' ICC or SEM, and so, calculation of minimal detectable difference (MDD) provides an indication of the magnitude of change required to be considered 'real' to aid researchers in the interpretation of results.

During kinematic analyses, the number of cameras and available laboratory space impact upon factors such as frame rate, resolution and desired capture volume. The resulting camera set-up can influence the coverage within the capture volume, which will impact upon marker detection - for example, areas of low coverage within the capture volume would likely increase marker drop-out rate. Furthermore, increasing the number of markers used has the consequence of increasing marker application and post-processing time (Vanrenterghem et al., 2010). In addition, there is potentially a decrease in the representativeness of the protocol through increased athlete interference with additional markers. It has been established that an LLT

marker set was sufficient for the accurate calculation of CoM location and associated variables (velocity, touchdown distance and turn of CoM) during bend sprinting (Chapter 3). For mean step velocity, touchdown distance and turn of CoM, ICCs in the range of 0.995-0.998 were reported showing excellent agreement between the simplified model and a whole-body marker set (Chapter 3). Since this reduced marker set has been shown to accurately represent full-body movements, it holds promise for use in future studies on bend sprinting. However, its reliability has yet to be established.

Therefore, the aim of this chapter was to determine the within- and between-day reliability of bend sprinting using 3D optoelectronic motion capture with an LLT marker set.

4.2. Methods

4.2.1. Participants

Following ethical approval from Sheffield Hallam University Research Ethics Committee, six sprinters (four males; mean age 20 ± 1 years; body mass 73.3 ± 3.0 kg; stature 1.79 ± 0.56 m and two females; mean age 22 ± 3 years; body mass 58.9 ± 1.4 kg; stature 1.66 ± 0.40 m) volunteered for this study. All athletes had experience of bend sprinting (200/400 m) and were active in training at the time of data collection. Mean personal best times were 22.76 ± 0.95 s (range: 22.00 - 24.10 s; 200 m, four males) and 64.00 ± 0.00 s (400 m, two females). Owing to the population under investigation and the requirement for experience the execution of a specific task, the number of participants in previous bend sprinting studies is typically in the range of six to nine and statistically significant differences have been found despite the smaller sample sizes used (Alt et al., 2015; Churchill et al., 2015; Churchill et al., 2016).

Furthermore, the findings from Alt et al. (2015) imply that velocity specific modulations are apparent in bend sprinting, and therefore extending the inclusion criteria may introduce variability into the sample. Thus, a smaller, but more homogenous, sample size was thought more appropriate. The study procedures were fully explained to participants who subsequently provided written informed consent.

4.2.2. Equipment

Kinematic data were collected using a 12-camera optoelectronic motion capture system (8 x Raptor model and 4 x Eagle model, Motion Analysis Corporation, Santa Rosa, CA, USA) sampling at 240 Hz. The experimental set-up is demonstrated in Figure 4.2.2.1 and fully described in section 3.2.2. Athletes ran primarily in the direction of the positive *x*-axis (anterior-posterior) in the capture volume, (see Figure 4.2.2.1) where the positive *y*-axis was directed vertically upwards (longitudinal) and the positive *z*-axis was orthogonal to the other two axes (mediolateral, pointing to the athletes' right).

A modified Vicon Plug-in Gait (PiG) marker set (LLT; Chapter 3) was used to model segments (torso, pelvis, thighs, shanks and feet, Figure 4.2.2.2). PiG has been used extensively in gait research (Kadaba, Ramakrishnan, & Wootten, 1990; Kulmala et al., 2017; Radzak, Putnam, Tamura, Hetzler, & Stickley, 2017). Although there are not yet any published data in sprinting, the unmodified PiG model is supported by reliability data during walking gait (Ferrari et al., 2008), revealing good reliability and correlation with other approaches including the Calibrated Anatomical System Technique (CAST; Benedetti, Catani, Leardini, Pignotti, and Giannini, 1998). Retro-reflective, spherical markers (12.7 mm diameter) were placed on the following anatomical landmarks of the left and right leg: lateral malleolus, medial malleolus,

shank (lower lateral 1/3), thigh (lower lateral 1/3 surface of the thigh), lateral femoral epicondyle, medial femoral epicondyle, greater trochanter, posterior superior iliac spine (left and right), anterior superior iliac spine (left and right), C7, T10, suprasternal notch, xiphoid process. Acromion process markers were included for the static trial only. All other markers remained for the movement trials.

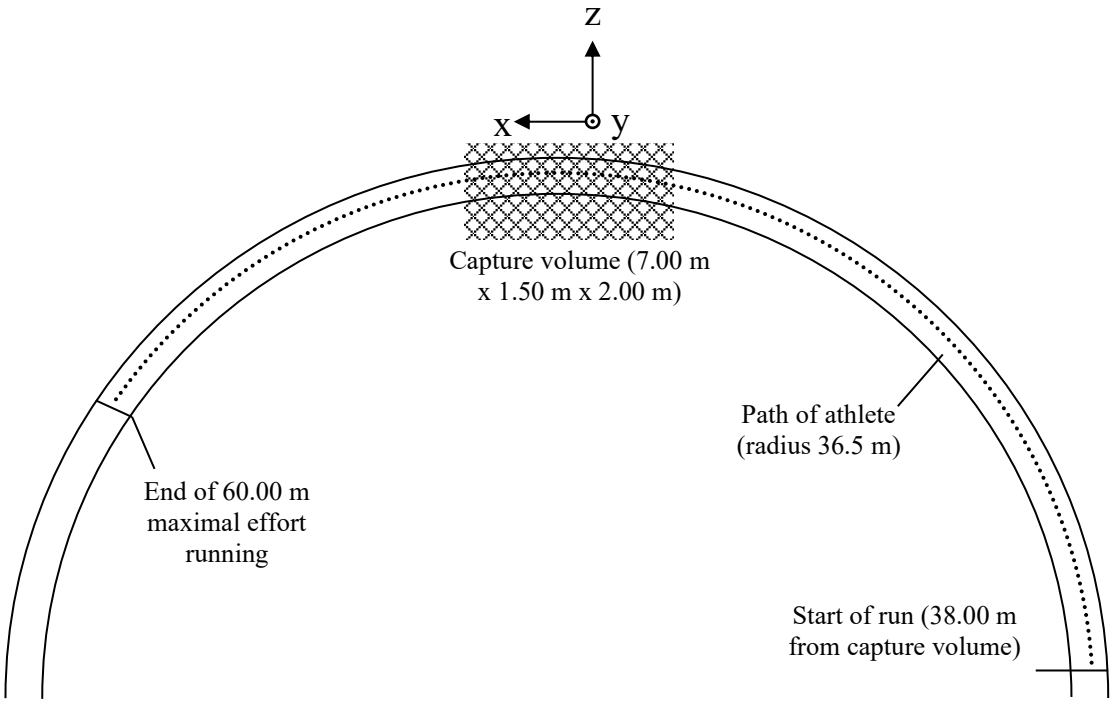

Figure 4.2.2.1 Plan view of test set-up (not to scale)

The PiG model represents the foot as a single unit. However, this simplistic approach does not permit the measurement of movements within the foot such as MTP dorsiflexion and plantar flexion which have been identified as important movements in sprinting (Bezodis et al., 2012; Smith et al., 2012). In addition, inversion and eversion may have importance during bend sprinting. Therefore, additional markers were placed on the posterior, medial and lateral calcaneus, 1st and 5th metatarsal bases, 1st, 2nd and 5th metatarsal heads and head of the 2nd toe (Smith et al., 2012, Figure 4.2.2.3). All foot markers were shoe-mounted and assumed to represent the movement

of the underlying foot. The foot was modelled as three segments; rearfoot, forefoot and toebox (Figure 4.2.2.3).

Multi-segment foot models require placement of the three calcaneus markers (posterior, medial and lateral) to be equidistant, and at the same height (Grant & Chester, 2015; Paik, Stebbins, Kothari, & Zavatsky, 2014). However, there are few easily palpable anatomical landmarks at the calcaneus (Grant & Chester, 2015), which makes repeatable marker placement difficult. Furthermore, McDonald et al. (2019) suggest variation in calcaneal marker placement can result in significant differences in ankle joint power. Thus, a consistent marker placement should be maintained across trials and conditions. Therefore, a custom-built block was used to enable consistent marker placement (height 3 cm, between-marker distance 3 cm, Figure 4.2.2.2).

Figure 4.2.2.2 Custom built block to enable consistent placement of calcaneus markers

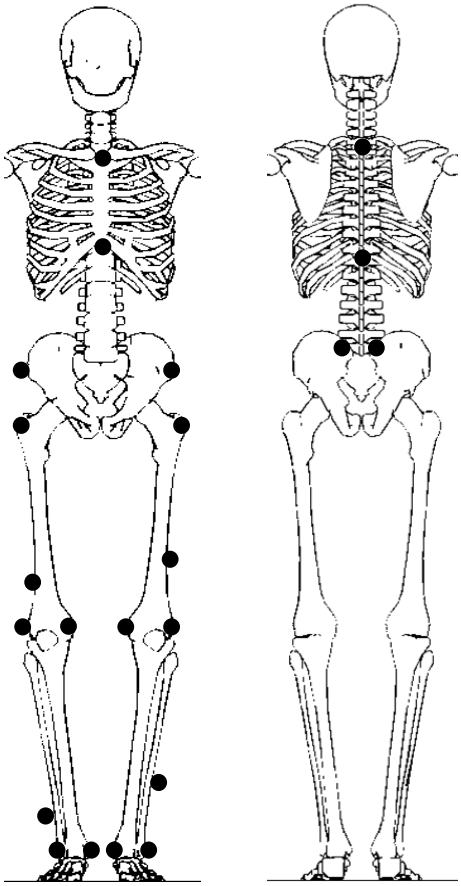

Figure 4.2.2.2 Lower limb and trunk marker set anatomical locations. Markers were placed on both sides of the body on the following landmarks: C7, T10, jugular notch, xiphoid process, anterior superior iliac spine (ASIS), posterior superior iliac spine (PSIS), greater trochanter, medial femoral epicondyle, lateral femoral epicondyle, thigh, tibia, medial malleolus, lateral malleolus.

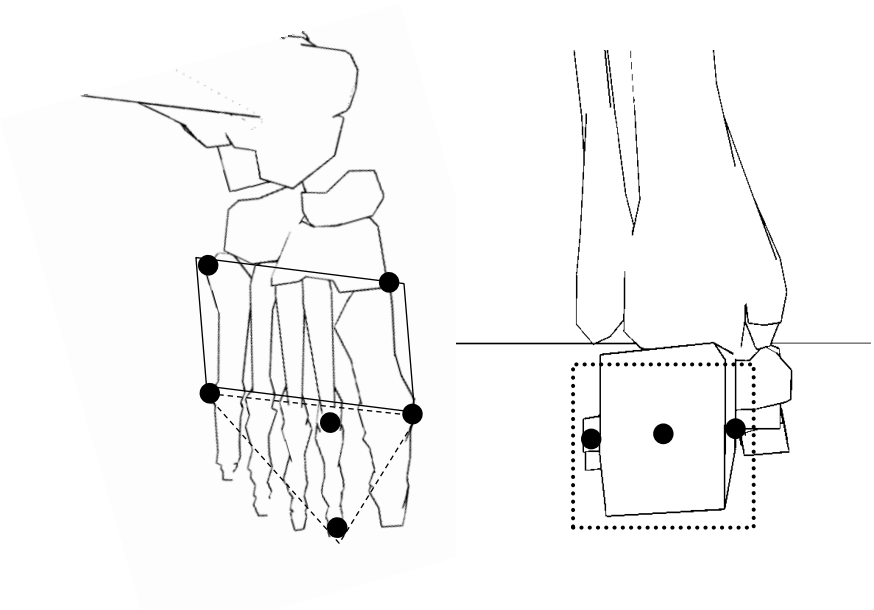

Figure 4.2.2.3 Multi-segment foot model marker placement and segment division. The solid line (-) represents the forefoot defined by the first and fifth metatarsal base and first, second and fifth metatarsal head. Dashed line (- - -) represents the toebox defined by first, second and fifth metatarsal heads and the head of second toe. Circular line (…) represents the rearfoot segment defined by posterior, lateral and medial calcaneus and a virtual inter-medius calcaneus marker.

Where possible, segments were defined according to ISB recommendations (Wu et al., 2002; Wu et al., 2005), with the exception of the multi-segment foot model which was defined in line with Cappozzo, Catani, Della Croce, and Leardini (1995) where the long axis of the foot was defined first. The segments were defined as follows:

Rearfoot

Segment definition: Posterior calcaneus, medial calcaneus, lateral calcaneus and virtual intermedius calcaneus marker.

- *Origin:* Posterior calcaneus marker.
- *y:* vector from the origin to intermedius calcaneus (midpoint of lateral and medial calcaneus markers) and its positive direction is proximal.
- *z:* defined by the *y*-axis and lateral calcaneus marker, pointing to the right (positive).
- *x:* orthogonal to the *yz* plane and the positive direction is dorsal.

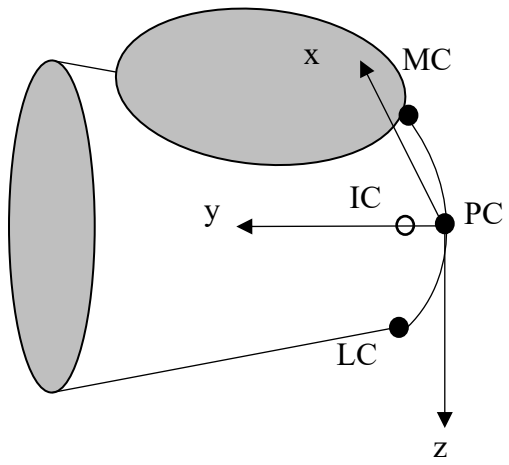

Figure 4.2.2.4 Rearfoot segment definition. L/P/MC = lateral/posterior/medial calcaneus, IC = intermedius calcaneus

Forefoot

Segment definition: 1st and 5th metatarsal bases and 1st and 5th metatarsal heads

- *Origin:* virtual landmark 1/3 of the way between the base of 1st and 5th metatarsal.
- *y:* joins the origin with the 2nd metatarsal head.
- *z:* orthogonal to a plane created by the *y*-axis and base of the 5th metatarsal, pointing to the right.
- *x:* orthogonal to the *yz* plane.

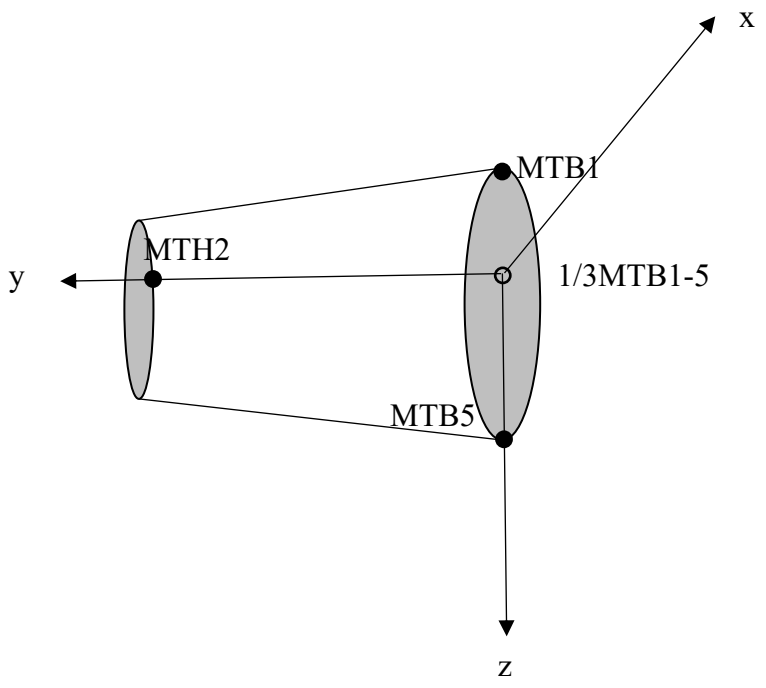

Figure 4.2.2.5 Forefoot segment definition. MTB1/5 = 1st and 5th metatarsal bases, MTH2 = 2nd metatarsal head, 1/3MTB1-5 = virtual landmark 1/3 of the way between MTB1 and MTB5

Toebox

Segment definition: 1st and 5th metatarsal heads and head of 2nd toe

- *Origin:* 2nd Metatarsal Head.
- *y:* joins the origin with the head of 2nd toe.
- *z:* defined by the *y*-axis and the 1st metatarsal head.
- *x:* orthogonal to the *yz* plane.

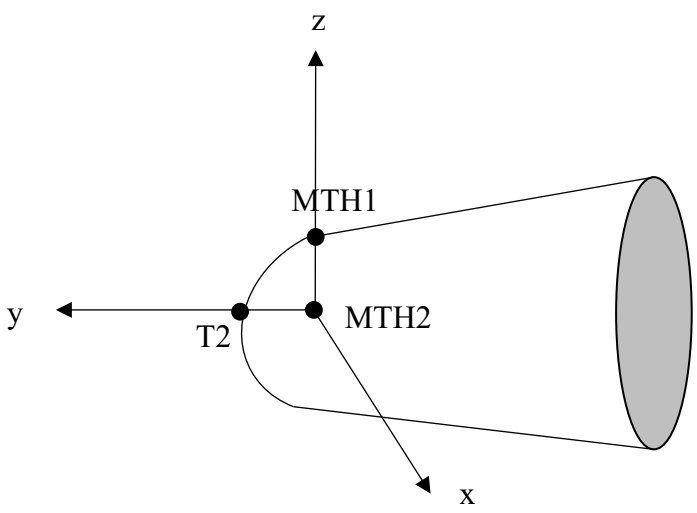

Figure 4.2.2.6 Toebox segment definition. MTH1 = first metatarsal head, MTH2 = second metatarsal head, T2 = head of second toe

Shank

Segment definition: virtual markers of the knee and ankle joint centres and tibia marker

- *Origin:* Intermedius malleoli (mid-point between lateral malleolus and medial malleolus).
- *z:* created from a unit vector passing from the medial malleolus to lateral malleolus, pointing to the right (positive).
- *x:* defined by the line perpendicular to the torsional plane of the tibia/fibula, pointing anteriorly with its positive direction forwards.
- *y:* defined by the line perpendicular to *z*- and *x*-axis with the positive direction proximal.

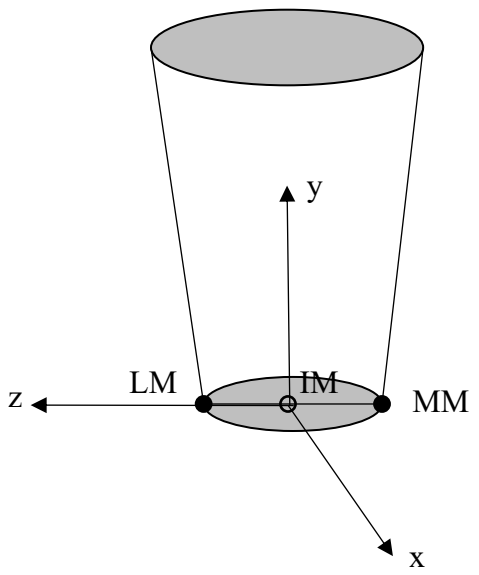

Figure 4.2.2.7 Shank segment definition. LM/MM = lateral / medial malleolus, IM = intermedius malleolus

Thigh

Segment definition: virtual markers of the hip and knee joint centres and the thigh marker

- *Origin:* hip joint centre of rotation.
- *y:* a line joining the origin with the midpoint between the femoral epicondyles, pointing upwards (positive).
- *z:* perpendicular to the *y*-axis, in the plane defined by the origin and femoral epicondyles, pointing to the right (positive).
- *x:* a line perpendicular to *y*- and *z*-axis, pointing anteriorly (positive).

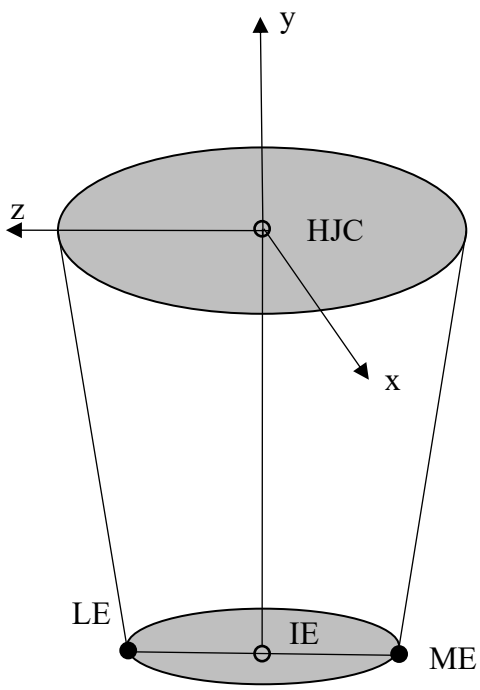

Figure 4.2.2.8 Thigh segment definition. HJC = hip joint centre, LE/ME = lateral and medial epicondyle, IE = inter-epicondyle

Pelvis

Segment definition: virtual marker at the midpoint of ASIS and both ASIS markers

- *Origin:* mid-point of the two ASIS markers.
- *z:* the line parallel to a line connecting the two ASIS landmarks, pointing to the right (positive).
- *x:* a line parallel to the plane defined by the midpoint of the two PSISs and the two ASIS landmarks, orthogonal to the *z*-axis and pointing anteriorly (positive).
- *y:* orthogonal to the *z-x* plane and its positive direction is upwards.

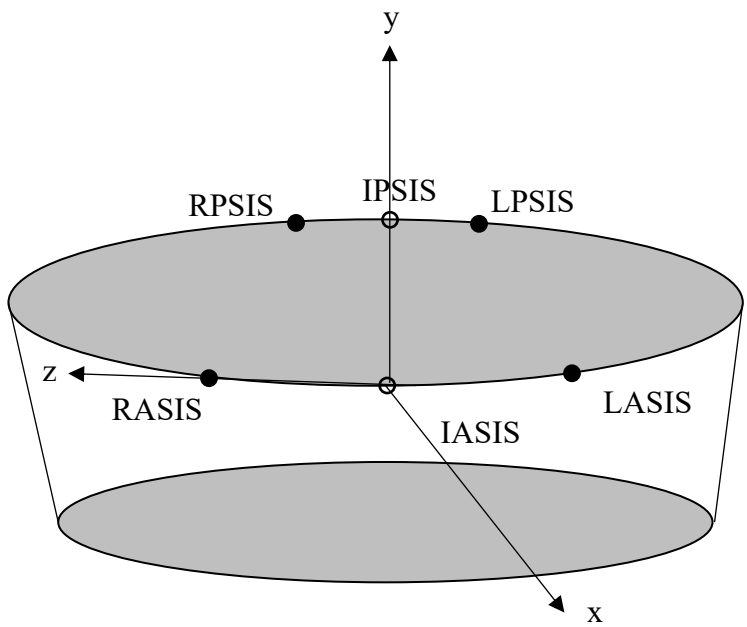

Figure 4.2.2.9 Pelvis segment definition. RPSIS/LPSIS = right / left posterior superior iliac spine, RASIS/LASIS = right/left anterior superior iliac spine, IPSIS = inter posterior superior iliac spine, IASIS = inter anterior superior iliac spine

Trunk

Segment definition: virtual markers: mid-point of C7 and jugular notch, the midpoint between the xiphoid process and T10 and mid-point between the jugular notch and xiphoid process

- *Origin:* coincident with the jugular notch.
- *y:* the line connecting the mid-point between the xiphoid process and T10 and the mid-point between the jugular notch and C7, pointing upward (positive).
- *z:* the line perpendicular to the plane formed by the jugular notch, C7, and the mid-point between the xiphoid process and T10, pointing to the right (positive).
- *x:* the common line perpendicular to the *y*- and *z*-axis, pointing forwards (positive).

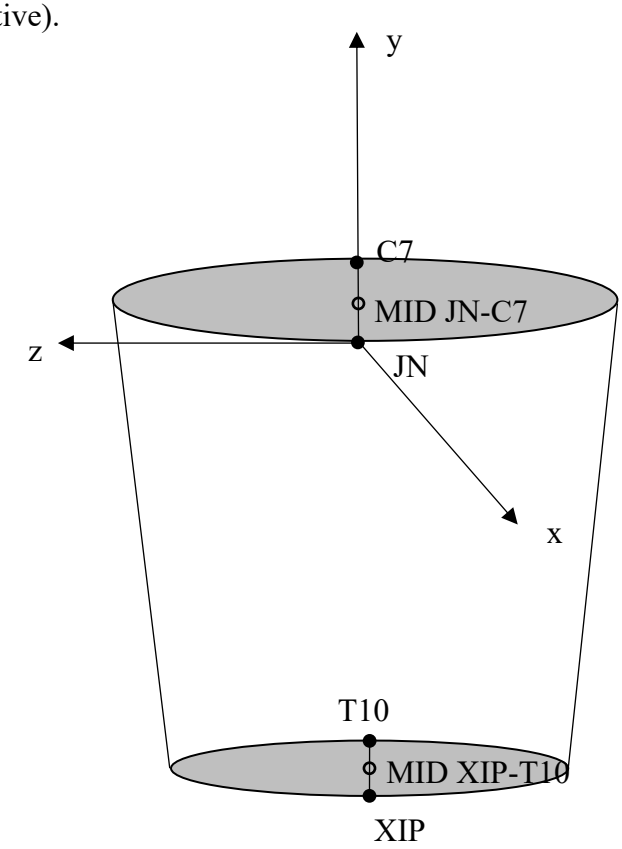

Figure 4.2.2.10 Trunk segment definition. JN = jugular notch, XIP = xiphoid process

4.2.3. Test-retest protocol

Data were collected on a flat standard indoor track surface with a reconstructed bend replicating lane 1 (radius 36.5 m) of a standard 400 m running track (IAAF, 2008). Lane 1 has the tightest bend radius (36.5 m compared to lane 8, 41.5 m). Therefore, any adaptations that occur as a consequence of bend radius were expected to be more apparent in lane 1 (Churchill et al., 2018). Following an individualised, standard competition warm-up, participants performed five trials at maximal effort for 60 m. Data collection started at 38 m, where athletes were likely to be at maximum speed (Krzysztof & Mero, 2013). Approximately eight minutes were allowed between trials to allow full recovery and avoid the onset of fatigue (Churchill et al., 2015). Participants were topless where possible or wearing form fitting clothing. In addition, participants wore the same pair of sprint spikes for each testing session and completed a full cool-down following the test protocol.

The test protocol was repeated between two days and one week later, with the second session occurring at approximately the same time of day (i.e., morning or afternoon). The marker set was applied by the same researcher at each testing session.

4.2.4. Data processing

Cortex software (version 5.3, Motion Analysis Corporation, Santa Rosa, CA, USA) was used to track and export raw 3D marker coordinate data. Automatic gap filling was performed using a cubic spline on all gaps <10 frames. Raw marker positions were filtered at 14-18 Hz using a low-pass, fourth-order recursive Butterworth filter. Trunk, pelvis and thigh markers were filtered at 18 Hz, shank and ankle markers at 16 Hz and foot markers at 14 Hz. These cut-off frequencies were chosen using residual analysis with a frequency range based upon previous sprint and

multi-segment foot literature with a range of 7 - 20 Hz (Churchill et al., 2015; Hunter et al., 2004a; Hunter et al., 2004b; Milner & Brindle, 2016; Queen, Gross, & Liu, 2006). Segments, LCS and joint centres were defined and constructed in Visual 3D software based on a static standing trial (version 6, C-Motion, Rockville, MD, USA). Body segment parameters were estimated from de Leva (1996) and adjusted to allow the addition of 0.2 kg to each foot which represents the mass of a spiked shoe (Hunter et al., 2004b). For CoM calculations, a single segment foot was implemented with the multi-segment foot used for other kinematic calculations only.

4.2.5. Calculation of variables

Descriptive statistics (mean and standard deviation) were calculated for spatio-temporal and kinematic variables found to be of importance in previous bend sprinting research were selected for measurements and evaluation (Alt et al., 2015; Churchill et al., 2015). All variables were calculated separately for the left and right step. Left and right steps were defined by the foot that initiated the step.

Joint (orientation) angles were defined as the distal segment relative to the proximal segment, with the exception of the trunk that was defined relative to the lab coordinate system. The Cardan sequence *zxy* (multi-segment foot angles: *zyx*) was used in line with ISB recommendations (Wu et al., 2002; Wu et al., 2005). Peak joint angles during the stance phase were calculated to enable standardisation of results with previous research (e.g. Alt et al., 2015). Values for the left limb in the transverse and frontal planes were multiplied by minus one for ease of interpretation. *Touchdown and take-off events* were defined using vertical force data where available. The mean plus two standard deviations of the last three seconds of vertical ground reaction force data (where there was zero load on the force plate) were used as a threshold (Bezodis et al.,

2007). For the second step or trials where force data was not recorded, the MTH5 marker was used to determine touchdown and take-off. The mean plus two standard deviations of the vertical coordinates of the left and right MTH5 in the static trial were calculated and used as a threshold for ground contact in each participant. For each foot, touchdown was considered as the first data point where the vertical coordinate of the marker dropped below the defined threshold and vice-versa for take-off (Bezodis et al., 2007). Analysis of the difference in key variables when calculated from data with each of the two methods of touchdown identification has been provided in Appendix A. Coefficient of variation (CV) was <1% for the sample of variables calculated. A CV of < 10 % is thought to represent very good reliability between trials (Atkinson & Nevill, 1998). Therefore, it is appropriate to make use of these different methods since any error present in the identification of touchdown does not propogate into notable differences in the calculation of variables of interest. *Absolute speed* was calculated using the first central difference technique from the horizontal distance travelled in the anterior direction by the CoM. The mean of the instantaneous speeds was calculated from the first frame of ground contact to the last frame of the flight phase with the contralateral foot to give absolute speed over a step (Churchill et al., 2015). *Directional step length* (Figure 4.2.5.1) was calculated relative to the direction of travel. A vector between the horizontal positions of the 2nd metatarsal head at consecutive ground contacts was created. A step progression vector was then created between the horizontal positions of the CoM at consecutive ground contacts and divided by its norm to create a unit vector. The dot product of the two vectors gave directional step length (Churchill et al., 2015). *Step frequency* was calculated as absolute speed divided by directional step length. *Contact time* was the time from touchdown to take-off of

the same leg and *flight time* the total step time (touchdown of one foot to touchdown of the contralateral foot) minus contact time.

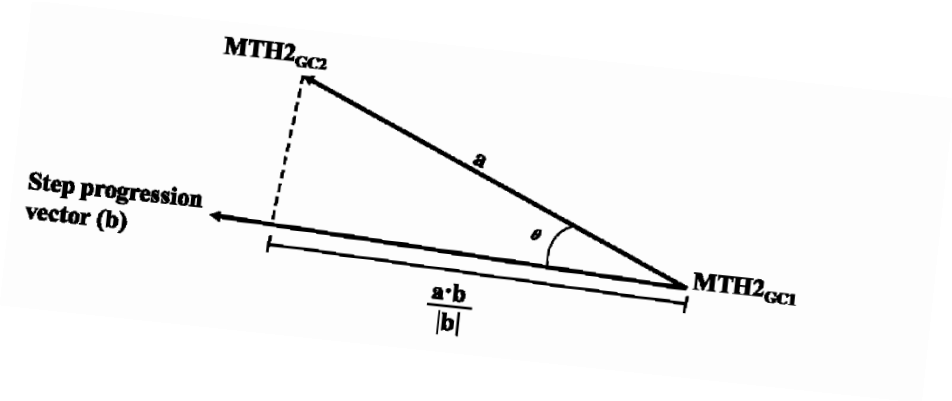

Figure 4.2.5.1 Calculation of directional step length where GC represents ground contact and MTH2 represents the second metatarsal head

Touchdown distance (the horizontal displacement between the CoM and second metatarsal head at touchdown) was calculated using an instantaneous progression vector for the CoM (calculated from the horizontal position of the CoM one frame before the instant of interest to the horizontal position of the CoM one frame after the instant of interest, then divided by its norm to create a unit vector). A horizontal vector from the CoM to the 2nd metatarsal head of the touchdown limb was also calculated. The dot product of the horizontal vector onto the instantaneous progression vector gave touchdown distance (Churchill et al., 2015).

4.2.6. Reliability measures

The reliability of the marker set was established using ICC tests. ICCs for absolute agreement were used to determine the reliability between sessions (ICC 3,*k*). Within-day reliability was determined using ICC (3,1) and calculated for all trials on the first day of testing. ICCs were interpreted according to Cicchetti (1994), where < 0.40 represents *poor* agreement; 0.40 to 0.59 *fair* agreement; 0.60 to 0.75 *good* agreement and > 0.75 *excellent* agreement. In accordance with recommendations from

Koo and Li (2016), 95% confidence intervals (CI) were also presented and Cicchetti (1994) descriptors were applied to the interpretation of CIs. As recommended by Koo and Li (2016) for a variable to be considered as having 'excellent' reliability, both upper and lower bounds must fall within the excellent range (i.e., > 0.75).

Standard error of measurement (SEM) was calculated using the formula (Weir, 2005):

Standard deviation of the mean difference (SD) x $\sqrt{1 - ICC}$ *Equation 1*

Minimal detectable difference (MDD) was calculated using the formula (Weir, 2005):

1.96 x SEM x $\sqrt{2}$ *Equation 2*

4.3. Results

For between-day reliability (ICC 3, *k*), analysis of 95% CI revealed all but two spatio-temporal variables (Table 4.3.1, Table 4.3.2) were fair to excellent (0.419 - 1.000). Right touchdown distance and left step length were poor to excellent (0.180 - 0.980). For all variables, within-day reliability (ICC 3, 1: 0.258 - 1.000) was greater than between-day reliability (ICC 3, *k*: 0.180 - 0.975). Right step frequency displayed a between-day MDD of 0.16 Hz, whereas right and left contact time had a between-day MDD of 0.02 s. Contact time also demonstrated a small between-day SEM (0.006-0.007 s). Within-day SEM and MDD were smaller when compared to between-day values.

For joint kinematics (Table 4.3.3, Table 4.3.4), 29 of 44 variables demonstrated excellent between-day reliability when analysing the 95% CI (0.780 - 0.999). Six

frontal and transverse plane variables (left knee internal rotation, right hip external rotation, right knee abduction, right knee adduction, right knee external rotation, right ankle external rotation) demonstrated poor to excellent reliability (0.075 - 0.985). Within-day reliability (ICC 3, 1: 0.228-0.999) was greater than between-day variability (ICC 3, *k,* 0.075 - 0.999) for most joint kinematic variables. MDD ranged from 1-11° across all variables. Between-day SEM values were < 4° across all conditions, however, within-day SEM and MDD were smaller.

Table 4.3.1 Left step spatio-temporal variables. ICC (3, 1) represents within-day reliability and ICC (3, k) between-day reliability. 95% lower- (LB) and upper bound (UB) confidence intervals are presented. Variables showing less than excellent (<0.75) reliability are highlighted with an asterisk (*). ± indicates the standard deviation of the group means.

Variable	Left		ICC (3, 1)	95% LB	95% UB	SEM	MDD	ICC (3, *k*)	95% LB	95% UB	SEM	MDD
	Day One	***Day Two***										
Absolute speed (m/s)	7.89 ± 0.75	8.01 ± 0.67	0.990	0.964	0.999	0.02	0.04	0.985	0.946	0.989	0.03	0.08
Directional step length (m)	1.94 ± 0.08	2.00 ± 0.08	0.832	0.315*	0.995	0.03	0.08	0.738*	0.184*	0.980	0.04	0.10
Contact time (s)	0.128 ± 0.01	0.127 ± 0.01	0.949	0.748	0.994	<0.01	0.01	0.815	0.419*	0.933	0.007	0.02
Flight time (s)	0.122 ± 0.03	0.126 ± 0.02	0.857	0.456*	0.983	<0.01	0.01	0.796	0.536*	0.911	0.01	0.03
Step frequency (Hz)	4.07 ± 0.32	4.01 ± 0.26	0.981	0.898	1.000	0.03	0.07	0.975	0.834	1.000	0.03	0.08
Touchdown distance (m)	0.40 ± 0.08	0.42 ± 0.08	0.791	0.258*	1.000	0.02	0.06	0.701*	0.436*	0.855	0.02	0.07

Table 4.3.2 Right step spatio-temporal variables. ICC (3, 1) represents within-day reliability and ICC (3, k) between-day reliability. 95% lower- (LB) and upper bound (UB) confidence intervals

Variable	Right		ICC (3,1)	95% LB	95% UB	SEM	MDD	ICC (3, *k*)	95% LB	95% UB	SEM	MDD
	Day One	*Day Two*										
Absolute speed (m/s)	7.87 ± 0.78	8.01 ± 0.67	0.973	0.908	0.997	0.02	0.04	0.984	0.944	0.999	0.03	0.08
Directional step length (m)	1.93 ± 0.11	2.00 ± 0.11	0.939	0.782	0.993	0.03	0.08	0.924	0.768	0.991	0.03	0.09
Contact time (s)	0.108 ± 0.01	0.108 ± 0.01	0.963	0.826	0.996	<0.01	<0.01	0.878	0.734	0.944	0.006	0.02
Flight time (s)	0.119 ± 0.03	0.113 ± 0.05	0.935	0.693	0.995	0.003	0.01	0.761	0.420*	0.897	0.006	0.02
Step frequency (Hz)	4.09 ± 0.33	4.02 ± 0.27	0.949	0.818	0.994	0.06	0.16	0.958	0.869	0.995	0.06	0.16
Touchdown distance (m)	0.34 ± 0.07	0.38 ± 0.07	0.982	0.867	0.997	<0.01	<0.01	0.684*	0.180*	0.874	0.03	0.08

are presented. Variables showing less than excellent (<0.75) reliability are highlighted with an asterisk (*). ± indicates the standard deviation of the group means.

Table 4.3.3 Left step joint kinematics. ICC (3, 1) represents within-day reliability and ICC (3, k) between-day reliability. 95% lower- (LB) and upper bound (UB) confidence intervals are presented. Variables showing less than excellent (<0.75) reliability are highlighted with an asterisk (*). ± indicates the standard deviation of the group means.

Peak joint angle during stance (°)	Left		ICC	95%	95%	SEM	MDD	ICC	95%	95%	SEM	MDD
	Day One	***Day Two***	(3, 1)	LB	UB			(3, *k*)	LB	UB		
Hip Flexion	42 ± 8	38 ± 16	0.926	0.763	0.988	1.92	5	0.930	0.782	0.992	2.55	7
Hip Extension	-15 ± 5	-14 ± 11	0.975	0.922	0.996	0.84	2	0.917	0.738	0.990	2.36	7
Hip Abduction	-5 ± 3	-5 ± 4	0.946	0.825	0.991	0.69	2	0.941	0.714	0.999	0.87	2
Hip Adduction	9 ± 4	8 ± 5	0.988	0.960	0.998	0.24	1	0.956	0.845	0.997	0.58	2
Hip Internal Rotation	-2 ± 9	-2 ± 8	0.992	0.973	0.999	0.26	1	0.989	0.965	0.999	0.42	1
Hip External Rotation	-16 ± 8	-14 ± 7	0.963	0.861	0.996	0.55	2	0.967	0.897	0.996	0.72	2
Knee Flexion	-40 ± 5	-42 ± 9	0.952	0.803	0.997	0.81	2	0.967	0.882	0.998	0.87	2
Knee Extension	-18 ± 7	-18 ± 7	0.975	0.911	0.997	0.70	1	0.978	0.932	0.997	0.54	1
Knee Abduction	-3 ± 3	-2 ± 4	0.969	0.890	0.996	0.57	2	0.936	0.780	0.995	1.33	4
Knee Adduction	4 ± 4	3 ± 3	0.942	0.815	0.991	0.38	1	0.937	0.808	0.992	0.40	1
Knee Internal Rotation	7 ± 7	8 ± 10	0.947	0.814	0.994	1.18	3	0.782	0.190*	0.985	2.39	7
Knee External Rotation	-13 ± 9	-9 ± 10	0.956	0.862	0.993	1.55	4	0.933	0.794	0.992	2.05	6
Ankle Dorsiflexion	107 ± 6	108 ± 9	0.962	0.865	0.996	0.96	3	0.934	0.795	0.992	2.37	7
Ankle Plantar flexion	63 ± 12	58 ± 10	0.960	0.850	0.995	1.94	5	0.932	0.786	0.992	3.87	11
Ankle Eversion	-10 ± 13	-12 ± 13	0.994	0.979	0.999	0.32	1	0.971	0.909	0.996	1.06	3
Ankle Inversion	5 ± 14	6 ± 11	0.992	0.972	0.999	0.49	1	0.970	0.907	0.996	1.85	5
Ankle Internal Rotation	24 ± 6	22 ± 6	0.949	0.819	0.994	0.66	2	0.852	0.549*	0.982	2.31	6
Ankle External Rotation	3 ± 5	4 ± 3	0.976	0.910	0.997	0.69	2	0.871	0.590	0.985	1.76	5
Midfoot Inversion	0 ± 4	0 ± 3	0.962	0.860	0.996	0.53	1	0.872	0.595*	0.985	1.64	5
Midfoot Eversion	7 ± 5	7 ± 1	0.985	0.948	0.998	0.34	1	0.877	0.603*	0.986	1.88	5
MTP Dorsiflexion	36 ± 8	38 ± 6	0.995	0.980	0.999	0.38	1	0.914	0.729*	0.990	2.21	6
MTP Plantar flexion	13 ± 5	13 ± 6	0.906	0.648*	0.989	0.97	3	0.840	0.504*	0.981	2.20	6

Table 4.3.4 Right step joint kinematics. ICC (3, 1) represents within-day reliability and ICC (3, k) between-day reliability. 95% lower- (LB) and upper bound (UB) confidence intervals are presented. Variables showing less than excellent (<0.75) reliability are highlighted with an asterisk (*). ± indicates the standard deviation of the group means.

Peak joint angle during stance (°)	Right		ICC	95%	95%	SEM	MDD	ICC	95%	95%	SEM	MDD
	Day One	*Day Two*	(3,1)	LB	UB			(3, *k*)	LB	UB		
Hip Flexion	39 ± 10	43 ± 11	0.909	0.714	0.985	1.81	5	0.883	0.580	0.992	3.15	9
Hip Extension	-15 ± 8	-14 ± 15	0.989	0.962	0.999	0.40	1	0.961	0.861	0.997	1.70	5
Hip Abduction	-7 ± 4	-6 ± 4	0.963	0.871	0.996	0.46	1	0.966	0.896	0.996	0.46	1
Hip Adduction	4 ± 6	6 ± 5	0.985	0.945	0.998	0.40	1	0.976	0.927	0.997	0.41	1
Hip Internal Rotation	3 ± 5	4 ± 8	0.923	0.733*	0.991	1.36	4	0.907	0.705*	0.989	1.46	4
Hip External Rotation	-9 ± 2	-9 ± 5	0.761	0.228*	0.962	2.41	7	0.752	0.200*	0.971	2.24	6
Knee Flexion	-44 ± 5	-42 ± 7	0.860	0.461*	0.984	2.21	5	0.831	0.479*	0.980	1.90	5
Knee Extension	-18 ± 7	-16 ± 8	0.951	0.822	0.994	0.70	1	0.972	0.913	0.997	0.42	1
Knee Abduction	-3 ± 2	- 4 ± 3	0.891	0.613*	0.987	0.88	2	0.778	0.308*	0.959	0.55	2
Knee Adduction	2 ± 1	3 ±4	0.855	0.320*	0.978	0.87	2	0.809	0.493*	0.990	1.23	3
Knee Internal Rotation	1 ± 8	-2 ± 9	0.961	0.862	0.995	1.01	3	0.973	0.886	0.999	1.09	3
Knee External Rotation	-14 ± 4	-13 ± 9	0.807	0.327*	0.997	1.64	5	0.739*	0.075*	0.982	3.67	10
Ankle Dorsiflexion	98 ± 6	97 ± 8	0.954	0.854	0.993	1.25	3	0.940	0.814	0.993	1.10	3
Ankle Plantar flexion	52 ± 13	51 ± 13	0.944	0.804	0.993	1.52	4	0.961	0.864	0.997	1.37	4
Ankle Eversion	-4 ± 8	-4 ± 7	0.988	0.956	0.999	0.60	2	0.897	0.705*	0.983	2.68	6
Ankle Inversion	12 ± 4	12 ± 9	0.961	0.874	0.994	1.38	4	0.816	0.294	0.987	3.33	9
Ankle Internal Rotation	-7 ± 4	- 6 ± 6	0.948	0.815	0.994	1.06	3	0.922	0.734	0.994	1.25	3
Ankle External Rotation	-17 ± 3	- 16 ± 2	0.929	0.708	0.995	0.75	2	0.793	0.353*	0.976	1.34	4
Midfoot Inversion	-9 ± 5	-6 ± 4	0.937	0.799	0.990	0.92	3	0.827	0.510*	0.978	2.84	8
Midfoot Eversion	-3 ± 4	0 ± 3	0.960	0.887	0.996	0.77	2	0.880	0.639*	0.986	1.66	5
MTP Dorsiflexion	36 ± 6	36 ± 5	0.918	0.703	0.990	1.18	3	0.914	0.785	0.994	1.91	5
MTP Plantar flexion	12 ± 5	10 ± 4	0.945	0.804	0.994	1.53	4	0.908	0.839	0.989	1.77	5

4.4. Discussion

The aim of this study was to determine the between- and within-day reliability of a lower limb and trunk marker set during maximal velocity bend sprinting. All athletes were experienced bend sprinters and mean absolute speed was similar between days. All variables (both spatio-temporal and kinematic) demonstrated excellent within-day reliability. Data from this study demonstrated consistently poorer between-day reliability than within-day reliability. When compared to between-day reliability, greater within-day reliability has been a common finding throughout previous reliability investigations involving running (e.g., Alenezi et al., 2016; Ferber et al., 2002). It is not possible to quantify the error arising from soft tissue artefact and marker misplacement within the current body of work. However, Leardini, Chiari, Croce, and Cappozzo (2005) concluded from a review of literature that soft tissue artefact is most prominent at the thigh compared with other lower limb segments, with Akbarshahi et al. (2010) reporting mean artefact of 9.7 mm in the mediolateral direction with skin-mounted thigh markers during treadmill walking in typical male adults. However, artefact during sprinting, which occurs at a higher velocity than walking, is likely to be higher. The increase in artefact at higher speeds is likely offset somewhat by the population of athletes used within the current programmes of research. Large differences in soft tissue artefact between participants are typical (Leardini et al., 2005), and so the contribution of error associated with soft tissue artefact and marker placement to the present study is likely reduced due to the lean body composition and consequently lower adipose tissue of the athletes involved and the marker set being applied by the same experienced researcher for all participants. In addition, given that the 3D residual for the optoelectronic camera system was calibrated to ≤0.4 mm for

each instance of testing, the majority of within day variability can likely be attributed to human movement variability in task execution as opposed to measurement error.

Between-day reliability for kinematic variables during walking and running has been reported with ICCs (without 95% CI's) in the range of 0.51 - 0.72 (Alenezi et al., 2016); 0.54 - 0.93 (Ferber et al., 2002) and 0.644 - 0.993 (Milner & Brindle, 2016). In comparison to between-day reliability, within-day reliability for kinematic variables is typically greater: 0.63 - 0.94 (Alenezi et al., 2016); 0.92 - 0.99 (Ferber et al., 2002) and 0.881 - 0.994 (Milner & Brindle, 2016). Therefore, the between- (0.739 - 0.989) and within-day (0.761 - 0.995) reliability demonstrated for joint kinematics within the present study are comparable to previous research in walking and running. Greater within-day reliability suggests that, where possible, data for each individual athlete should be collected during a single session. Should this not be appropriate, the between-day MDDs provide an indication of the margin for error that should be applied when interpreting results.

SEM and MDD provide an indication of the magnitude of change required in experimental studies to be confident that a real change has occurred. The present findings demonstrated an MDD of 2° (left step) and 1° (right step) for peak hip adduction angles comparing favourably to the MDD of 6.90° during running and 8.37° in cutting reported previously (Alenezi et al., 2016). It is likely these differences can be attributed to the inclusion of recreational athletes by Alenezi et al. (2016) in comparison to the present study where athletes were trained and experienced in the execution of a specific task. Moreover, the cutting task used by Alenezi et al. (2016) may also contribute to these differences since it may be difficult for non-expert participants to replicate the movement consistently. In addition, Alenezi et al. (2016)

found knee internal rotation angle during the cutting manoeuvre (which due to its lateral change of direction may share some similarities with bend sprinting) demonstrated the lowest between-day ICC (0.40) with an MDD of 11.3°. This is similar to the current findings, where one of the lowest between-day ICC was left knee internal rotation angle (0.782) with an MDD of 7°. Whilst this is larger than the 5° difference in left knee internal rotation angle reported by Alt et al. (2015), the reliability can be increased by collecting data on the same day. Doing so would decrease the required MDD from 7° to 3°, thus making the protocol sensitive to smaller changes such as those reported by Alt et al. (2015).

Touchdown distance and left step length in this study failed to achieve excellent between-day reliability, supporting previous findings that touchdown distance was one of the least reliable variables examined during straight-line sprinting (Hunter et al., 2004a). In addition, Standing and Maulder (2017) reported between-day ICCs of 0.65 and 0.44 for step length during the first and third steps of the acceleration phase. However, Hunter et al. (2004a) showed that reliability increased for all variables when averaging across three trials, suggesting a single trial is insufficient to capture the natural variance within an athlete's technique. Therefore, as also demonstrated by the results of average measures ICC (3, *k*) here, future research should, where possible, use an average of multiple trials to improve the reliability of variables such as step length and touchdown distance. Step length results of the present study demonstrate excellent within-day reliability for both steps, however high standard deviations were reported, suggesting step length is variable both between participants (SD: 0.08 - 0.11 m) and between-days (ICC 3, *k*: 0.184 - 0.991). These variations in step length might contribute towards the different results found between

previous bend sprinting studies. For example, Churchill et al. (2015) and Churchill et al. (2016) suggested a reduction in right step length is present on the bend, while Alt et al. (2015) found neither left nor right step length was affected during bend sprinting. However, this may have been a result of the different protocols used, since Alt et al. (2015) measured sub-maximal velocity compared to Churchill et al. (2015) and Churchill et al. (2016) who evaluated maximal velocity. The present study results provide increased clarity for future research on what constitutes a real change in step length. The ICCs for the remaining spatio-temporal variables represented excellent agreement for both between- and within-day reliability, with small (e.g. contact time 0.006 - 0.007 s) SEM reported throughout. Notwithstanding the poor and fair 95% CI reported for some ICCs, the resulting MDD is low enough to detect changes in spatio-temporal variables between conditions. For example, a 0.08 m MDD has been established for right step length. Churchill et al. (2015) reported a decrease of 0.10 m in the right step length on the bend compared to the straight at maximal speed. In further research also at maximal speed, Ishimura and Sakurai (2016) reported a difference of 0.14 m between right and left step length on the bend. Therefore, the marker set is reliable for future use with spatio-temporal variables.

Reliability of sagittal plane variables was generally greater than variables calculated in the frontal and transverse planes, replicating common findings of reliability analyses. For example, a review of reliability in kinematic measures of walking gait demonstrated the lowest reliability, and the highest error occurred most frequently in the transverse plane (McGinley, Baker, Wolfe, & Morris, 2009). In addition, the values reported here are consistent with previous reliability investigations of multi-segment foot models during walking (Bishop et al., 2013; Deschamps et al.,

2012) and running (Milner & Brindle, 2016). Joints at the foot generally exhibit smaller ranges of motion than other segments. Therefore, determining true differences from error can be more of an issue at segments of the foot. However, comparison of the MDDs with previous bend sprinting literature suggests the protocol is sensitive enough to detect the magnitude of change previously reported. For example, Alt et al. (2015) and Churchill et al. (2015) have reported an increase in left hip adduction on the bend compared with the straight of 6° and 7° respectively. The present study established an MDD of 1° and 2° for within- and between-day protocols. In addition, although right ankle external rotation demonstrated poor to excellent between-day reliability, the associated MDD is 4°, which is smaller than the 5° difference between left and right foot on the bend reported by Alt et al. (2015). In addition, right ankle external rotation MDD can be decreased further to 2° by collecting data on the same day. Therefore, the marker set can reliably be used in future research.

A radius replicating lane one (36.5 m) was used in this study. Whilst this may be most useful from a research perspective since technical adaptations have been shown to be more prominent in lanes with a smaller radius (Churchill et al., 2018), athletes tend to avoid training in this lane, which may have contributed towards variance between days.

4.5. Conclusion

The reliability of an LLT marker set with a multi-segment foot has been established for bend sprinting. Overall, between-day ICCs were fair to excellent for all variables and comparable to those previously reported during straight-line walking and running gait. Within-day reliability was greater than between-day reliability, suggesting that, where possible, data collection for a single athlete should take place

on the same day. The between-day data presented considers variance in athlete technique alongside the reliability of the equipment set-up, calibration, random error and marker placement. As such, this will inform protocol design and the determination of meaningful differences between conditions in future kinematic studies of bend sprinting. The LLT marker set is a reliable model to use in future analyses of bend sprinting. However, results should be interpreted with the reported MDD's in mind.

Chapter Five: THE EFFECT OF THE BEND ON TECHNIQUE AND PERFORMANCE IN THE ACCELERATION PHASE OF SPRINTING

THE WORK FROM THIS CHAPTER FORMED THE BASIS OF THE FOLLOWING PEER-REVIEWED JOURNAL ARTICLE:

Judson, L. J., Churchill, S. M., Barnes, A., Stone, J. A., Brookes, I. & Wheat, J. (2019). Kinematic modifications of the lower limb during the acceleration phase of bend sprinting. *Journal of Sports Science.* doi: 10.1080/02640414.2019.1699006

5. The effect of the bend on technique and performance in the acceleration phase of sprinting

5.1. Introduction

In track and field sprint events longer than 100 m, more than half the total distance is run on a curved portion of track (Meinel, 2008). Research demonstrates a decrease in maximum velocity when sprinting on the bend in an anti-clockwise direction (which is the standard direction of travel in athletics competition) compared with the straight which has been attributed to kinetic, kinematic and spatio-temporal adaptations (Churchill et al., 2015; Churchill et al., 2016). However, the current understanding of biomechanical adaptations during anti-clockwise bend sprinting in the acceleration phase is limited. Identification of these affected parameters could aid overall race performance through the development of targeted training programmes and increased specificity of athlete preparation.

During bend sprinting at maximal speed, mean body lateral lean angles of 10° and 15° at touchdown have been reported in the left and right step, respectively (Churchill et al., 2015). This lateral lean is necessary to counteract the moment produced by the mediolateral force required to change direction. The configuration of the lower limb is therefore dictated by the lateral lean and constrained by the need to complete an anti-clockwise left hand turn. Therefore, several kinematic changes of the lower limb exist during bend sprinting, which occur predominantly in the frontal and transverse planes (Alt et al., 2015; Churchill et al., 2015) and are thought to be a consequence of lateral lean (Churchill et al., 2015). More specifically, the left limb is characterised by a mean increase in peak hip adduction of approximately 6° during bend sprinting at 40 m compared with the straight (Alt et al., 2015; Churchill, 2015). Furthermore, a high left peak ankle eversion angle (e.g. 13° Alt et al., 2015; > 35° Luo

and Stefanyshyn, 2012a) has been reported, but in protocols that are not representative of a competitive elite environment, for example, at sub-maximal speed (Alt et al., 2015) and with a smaller radius (2.5 m, Luo & Stefanyshyn, 2012a). It has previously been suggested that excessive hip adduction and ankle eversion are associated with injury, particularly at the knee (Hreljac, 2004; Li et al., 2015). Hence, understanding the kinematics of bend sprinting technique may provide insight into possible injury mechanisms. Therefore, further investigation with a protocol more closely replicating race conditions is warranted.

In the right limb, a mean 4° increase in internal knee rotation on the bend compared with the straight is thought to contribute to a rotational strategy which serves to control horizontal plane motion (Alt et al., 2015). This finding did not reach the alpha level $p < 0.05$, but due to the small sample size ($n = 6$) was reported as a tendency ($p < 0.1$, Alt et al., 2015), suggesting this should be interpreted cautiously until further evidence is available. However, bend sprinting did result in a 3° increase in peak right ankle external rotation compared with the straight (Alt et al., 2015). Despite Alt et al. (2015) providing some initial findings using a controlled sub-maximal velocity, gaining further evidence during representative performance conditions (such as during acceleration) would enhance the current evidence base.

Spatio-temporal parameters such as contact time, step frequency and step length are fundamental components of sprint performance, with these parameters being affected during bend sprinting. For example, Alt et al. (2015) found an increase in left contact time on the bend compared with the straight at sub-maximal speed. This increase in contact time is consistent with others at maximal speed (Churchill et al., 2015; Churchill et al., 2016; Ishimura & Sakurai, 2010; Ishimura et al., 2013). However, the evidence base regarding spatio-temporal variables is sometimes

contradictory. For example, a reduction in right step length on the bend compared with the straight at maximal speed has been reported by several authors (Churchill et al., 2015; Churchill et al., 2016; Ishimura et al., 2013). This reduction was considered responsible for a loss of velocity on the bend compared with the straight (Churchill et al., 2015), highlighting the importance of spatio-temporal variables and their relationship with performance. However, step length was unaffected during sub-maximal bend sprinting (Alt et al., 2015). Moreover, the majority of available research has focussed on maximal and sub-maximal speed bend sprinting (Alt et al., 2015; Churchill et al., 2015; Churchill et al., 2016; Ishimura et al., 2013). The limited research available in the acceleration phase of sprinting at maximal effort showed both left and right step lengths were reduced on the bend compared with the straight (Stoner & Ben-Sira, 1979). Therefore, further research is required regarding the effect of the bend during the acceleration phase on spatio-temporal aspects of technique and performance.

Alt et al. (2015) suggested some adaptations may be velocity dependent. Thus, during the acceleration phase, where athletes have not yet reached maximum velocity, the kinematic demands of bend sprinting may be different from the maximum speed phase. It is possible that adaptations such as increased hip adduction and ankle eversion are less prominent during acceleration. Moreover, the maximum velocity a sprinter is able to attain is dependent on the sprinters' ability to accelerate. Consequently, any adaptations present in the acceleration phase of bend sprinting may impact upon overall race performance. However, the acceleration phase (0 - 40 m) has received little attention within the bend sprinting literature. Therefore, the aim of the present study was to investigate the effect of bend sprinting on the kinematic and spatio-temporal parameters of the lower limb during the acceleration phase. It was

hypothesised bend sprinting would result in greater adaptations in the frontal and transverse planes than on the straight.

5.2. Methods

5.2.1. Participants

Ethical approval was provided by the Sheffield Hallam Research Ethics Committee. Nine male sprinters (mean age 22 ± 4 years; body mass 71.48 ± 9.47 kg; stature 1.81 ± 0.06 m) with experience of bend sprinting (200 and /or 400 m) volunteered to participate in this study. The sample size was largely determined by convenience sampling. However, the number is within the range used in the previous bend sprinting literature (Alt et al., 2015; Churchill et al., 2015; Churchill et al., 2016). To standardise ability with previous research (22.60 ± 0.33 s, Alt et al., 2015; 22.15 ± 0.93 s, Churchill et al., 2015), the inclusion criteria required a 200 m personal best of 23.5 s or faster (mean 22.70 ± 0.49 s, range 21.8 - 23.43 s). All athletes were active in training and injury free at the time of data collection. The study procedures were fully explained to participants who subsequently provided written informed consent.

5.2.2. Experimental set-up

The experimental set-up is demonstrated in Figure 5.2.1.1. Kinematic data were collected using a 15-camera optoelectronic motion capture system (13 x Raptor model and 2 x Eagle model, Motion Analysis Corporation, Santa Rosa, CA, USA) sampling at 200 Hz. A right-handed lab coordinate system was defined using a rigid L-frame with four markers at known locations. Athletes ran primarily in the direction of the positive *x*-axis (anterior-posterior), where the positive *y*-axis was directed vertically upwards (longitudinal) and the positive *z*-axis (mediolateral) was pointing to the athletes' right. A three-marker wand (length 500 mm) was used within the

calibration volume to scale the individual camera intrinsic and extrinsic parameters. The calibration volume (7 m long, 3 m wide and 1.5 m high) was located tangentially to the apex of the curve to record data through the 10 - 17 m section of the 30 m sprints. Data were collected specifically at this distance as Morin et al. (2015) identified the production of horizontal impulse in the first twenty metres of a sprint as a major determinant of sprint acceleration performance. Furthermore, Stoner and Ben-Sira (1979) measured sprints on the bend vs. straight at 12 m, and data collection at this point provides standardisation allowing comparisons with previous research.

For the identification of gait events, a force plate (Kistler, Model 9287BA, 900 x 600 mm) was embedded into the track surface at approximately 12 m. A modified Vicon Plug-in Gait (PiG) marker set (lower limb and trunk; 4.2.2) was used to model the torso, pelvis, thighs, shanks and feet segments (toebox, forefoot, rearfoot). For full details of marker location, please see Section 4.2.2. The marker set was applied by the same researcher for all participants to reduce variability in marker placement.

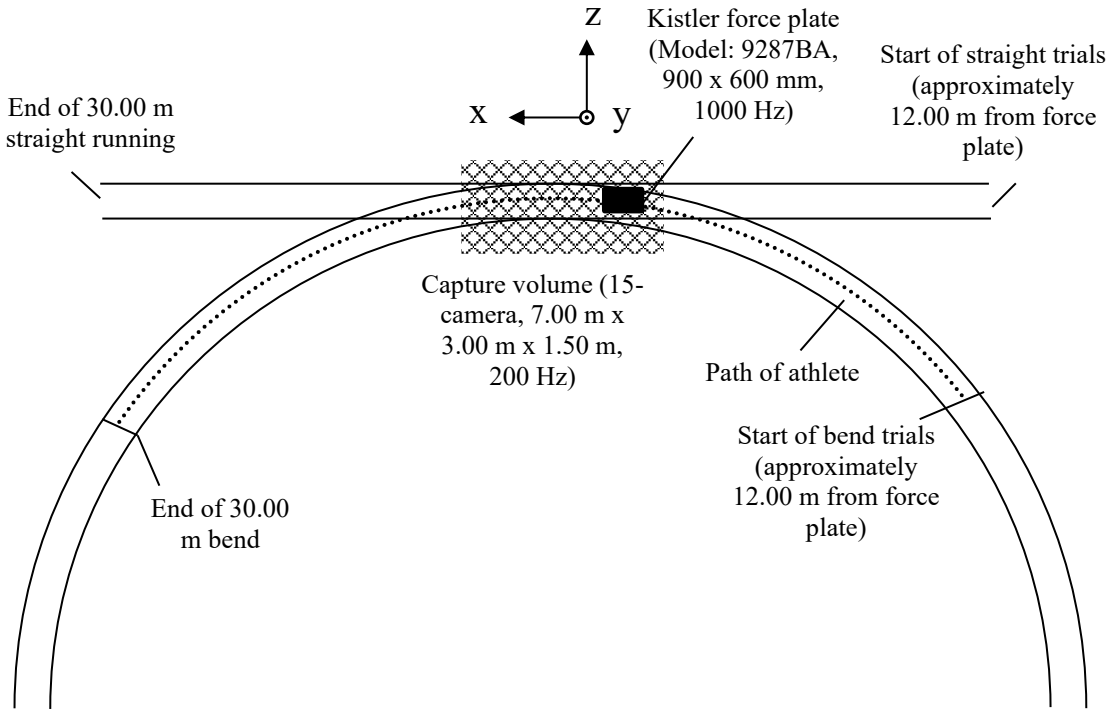

Figure 5.2.1.1 Plan view of experimental set-up (not to scale).

5.2.3. Protocol

Data collection took place on a standard flat indoor track surface. A bend replicating lane 1 (radius 36.5 m) of a standard 400 m running track (IAAF, 2008) was reconstructed, and a 30 m section of straight track was used for straight trials. For bend trials, cones were placed at 1 m intervals to aid with guiding the athlete during the drive phase. A lane width of 1.22 m was used. The order of bend and straight trials was randomised to minimise order effects. Participants completed a typical warm-up followed by up to six maximal effort trials for 30 m from starting blocks in both bend and straight conditions. Athletes were instructed to accelerate maximally for the full 30 m, and '*on your marks, set, go*' signal was used. To avoid the onset of fatigue, approximately eight minutes rest were allowed between trials (Churchill et al., 2015). Participants wore their own sprint spikes for the testing session and were topless with form fitting shorts allowing the majority of markers to be placed directly on to the skin.

5.2.4. Data processing

Raw 3D marker coordinate data was tracked using Cortex software (version 5.3, Motion Analysis Corporation, Santa Rosa, CA, USA). Automatic gap filling (cubic spline) was performed; all gaps were <10 frames. Raw marker positions were filtered at 18 Hz using a low-pass, fourth-order recursive Butterworth filter. The cut-off frequency was determined with the use of residual analysis. Segments, LCS and joint centres were defined using Visual 3D software (version 6, C-Motion, Rockville, MD, USA). de Leva (1996) was used to estimate body segment parameters. In line with Hunter et al. (2004b), these values are typically adjusted by 0.2 kg to represent the typical mass of a sprint spike. However, owing to advances in technology which aim to reduce the weight of the shoe, it is possible the value of 0.2 kg is outdated. Therefore, the manufacturer and model of the shoe were recorded, allowing the values to be individually adjusted by 0.150 to 0.189 kg (representing the mass of individual participants' spiked shoe according to manufacturer guidelines) and increasing the accuracy of the estimations.

Vertical force data and methods described by Bezodis et al. (2007) were used to identify touchdown and take-off events, with the mean plus two standard deviations of the last three seconds of vertical ground reaction force data (where there was zero load on the force plate) were used as a threshold. All variables were measured individually for the left and right step. For touchdown of the second foot contact or trials where force data was not available, methods described by Bezodis et al. (2007) were used where the mean plus two standard deviations of MTH5 vertical coordinates in the static trial were used as a threshold to detect touchdown and take-off. Spatio-temporal variables (absolute speed, contact time, directional step length, turn of CoM,

touchdown distance, step frequency and flight time) were calculated following the methods of Churchill et al. (2015), described in full in Section 4.2.5.

For the calculation of race velocity in bend trials, a four-quadrant inverse tangent was used to calculate the angle between CoM position at each time point. The difference between these angles at consecutive time points was used to calculate race displacement:

race displacement = $\theta_d r$ *Equation 3*

where θ_d represents the difference in angle and r is the radius of the race line (36.7 m). First central difference technique was then used to calculate the instantaneous velocity of the CoM relative to the race line. Race step length was calculated using a similar method, where the angle between the MTP at two consecutive ground contacts was calculated (θ), then used to calculate race step length with the following equation, where r is the radius of the race line (36.7 m):

race step length = θr *Equation 4*

Joint orientation angles during the stance phase were defined as the distal segment relative to the proximal segment. Joint angles were calculated using the cardan sequence *zxy* (multi-segment foot angles: *zyx*) and cropped to the stance phase. To enable standardisation with previous bend sprinting research (e.g. Alt et al., 2015), peak angle during stance was then calculated and averaged across three trials for each participant. Furthermore, bend sprinting research has reported peak ankle eversion angles close to that considered to cause injury if reached repeatedly (Alt et al., 2015; Clarke et al., 1984). Therefore, the analysis of peak angles could assist in developing injury prevention strategies by identifying which joints are at risk and how. For ease of interpretation, values of the left limb were multiplied by minus one. Body lateral lean was calculated using 3D orientation angles, based on methods outlined by

(Yeadon, 1990). First, a CoM progression vector was calculated using the first central difference technique at the frame before and after the instant of interest. This was then divided by its norm to create a unit vector, *i* representing forward progression. Unit vector *j*, representing vertical progression, was defined as [0 1 0]. The cross product of these two unit vectors was then divided by its norm to give unit vector *k* (mediolateral progression):

$$k = \frac{i \times j}{\| i \times j \|} \qquad \textit{Equation 5}$$

A unit vector matrix for the progression coordinate system was then constructed:

$$[\text{PROG}] = \begin{bmatrix} i_x & i_y & i_z \\ j_x & j_y & j_z \\ k_x & k_y & k_z \end{bmatrix} \rightarrow \qquad \textit{Equation 6}$$

A body coordinate system was then created using the *i* unit vector from the CoM progression matrix. A temporary second unit vector (*j*), was created from the second metatarsal head (MTH2) and CoM location, and divided by its norm. Vector *k* was then created using the cross product of *i* and *j*:

$$k = i \times j \qquad \textit{Equation 7}$$

j was then recalculated using the cross product of *k* and *i*:

$$j = k \times i \qquad \textit{Equation 8}$$

A unit vector matrix for the body coordinate system was then created:

$$[\text{BODY}] = \begin{bmatrix} i_x & i_y & i_z \\ j_x & j_y & j_z \\ k_x & k_y & k_z \end{bmatrix} \rightarrow \qquad \textit{Equation 9}$$

The RTM was the dot product of the two matrices:

$$[\text{RTM}] = [\text{BODY}][\text{PROG}]' \qquad \textit{Equation 10}$$

For each rotation, a direction cosine matrix can be defined:

$$[R_z] = \begin{bmatrix} 1 & 0 & 0 \\ 0 & \cos\alpha & \sin\alpha \\ 0 & -\sin\alpha & \cos\alpha \end{bmatrix}$$ *Equation 11*

$$[R_x] = \begin{bmatrix} \cos\beta & 0 & -\sin\beta \\ 0 & 1 & 0 \\ \sin\beta & 0 & \cos\beta \end{bmatrix}$$ *Equation 12*

$$[R_y] = \begin{bmatrix} \cos\gamma & \sin\gamma & 0 \\ -\sin\gamma & \cos\gamma & 0 \\ 0 & 0 & 1 \end{bmatrix}$$ *Equation 13*

The direction cosine matrix, [R], is the product of $[R_y]$, $[R_x]$ and $[R_z]$:

[R]=

$$\begin{bmatrix} \cos\beta\cos\gamma - \sin\alpha\sin\beta\sin\gamma & \cos\beta\sin\gamma + \cos\gamma\sin\alpha\sin\beta & -\cos\alpha\sin\beta \\ -\cos\alpha\sin\gamma & \cos\alpha\cos\gamma & \sin\alpha \\ \sin\beta\cos\gamma + \sin\alpha\cos\beta\sin\gamma & \sin\gamma\sin\beta - \cos\beta\cos\gamma\sin\alpha & \cos\alpha\cos\beta \end{bmatrix}$$

Equation 14

It was then possible to solve for α, representing body lateral lean:

$\alpha = \sin^{-1}(R_{23}) = \sin^{-1}(RTM_{23})$ *Equation 15*

MDD indicates the magnitude of change required to be considered 'real'. Where the difference between conditions exceeds the MDD, it can be considered a change due to the experimental condition and not natural athlete variance or protocol error. Therefore, peak angles and spatio-temporal variables were interpreted with reference to the MDD, identified in Chapter 4. Variables failing to meet the MDD were not interpreted further.

5.2.5. Statistical analysis

Descriptive statistics (mean, standard deviation and percent difference) were calculated for all variables. A group design approach was taken throughout the thesis. The Shapiro-Wilk normality test ($p > 0.05$) was used to confirm the normal distribution

of data. Differences between the bend and straight conditions for the left and right limb were assessed using a two-way repeated measures Analysis of Variance (ANOVA, condition: bend vs. straight, limb: left vs. right) for each dependent variable. Due to a small sample size, the study may be statistically underpowered, and so the chance of detecting a true effect is reduced. Unlike significance tests, effect size places emphasis on the size of the difference (Coe, 2002). Therefore, results were also interpreted using effect size. Cohen's *d* provides an estimate of effect with a population and so can be biased for small samples ($n < 20$), resulting in an overestimation of the true population effect (Lakens, 2013), since variations have a larger influence on smaller samples (Schweizer & Furley, 2016). Therefore, Hedges' *g* was used, which includes a correction for smaller sample sizes, calculated using the following equation (Durlak, 2009):

$$g = \frac{M_1 - M_2}{sd} \times \left(\frac{n-3}{n-2.25}\right) \times \sqrt{\frac{n-2}{n}} \qquad \textit{Equation 16}$$

where M_1 - M_2 is the difference between the group means (*M*), *sd* is the pooled standard deviation and *n* is the total sample size. Cohen (1988) guidelines were used for the interpretation of effect size, where $g < 0.20$ represents a trivial difference, $0.20 \geq 0.50$ indicating a small difference, $0.50 \geq 0.80$ a moderate difference and ≥ 0.80 a large difference between means.

5.3. Results

5.3.1. Spatio-temporal variables

There was a 2% reduction in absolute speed on the bend compared with the straight for the left step ($g = 0.53$, Table 5.4.1.1). During bend sprinting, absolute speed was faster for the right step compared with the left step ($g = 0.64$). However, there was no significant main effect for condition, $F_{(1, 8)} = 0.574$, $p = 0.47$ or limb, $F_{(1, 8)} = 2.994$,

p = 0.122. For race velocity, which takes into consideration the progression of the athlete with respect to the actual race distance, there was no main effect for condition ($F_{(1, 8)}$ = 2.673, p = 0.141, Table 5.4.1.1). However, there was a significant condition x limb interaction ($F_{(1, 8)}$ = 19.467, p = 0.002, Table 5.4.1.1) due to shorter race step lengths on the bend compared with the straight.

For step frequency, there was a significant condition x limb interaction, $F_{(1, 8)}$ = 12.144, p = 0.008, due to the left step on the bend being lower compared with the left step on the straight (g = 0.66) and the right step on the bend (g = 0.61). There was also a condition x limb interaction for touchdown distance, $F_{(1,8)}$ = 5.477, p = 0.04, where left step touchdown distance was longer on the bend (0.30 ± 0.05 m) compared with the straight (0.25 ± 0.05 m). For contact time, there was a significant main effect for condition, $F_{(1, 8)}$ = 6.111, p = 0.039 (g = 1.50 left step; 0.27 right step), with contact being longer on the bend compared with the straight. A significant condition x limb interaction was also reported, $F_{(1, 8)}$ = 7.801, p = 0.023 showing the increase in contact time on the bend was greater in the left step compared with the right step (g = 0.57).

5.3.2. Joint kinematics

For joint kinematics, there was a condition x limb interaction for peak hip adduction angle, $F_{(1, 8)}$ = 12.093, p = 0.008. Peak left step hip adduction was greater on the bend (8°) compared with the left step on the straight (4°) and the right step on the bend (6°, Table 5.3.2.2). In addition, the condition x limb interaction for peak hip external rotation was non-significant, $F_{(1, 8)}$ = 3.859, p = 0.085. However, a large effect size was observed, suggesting higher peak left hip external rotation (g = 0.89) on the bend compared with the straight. There was a condition x limb interaction for peak hip abduction joint angle ($F_{(1, 8)}$ = 6.075, p = 0.039), with the right limb being more abducted on the bend compared with the straight. There was a condition x limb

interaction for body lateral lean at touchdown, $F_{(1, 8)} = 26.697$, $p = 0.001$ which was greater in both the left and right step on the bend (left step -5°; right step -12°) compared with the straight (left step 6°; right step -5°). No significant interactions were reported for any variables at the knee.

Left step peak ankle internal rotation was greater on the bend compared with the straight and the right step on the bend resulting in a condition x limb interaction ($F_{(1, 8)} = 17.091$, $p = 0.003$). Although no main effect was reported for peak ankle eversion ($F_{(1, 8)} = 1.247$, $p = 0.297$), left step peak ankle eversion was 55% greater on the bend compared with the straight ($g = 0.88$). At the midfoot, there was a significant condition x limb interaction ($F = 11.768$, $p = 0.009$) for peak midfoot eversion. Peak midfoot eversion increased in the left step on the bend compared with the straight ($g = 0.76$), whereas it decreased in the right step on the bend compared with the straight ($g = 0.70$).

A significant condition x limb interaction was reported for peak midfoot inversion, $F_{(1, 8)} = 6.238$, $p = 0.037$, due to an increase in right step peak midfoot inversion on the bend compared with the straight and the left step on the bend ($g = 0.90$). There was no significant condition x limb interaction for MTP angular velocity ($F_{(1,8)} = 1.672$, $p = 0.232$). However, a moderate effect size between the left step on the bend and straight was observed ($g = 0.50$).

Table 5.3.2.1 Spatio-temporal variables. Group mean ± standard deviation. Significant main effects are marked with *. Significant interactions are marked with #.

	Straight		**Bend**		**Effect size (*g*) (% difference)**				
	Left	**Right**	**Left**	**Right**	**Left vs. right straight**	**Left vs. right bend**	**Straight vs. bend left**	**Straight vs. bend right**	**MDD met? (left / right)**
Absolute speed (m/s)	7.98 ± 0.34	8.00 ± 0.20	7.81 ± 0.30	7.98 ± 0.34	0.12(0%)	0.48(2%)	0.52 (2%)	0.05 (0%)	Yes / no
Race velocity (m/s)	7.98 ± 0.34	8.00 ± 0.20	7.76 ± 0.32	7.86 ± 0.27	0.12 (0%)	0.32 (1%)	0.64 (3%)	0.56 (2%)	n/a
Contact time (s)	0.107 ± 0.007	0.111 ± .012	0.119 ± 0.007	0.114 ± 0.008	0.34 (4%)#	0.57 (4%)#	1.50 (11%)*#	0.27 (24%)*#	Yes / yes
Flight time (s)	0.135 ± 0.019	0.133 ± 0.016	0.135 ± 0.021	0.124 ± 0.016	0.10(2%)	0.53 (9%)	0.01 (0%)	0.51 (7%)	No / yes
Step Frequency (Hz)	4.33 ± 0.25	4.29 ± 0.22	4.11 ± 0.37	4.30 ± 0.22	0.18 (1%)#	0.61 (5%)#	0.66 (5%)#	0.09 (1%)#	Yes / no
Directional step length (m)	1.84 ± 0.11	1.87 ± 0.08	1.90 ± 0.12	1.84 ± 0.07	0.26 (2%)#	0.55 (3%)#	0.48 (3%)#	0.35 (2%)#	No / no
Race step length (m)	1.84 ± 0.11	1.87 ± 0.08	1.53 ± 0.10	1.37 ± 0.08	0.26 (2%)#	1.70 (12%)*#	2.89 (17%)* #	6.16 (37%)* #	n/a
Touchdown distance (m)	0.25 ± 0.06	0.26 ± 0.07	0.30 ± 0.05	0.27 ± 0.08	0.12 (4%)#	0.49 (10%)#	0.95 (29%) #	0.11 (4%)#	Yes / yes
Turn of CoM (°)			2.48 ± 0.91	2.61 ± 0.86			0.13 (5%)		n/a

Table 5.3.2.2 Joint kinematics. Group mean ± standard deviation. Significant main effects are marked with *. Significant interactions are marked with #.

Peak angle (°)	Straight		Bend		Effect size (*g*) (% difference)				
	Left	Right	Left	Right	Left vs. right straight	Left vs. right bend	Straight vs. bend left	Straight vs. bend right	MDD met? (left / right)
Hip abduction	-6 ± 4	-6 ± 3	- 6 ± 3	-8 ± 3	0.08 (27%)#	0.66 (21%)#	0.22 (20%)#	0.50 (28%)#	No / yes
Hip adduction	4 ± 5	7 ± 3	8 ± 4	6 ± 4	0.49 (72%)#	0.63 (30%)#	1.09 (106%)#	0.24 (31%)#	Yes / yes
Hip internal rotation	2 ± 8	5 ± 4	1 ± 9	7 ± 5	0.41 (104%)	0.75 (126%)	0.15 (86%)	0.41 (38%)	Yes / no
Hip external rotation	-9 ± 8	-10 ± 9	-16 ± 7	-8 ± 4	0.13 (11%)	1.22 (89%)	0.89 (51%)	0.28 (14%)	Yes / no
Knee abduction	-2 ± 4	-1 ± 7	-2 ± 4	0 ± 4	0.03 (75%)	0.39 (23%)	0.03 (0%)	0.21(93%)	No / no
Knee adduction	5 ± 5	5 ± 4	5 ± 4	6 ± 6	0.10 (26%)	0.15(17%)	0.05 (5%)	0.05 (21%)	No / no
Knee internal rotation	-1 ± 8	-5 ± 8	-1 ± 6	-5 ± 9	0.37 (70%)	0.52 (80%)	0.02 (18%)	0.07 (11%)	No / no
Knee external rotation	-15 ± 7	-13 ± 7	-14 ± 6	-15 ± 8	0.18 (6%)	0.18 (4%)	0.14 (5%)	0.22 (6%)	No / no
Ankle inversion	14 ± 9	10 ± 9	11 ± 9	12 ± 9	0.34 (48%)#	0.06 (6%)#	0.22 (33%)#	0.19 (16%)#	Yes / no
Ankle eversion	-2 ± 9	-4 ± 10	-5 ± 9	-3 ± 10	0.15 (36%)	0.12 (23%)	0.88 (55%)	0.02 (8%)	Yes / no
Ankle internal rotation	2 ± 4	3 ± 5	12 ± 7	1 ± 7	0.25 (44%)*#	1.95 (562%)*#	1.70 (346%)*#	0.46(108%)*#	Yes / no
Ankle external rotation	-10 ± 5	-10 ± 3	-5 ± 5	-9 ± 5	0.13 (9%)	0.85 (42%)	0.95 (50%)*	0.20 (6%)	Yes / no
Midfoot inversion	-7 ± 5	-7 ± 5	-5 ± 4	-12 ± 4	0.03 (6%)#	1.48 (63%)#	0.30 (41%)#	0.90 (69%)#	Yes / yes
Midfoot eversion	0.3 ± 5	-0.3 ± 5	4 ± 3	-4 ± 4	0.13 (209%)#	1.73 (184%)#	0.79 (956%)#	0.72 (1271%)#	Yes / yes
MTP angular velocity (°/s)	776 ± 239	732 ± 120	694 ± 168	704 ± 176	0.25 (6%)	0.06 (2%)	0.50 (11%)	0.15 (4%)	n/a
Body lateral lean at touchdown	6 ± 3	-5 ± 1	- 5 ± 2	-12 ± 2	3.24 (221%)*#	2.98 (62%)*#	4.01 (168%)*#	3.39 (78%)*#	n/a

5.4. Discussion

This study aimed to investigate the effect of bend versus straight-line sprinting during the acceleration phase on the kinematic and spatio-temporal parameters of the lower limb. Variables were interpreted with reference to the MDDs determined in Chapter 4. All variables demonstrating significant outcomes met or exceeded the identified MDD, with the exception of directional step length and ankle inversion.

A moderate effect size was observed when comparing absolute speed on the bend and the straight for the left (g = 0.52, 2%) step. Whilst the reported effect size suggests these reductions are moderate, a 2% reduction may be meaningful in terms of competitive race performance. For the left step, the 2% reduction found in the present study is the same as the 2% reported in previous research into the acceleration phase of bend sprinting (Stoner & Ben-Sira, 1979). Similarly, to Churchill et al. (2015) at maximal speed, the reduction in left step velocity on the bend can be attributed to a reduction in left step frequency. Moreover, an increase in left step touchdown distance was apparent on the bend compared with the straight. Churchill et al. (2015) suggest the reduction in right step absolute speed is due to a shorter right directional step length on the bend compared with the straight. However, no reduction in right step absolute speed was observed in the present study. A small (g = 0.35) decrease in right directional step length on the bend compared with the straight was reported, although the difference (0.03 m) does not meet the minimum detectable difference (MDD) of 0.08 m identified in Chapter 4. Therefore, the results suggest maintaining a similar right directional step length on the bend and straight aided in avoiding a reduction in right step absolute speed.

A main effect for condition was reported with a reduction in race step length on the bend compared with the straight in both the left (g = 2.89) and right steps (g = 6.16). Race step length takes into account the progression with respect to the official race distance in each step. The reductions reported here are up to twice as great as those found by Churchill et al. (2015) and Churchill et al. (2016) at maximal speed. The radius in the present study was 36.5 m (lane one), whilst Churchill et al. (2015) and Churchill et al. (2016) examined a 37.72 m radius (lane two), which might have some impact on the results. Furthermore, athletes tend to try and maintain a straight path for as long as possible during the acceleration phase. Whilst athletes were not running straight at the point of data collection, doing so in the earlier phases of the race may result in athletes not closely following the race line and consequently, a 3 and 2% decrease in race velocity for the left and right steps, respectively. Therefore, sprinting to maintain a straight path during the acceleration phase may not be an effective strategy.

During bend sprinting, an increase in peak left hip adduction (bend = 8°, straight = 5°, g = 1.09), combined with a non-significant increase in peak left hip external rotation (bend = 16°, straight = 9°, g = 0.89) was reported compared with straight-line sprinting. This supports research during sub-maximal effort bend sprinting at approximately 9.26 m/s which reported peak left hip adduction (14°) and external rotation (22° Alt et al., 2015). The excessive hip adduction observed might have implications for injuries, particularly at the knee (Li et al., 2015). For example, it is expected that iliotibial band tension would increase with hip adduction, potentially resulting in iliotibial band syndrome (Chuter & Janse de Jonge, 2012; Powers, 2010). In addition, greater hip adduction has also been associated with patellofemoral pain

(Neal, Barton, Birn-Jeffery & Morrissey, 2019). Both iliotibial band syndrome and patellofemoral pain were recorded by Beukeboom et al. (2000) in a season long evaluation of injuries in indoor track athletes. Therefore, high peak hip adduction may be a precursor for injury. Strength and conditioning programmes should aim to increase strength in the frontal and transverse planes to ensure athletes are sufficiently prepared to withstand this high adduction angle. These results suggest non-sagittal plane hip movement may be an important kinematic modification in bend sprinting compared to straight-line sprinting.

The present study observed an increase in peak left step ankle eversion on the bend (-5° ± 9°) compared with the straight (-2° ± 9°). These findings support the notion that the left limb is associated with a stabilising role achieved through the combination of greater hip adduction and ankle eversion (Alt et al., 2015). An increase in left step peak midfoot eversion was also observed in the present study, suggesting the stabilising role of the left hip and ankle joints might extend to the midfoot. Whilst increased eversion enables the attenuation of impact forces (Hreljac, 2004), it is also linked with medial tibial stress syndrome and patellofemoral pain syndrome (Chuter & Janse de Jonge, 2012), both of which were amongst the most frequently reported injuries in indoor bend sprinters over a season (Beukeboom et al., 2000). Therefore, strengthening the evertor muscles of the left foot and ankle should be prioritised to reduce the risk of injury. It is apparent that the left limb is in a complex segmental arrangement which might compromise force production and therefore be responsible for the loss of speed observed on the bend. As Chang and Kram (2007) suggested, it is possible that modifications in the transverse and frontal planes restrict the capacity of muscles to operate and produce force in the sagittal plane. Therefore, analysis of joint moments during bend sprinting is warranted.

In general, eversion occurs during the first 15% of stance due to the eccentric contraction of invertors such as tibialis posterior and anterior (Chan & Rudins, 1994). As bi-planar muscles, whilst they are predominantly invertors, they also have a role to play in plantar flexion of the foot and ankle (Palastanga, Field, & Soames, 2006). Simulations (Debaere et al., 2015) and later experimental data (Brazil et al., 2017) suggested kinetics of the ankle joint play a dominant role in the acceleration of the centre of mass during the stance phases of early acceleration in straight-line sprinting. It appears the increased left step eversion and ankle internal rotation might place the foot in a disadvantageous position, compromising the ability to produce propulsive force.

A moderate (g = 0.50) effect size suggests there might be a decrease in MTP joint angular velocity during the left step on the bend compared to the straight. Krell and Stefanyshyn (2006) established that faster male sprinters elicited higher maximal rates of MTP extension. Therefore, decreased angular velocity of the MTP joint might be a contributing factor to the decrease in sprint performance found on the bend. However, further research is required to strengthen this conclusion.

Based on the results of the present study, adaptations of the right limb during the acceleration phase of bend sprinting can be characterised by an increase in hip abduction. In addition, the present study did not observe a change in peak right ankle external rotation or internal knee rotation. These two factors were suggested by Alt et al. (2015) to contribute towards a rotational strategy of the right limb. However, the findings of this study do not support this during the acceleration phase. This further highlights the left and right limb have different functions on the bend, whilst also advancing the notion that the key to understanding the limits of bend sprinting performance in an anti-clockwise direction lies within the left limb.

There was a large increase in body lateral lean at touchdown on the bend (left step: -5° ± 2; right step -12° ± 2) compared with the straight (left step: 6° ± 3; right step: -5° ± 1). These findings, combined with the aforementioned kinematic adaptations, support the suggestion from Churchill et al. (2015) that the increase in lateral lean angle found on the bend might be responsible for inducing kinematic adaptations in the lower limb. However, the observed body lateral lean in the present study was lower than the -10° (left step) and -15° (right step) lean angles reported during maximum speed (Churchill et al., 2015), suggesting these smaller changes accumulate during the acceleration phase, resulting in greater changes at faster speeds. To ensure the transfer of strength training to sports performance, the principle of training specificity is of paramount importance (Young, 2006). Coaches tend to prefer the specificity of training is addressed by adding resistance to sporting movements rather than attempting to make gym exercises more sports-specific (Burnie et al., 2017). Therefore, as suggested by Churchill et al. (2016), the use of ropes or harnesses in training to provide resistance in a leaning position might be beneficial to performance. In addition, ensuring acceleration training is undertaken on the bend to promote further specificity is essential.

The adaptations reported in the present study during the acceleration phase on the bend compared with the straight are not as great as those reported at maximum speed. For example, Churchill et al. (2015) and Alt et al. (2015) reported peak left hip adduction values during bend sprinting of 11° and 14° respectively, compared with 8° in the present study. This suggests kinematic adaptations between the bend and straight become more prominent as velocity increases. However, greater adaptations have also been found at smaller radii when running at slower speeds (Chang & Kram, 2007; Luo

& Stefanyshyn, 2012a). Therefore, it is likely that a combination of radius and velocity are responsible for inducing kinematic adaptations. However, the effect of lane allocation has not yet been investigated during the acceleration phase, despite performance differences being observed across lanes at maximal velocity (Churchill et al., 2018).

5.5. Conclusion

In conclusion, the results of the present study demonstrate that the bend impacts upon kinematic and spatio-temporal parameters of sprint technique and performance during the acceleration phase. These results show that kinematic adaptations start early in the race and likely accumulate, resulting in greater adaptations at maximal speed and thus a greater reduction in speed. For example, in accordance with the mechanical principles of bend sprinting, and in particular the need to produce centripetal force which is proportional to the square of velocity, as athletes reach faster speeds the magnitude of centripetal force experienced will also increase. Thus, at faster speeds a greater lateral lean will be required to balance the greater mediolateral force and as a consequence of body configuration also result in greater adaptations at the lower limb. Furthermore, the reported kinematic adaptations are more prominent in the left limb. A recent study by Ohnuma, Tachi, Kumano, and Hirano (2018) compared technique on the bend and straight in 'good' and 'poor' bend sprinters - where athletes were categorised by their ability to maintain their maximum straight-line speed on the bend (i.e., those with a higher percentage difference in running speed were categorised as poor, and vice versa). It was concluded that better bend sprinters are those who are able to more closely maintain the same sagittal plane kinematics and kinetics as on the straight path. Therefore, coaches and athletes should

prioritise strategies to address the reported adaptations of the left limb, such as reducing touchdown distance and increasing step length on the bend. Whilst the results demonstrated within the present chapter highlight changes in technique during bend sprinting compared with the straight, we do not know how this impacts upon force production and propulsion in the acceleration phase. Moreover, an investigation of joint moments may be warranted to understand the mechanisms responsible for these adaptations and identify their role in restricting or aiding performance.

Chapter Six: FORCE PRODUCTION AND MTP JOINT AXIS USE DURING THE ACCELERATION PHASE DURING BEND SPRINTING

THE WORK IN THIS CHAPTER FORMED THE BASIS OF THE FOLLOWING PEER-REVIEWED JOURNAL ARTICLE:

Judson, L. J., Churchill, S. M., Barnes, A., Stone, J. A., Brookes, I. & Wheat J. (2019). Horizontal force production and multi-segment foot kinematics during the acceleration phase of bend sprinting. *Scandinavian Journal of Medicine & Science in Sports*. doi.org/10.1111/sms.13486

AND CONFERENCE PAPER:

Judson, L. J., Churchill, S. M., Barnes, A., Stone, J. A. & Wheat, J. (2018). Metatarsophalangeal joint push-off axis during sprinting on the bend and straight. *BASES Annual Conference, Harrogate.*

6. Force production and kinetics of the acceleration phase during bend sprinting

6.1. Introduction

Faster speeds are associated with higher peak vertical forces during maximal velocity treadmill sprinting (Weyand et al., 2010). However, rather than solely producing greater peak forces, faster speeds are more dependent on the ability to produce these forces rapidly, meaning the production of high vertical force over a short contact time is crucial (Weyand et al., 2010). During anti-clockwise over-ground bend sprinting, left step contact times are longer than during straight-line sprinting (Alt et al., 2015; Churchill et al., 2015; Ishimura & Sakurai, 2010; Ishimura et al., 2013). Therefore, with the findings of Weyand et al. (2010) in mind, the magnitude of force produced during the longer contact time on the bend is also of interest in understanding bend sprinting performance.

In the maximal velocity phase of bend sprinting, lower peak resultant forces have been reported for the left step on the bend than on the straight (Churchill et al., 2016). Additionally, inward forces are greater on the bend than the straight for both the left and right step, with the left limb producing a greater peak inward force compared with the right on the bend (Churchill et al., 2016). This limb asymmetry in force production could hold important insights in understanding bend sprinting performance. This asymmetry can be quantified using the 'symmetry angle' proposed by Zifchock, Davis, Higginson and Royer (2008) and used in straight-line sprint research by Exell, Irwin, Gittoes, and Kerwin (2017) who demonstrated higher levels of asymmetry in kinetic variables at maximal speed. However, the maximal velocity phase does not reflect the full requirements of performance across a 200 m or 400 m race and consideration of the acceleration phase on the bend is required.

Straight-line acceleration performance is not simply reliant upon the production of large forces, but rather the production of greater horizontal force as a proportion of the total amount of force applied (Morin et al., 2012; Rabita et al., 2015). Thus, 'ratio of force' has been proposed as a useful measure of performance during the acceleration phase of straight-line sprinting, rather than simply the evaluation of mean forces, as it places emphasis on the orientation of force rather than magnitude (Morin et al., 2012; Morin et al., 2011; Rabita et al., 2015). The necessity to generate centripetal force during bend sprinting might also affect the magnitude and orientation of vertical and anteroposterior forces, and thus ratio of force, however, this is yet to be investigated. In addition, Morin et al. (2015) identified propulsive impulse in the first 20 m of acceleration as a key determinant of acceleration performance over 40 m. This further reinforces the importance of orientation in force production, particularly as no correlations were observed for vertical or braking impulse (Morin et al. 2015). The generation of propulsive impulse could also be negatively affected during bend sprinting due to the need to produce centripetal force. Therefore, analysis of impulse and ratio of forces might provide important insight into performance changes between bend and straight sprinting.

Bojsen-Moller (1979) observed the MTP has two possible axes about which the foot can push off: transverse and oblique. The transverse axis runs through the heads of the first and second metatarsals, whereas the oblique axis runs through the second to fifth metatarsal heads (Bojsen-Moller, 1979). During push-off about the transverse axis, the calcaneocuboid joint is closely packed, which increases the effectiveness of the windlass mechanism and provides a more stable foot for push-off (Bojsen-Moller, 1979). Push-off at higher walking speeds is thought to use the transverse axis, thus it is deemed more effective than the oblique axis at generating

propulsive force in the direction of progression (Bojsen-Moller, 1979). Churchill et al. (2016) postulated that the inward lean of athletes during bend sprinting might promote the use of the less effective oblique axis for the left ground contact (but the more effective transverse axis for the right ground contact). Therefore, it is probable that athletes are less effective at generating propulsive force when using the oblique axis for the left step, which has been suggested as a limiting factor in bend sprinting (Churchill et al., 2016). Indeed, the MTP joint has been highlighted as making an important contribution to performance in straight-line sprinting (Krell & Stefanyshyn, 2006; Smith et al., 2014) and warrants investigation during bend sprinting.

In summary, force adaptations during the acceleration phase of sprinting on the bend are likely and this might contribute towards a decrease in performance compared with straight-line sprinting. Therefore, the aim of this study was to investigate force production and MTP axis use during sprinting on the bend compared with the straight. A secondary aim was to evaluate between limb differences to identify the existence of any asymmetry during bend sprinting. It was hypothesised that the oblique axis would be used by the left foot for push-off during bend sprinting, resulting in a decrease in propulsive force (and therefore sprint performance) in comparison with the straight.

6.2. Methods

6.2.1. Participants

Following institutional ethical approval, seven male sprinters (mean age 22 ± 4 years; body mass 68.32 ± 6.98 kg; stature 1.79 ± 0.06 m) volunteered to participate in this study. All athletes were experienced bend sprinters (200 and/or 400 m) and the inclusion criteria required a 200 m personal best of 23.5 s or faster (mean 22.70 ± 0.52 s, range 21.8 - 23.43 s). At the time of data collection, all athletes

were injury free and active in training. The study procedures were fully explained to participants who subsequently provided written informed consent.

6.2.2. Experimental set-up

The experimental set-up is provided in section 0. For CoM calculations, kinematic data were collected using a 15-camera optoelectronic motion capture system (13 x Raptor model and 2 x Eagle model, Motion Analysis Corporation, Santa Rosa, CA, USA) sampling at 200 Hz. A modified Vicon Plug-in Gait (PiG) marker set (lower limb and trunk; Chapter 4) was used to model the torso, pelvis, thighs, shanks and feet segments (toebox, forefoot, rearfoot). Full details of marker placement can be found in section 4.2.2.

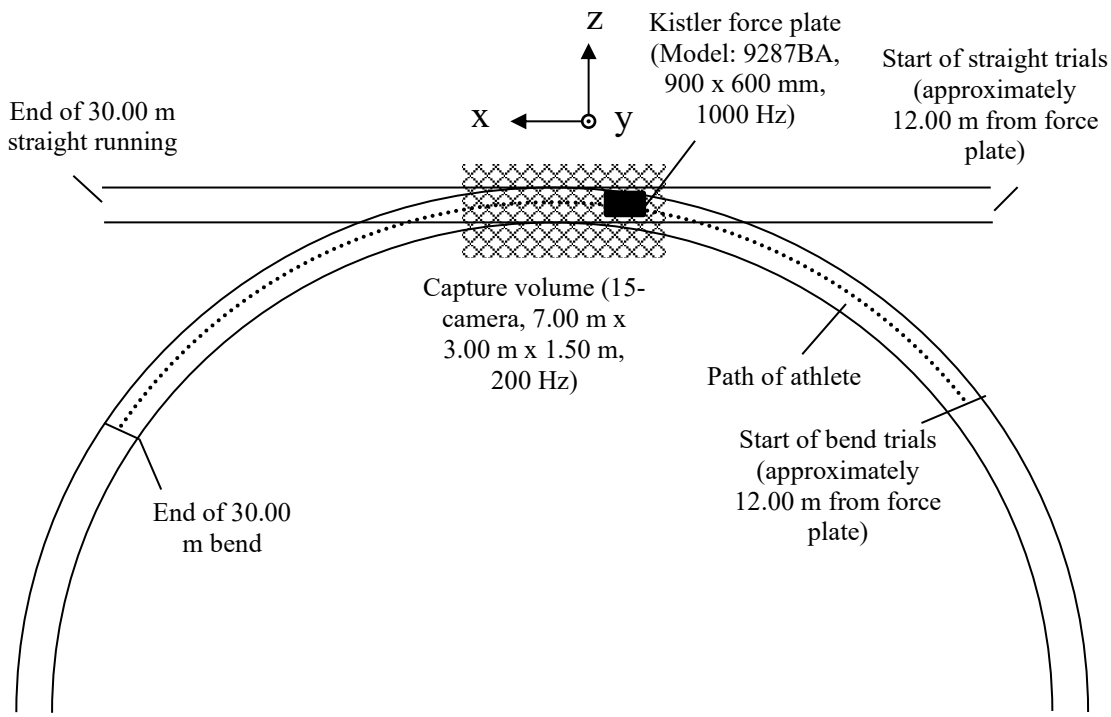

Figure 6.2.2.1 Plan view of experimental set-up (not to scale).

Kinetic data were collected using a Kistler force plate (Model: 9287BA, 900 x 600 mm) sampling at 1000 Hz. The force plate was embedded into the track surface and covered with a secured piece of synthetic track. The force platform was

configured to produce a rising edge 5 V signal at the onset of data collection, which was sampled by the motion capture system and used to temporally synchronise the kinematic and kinetic data.

6.2.3. Protocol

Data were collected on a flat standard indoor track surface with a reconstructed bend replicating lane 1 (radius 36.5 m) of a standard 400 m running track (IAAF, 2008). Straight-line trials were completed on a 30 m section of straight track. The order in which experimental conditions were presented to each participant was randomised to minimise order effects. Results from Morin et al. (2015) suggest the production of propulsive impulse in the first 20 m determines acceleration performance. Thus, it was decided to limit analysis to the 0 - 20 m section. Furthermore, only one study has examined the acceleration phase of bend sprinting, analysing data at 12 m (Stoner & Ben-Sira, 1979). Therefore, data were collected at approximately 12 m within the present study to enable comparison with previous research.

Participants completed their typical competition warm-up before performing up to six trials at maximal effort for 30 m in each condition (bend and straight, three left, three right). Starting blocks were used alongside an '*on your marks, set, go*' signal to maintain the representativeness of the protocol. For force data, a minimum of one successful right step and left step on the bend and one successful right step and left step on the straight were achieved. A successful trial was defined as contact being made with the force plate with the whole foot, without changes to their running gait caused by targeting. To achieve this, one researcher modified the start location of the athletes based upon warm-up trials, up to a maximum of one metre. Therefore, force data were collected in the range of 11 - 13 m. To further reduce the likelihood of targeting, participants were not informed of the force plate location. Approximately

eight minutes were allowed between trials to allow full recovery and avoid the onset of fatigue (Churchill et al., 2015). Participants wore their own sprint spikes for the testing session.

6.2.4. Data processing

Raw 3D marker coordinate data was analysed using Cortex software (version 5.3, Motion Analysis Corporation, Santa Rosa, CA, USA). Automatic gap filling, using a cubic spline, was performed. All gaps were <10 frames. A low-pass, fourth-order recursive Butterworth filter was applied to raw marker positions. Residual analysis was used to determine the cut-off frequency (18 Hz). Visual 3D (version 6, C-Motion, Rockville, MD, USA) was used to define and construct segments, LCS and joint centres. Where possible, ISB guidelines (Wu et al., 2002; Wu et al., 2005) were adhered to. However, the joint coordinate system for the multi-segment foot was defined in accordance with Cappozzo et al. (1995). Body segment parameters were estimated from de Leva (1996) and adjusted by 0.150 to 0.189 kg representing the mass of individual participants' spiked shoe according to manufacturer guidelines. Kinetic data were analysed using Matlab (v2017a, Mathworks, Natick, USA). Force data were filtered with a low-pass, fourth-order recursive Butterworth filter with a 150 Hz cut-off frequency, chosen with the use of residual analysis.

For force data for each participant, one successful trial for each condition was analysed, as was the case with Churchill et al. (2016). Where more than one successful trial was available, the first successful trial was used for analysis. A selection of variables calculated from additional trials that were not included in the analysis for this study have been presented in Appendix B, alongside CV.. The CV were in the range of 0.42 - 1.67 % for propulsive force and 1.40 - 5.74 % for braking impulse, supporting previous work from Hunter et al. (2004a) that demonstrated greater

reliability in propulsive measurements than measurements of braking. In addition, all values reported were < 10 %, which is indicative of very good reliability between trials (Atkinson & Nevill, 1998), supporting the use of a single trial for force plate data.

Touchdown and take-off events were identified using vertical force data, using the mean plus two standard deviations of the zero load vertical force as a threshold (Bezodis et al., 2007). All variables were calculated separately for the left and right step. Steps were defined by the foot that initiated the step.

Horizontal forces in the global coordinate system (GCS) were aligned with the direction of travel of the athlete for both bend and straight trials (Glaister, Orendurff, Schoen, & Klute, 2007). This was necessary due to the orientation of the force plate in the experimental set-up not being aligned with the direction of forward progression. To enable this alignment to take place, CoM data was up-sampled from 200 Hz to 1000 Hz using a cubic spline interpolation. An instantaneous progression vector was then calculated from the up-scaled horizontal CoM position one frame before and one frame after the instant of interest. The angle between the *x*-axis (anteroposterior) of the force plate and the CoM progression vector was then calculated. A direction cosine matrix was then used to rotate the forces bringing them into alignment with the direction of travel:

$$\begin{bmatrix} Fz' \\ Fx' \end{bmatrix} = \begin{bmatrix} \cos\theta & \sin\theta \\ -\sin\theta & \cos\theta \end{bmatrix} \begin{bmatrix} Fz \\ Fx \end{bmatrix} \qquad \textit{Equation 17}$$

Fz' and Fx' represent the horizontal ground reaction forces aligned with the direction of travel of the athlete, where Fz and Fx are the horizontal ground reaction forces in the GCS. θ is the angle between the GCS and body reference frame.

Impulse in each direction was calculated from absolute values using numerical integration of the force data and expressed relative to body mass, thus giving change

of direction and keeping consistent with previous bend sprinting research (Churchill et al., 2016). The symmetry angle (θ_{SYM}) was calculated with the following equation, proposed by Zifchock, et al. (2008):

$$\theta SYM = \frac{\left(45° - \arctan\left(\frac{X_{left}}{X_{right}}\right)\right)}{90°} \times 100$$

Equation 18

A θ_{SYM} value of 0% represents perfect symmetry between limbs, where 100% would indicate perfect asymmetry (Zifchock et al., 2008). The symmetry angle method was chosen for use over the symmetry index as Zifchock et al., (2008) reported it does not suffer from artificial inflation that can occur when a difference that is clinically irrelevant is divided by a much smaller reference value.

Ratio of force was calculated as the mean ratio of force in the direction of forward progression (relative to the direction of travel of the athlete's CoM) to resultant force (including mediolateral forces) during ground contact. The inclusion of mediolateral force in this equation differs from that proposed by Morin et al. (2011), which includes anteroposterior and vertical forces, only. Since mediolateral force can be considered negligible on the straight, this equation is sufficient for the analysis of straight-line acceleration. However, sprinting on the bend results in higher mediolateral forces, as demonstrated by Churchill et al. (2016). Thus, the inclusion of mediolateral force is necessary to appropriately assess the effectiveness of force application on the bend.

Following methods adapted from Smith et al. (2012), MTP push-off axis was determined using centre of pressure (CoP) data. CoP data were first aligned with a local foot coordinate system. The mediolateral position of the CoP and MTH2 marker

was then extracted during the propulsive phase of stance for each condition. The distance of the CoP from the MTH2 was then calculated for each frame, followed by calculation of the mean CoP position during the propulsive phase of stance. For ease of interpretation, data for the left foot were multiplied by -1, so a positive value indicated CoP was lateral for both the left and right foot. Consequently, a positive value would represent the use of the oblique axis, with a negative value representing the use of the transverse axis (Figure 6.2.4.1).

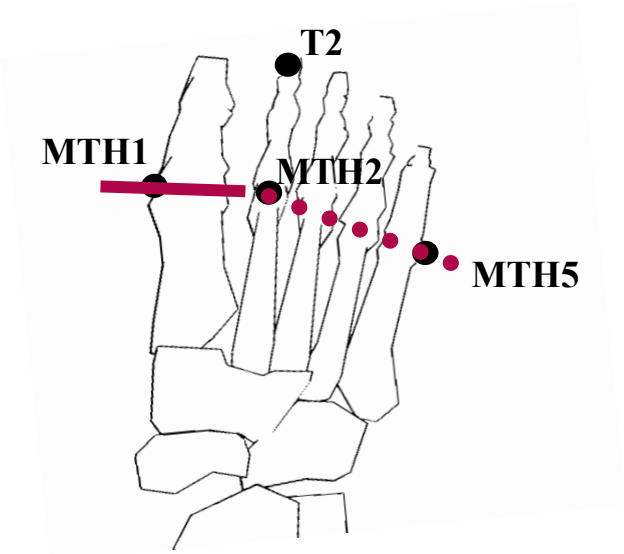

Figure 6.2.4.1 Right foot representation of the transverse (solid line ——) and oblique (dashed line - - -) axes of the foot. Where T2 represents marker at the second toe and MTH1, 2 and 5 the first, second and fifth metatarsal heads, respectively.

Descriptive statistics (mean, standard deviation and percent differences) were calculated for all variables. Normal distribution of the data for each variable was confirmed by the Shapiro-Wilk normality test ($p > 0.05$). For discrete variables, two-way repeated measures ANOVAs were performed, condition (bend vs. straight) x limb (left vs. right). Due to a small sample size, the study may be statistically underpowered, and so the chance of detecting a true effect is reduced. Therefore, results were also interpreted using effect size (Hedges' *g,* Equation 16). Cohen's (1988) guidelines were used for the interpretation of effect size, where $g < 0.20$ represents a trivial difference,

0.20 ≥ 0.50 indicating a small difference, 0.50 ≥ 0.80 a moderate difference and ≥ 0.80 a large difference between means.

Statistical parametric mapping (SPM; Friston, Ashburner, Kiebel, Nichols, & Penny, 2007) was used to statistically compare force production across the entire stance phase between conditions. Force data were first normalised to 101 data points, representing 0-100% of the stance phase. An SPM repeated measures two-way ANOVA was then performed separately at each of the 101-time points resulting in the output of a statistical parametric map (SPM{F}), using the equation:

$$P(t(q)_{max} > t^{*}{}_{1D}) = 1 - exp\left(- \int_{t^{*}1D}^{\infty} f_{0D}\,(x)dx - ED\right) = \alpha \quad \textit{Equation 19}$$

where $t^{*}{}_{1D}$ is the one-dimensional (1D) test statistic, $t(q)_{max}$ represents the maximum value in the 1D trajectory t, and the smoothness-dependent Euler density function is represented by ED (Friston et al., 2007). If SPM{F} exceeded the critical threshold, force production at these specific nodes could be considered statistically different. A collection of consecutive nodes exceeding the threshold and thus considered significant is termed a 'supra-threshold cluster'. In line with Colyer et al. (2018), clusters of fewer than five nodes were considered unlikely to be meaningful. SPM analyses were implemented using open source SPM code (SPM1D open-source package, spm1d.org) in MATLAB (v2017a, Mathworks, Natick, USA).

To establish whether there was a relationship between asymmetry and sprint performance, Pearson's correlations (*r*) were calculated between θ_{SYM} and mean velocity across the left and right steps. In accordance with Field (2009), an *r* value of .1 - .3 indicates a weak correlation, .3 - .5 a moderate correlation and >.5 a strong correlation.

6.3. Results

SPM revealed there were no changes in resultant force across bend and straight conditions (Figure 6.3.1, $F = 28.771$). Similarly, for vertical force (Figure 6.3.2), the critical threshold of $F = 31.573$ was not met, indicating there was no difference in vertical force production between conditions.

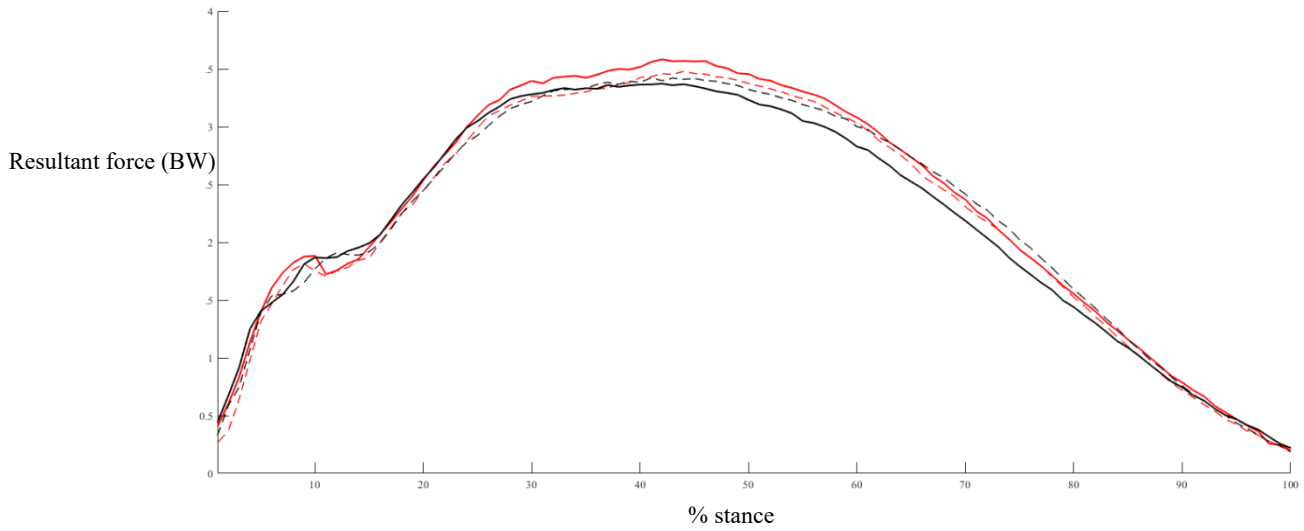

Figure 6.3.1 Group mean resultant force for the left (red) and right (black) steps on the bend (dashed line - - -) and straight (solid line ——). Shaded areas represent supra-threshold clusters indicating a significant main effect for condition.

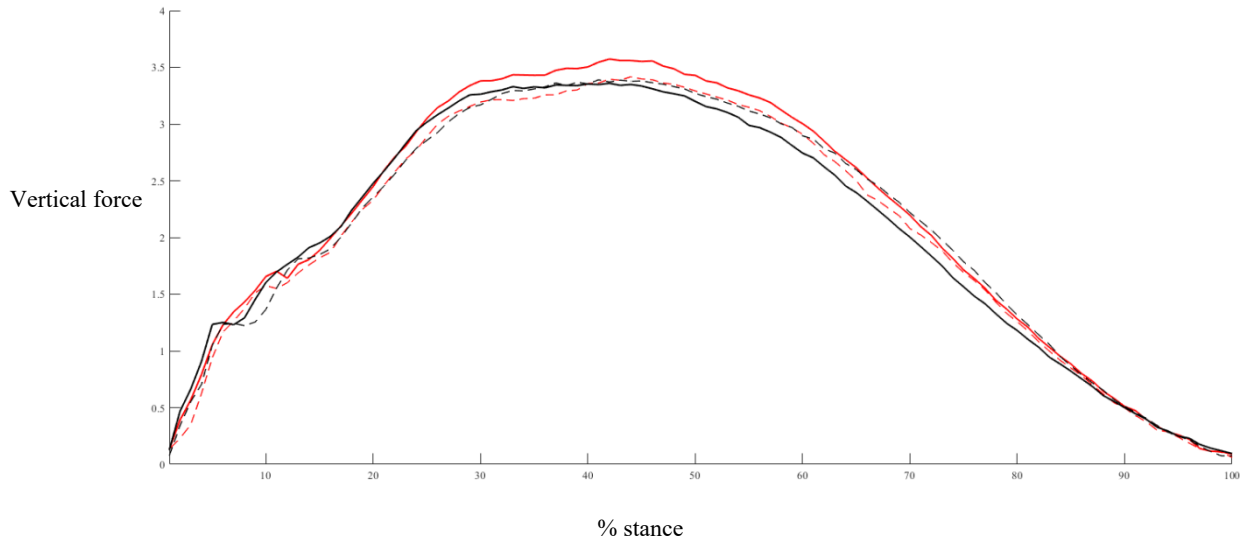

Figure 6.3.2 Group mean vertical force for the left (red) and right (black) steps on the bend (dashed line - - -) and straight (solid line ——). Shaded areas represent supra-threshold clusters indicating a significant main effect for condition.

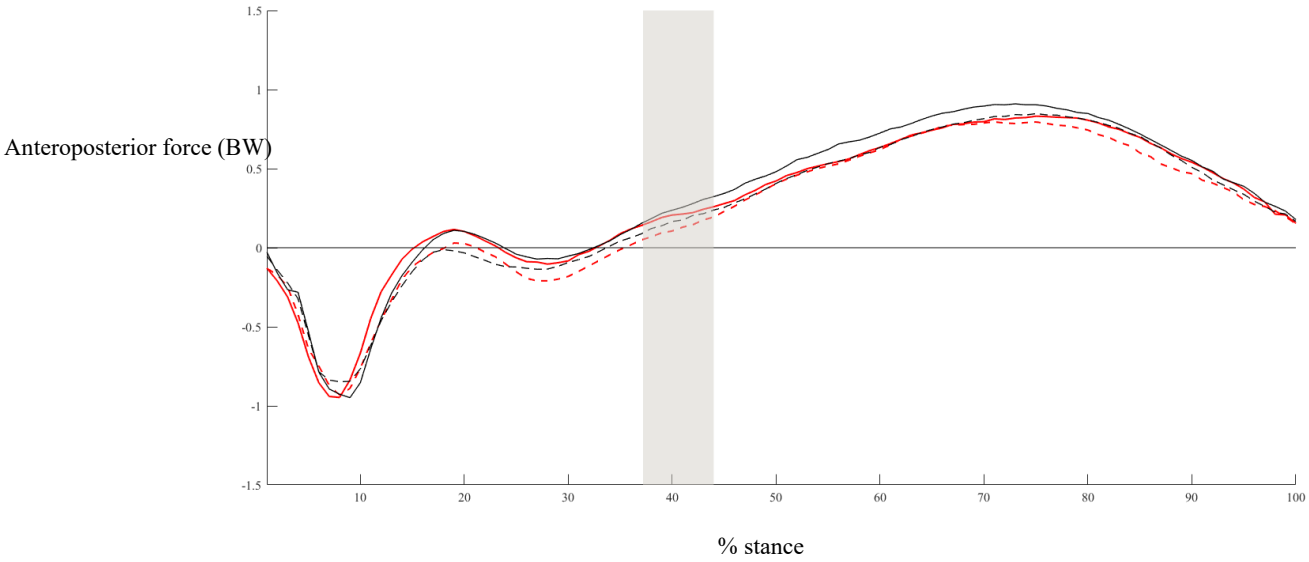

Figure 6.3.3 Group mean anteroposterior force for the left (red) and right (black) steps on the bend (dashed line - - -) and straight (solid line ——). Shaded areas represent supra-threshold clusters indicating a significant main effect for condition.

Anteroposterior force production during straight-line and bend sprinting was similar for the majority of the stance phase (Figure 6.3.3). However, one supra-threshold cluster (37-44%) exceeded the critical threshold of $F = 17.238$ for the main effect of condition, where anterior force was lower on the bend compared with the straight in both the left and right steps. The probability that a supra-threshold cluster of this size would be observed in repeated random samplings was $p < 0.001$.

One supra-threshold cluster exceeded the critical threshold ($F = 15.309$) for main effect of condition when comparing mediolateral force on the bend and straight (3-96%, $p < 0.001$). This was due to an increase in mediolateral force production across the majority of the stance phase on the bend (Figure 6.3.4). There was also a significant main effect for limb, with two supra-threshold clusters found at 1-12% and 75-100% of stance. At 1-12%, mediolateral force was greater in the right step than left, whilst at 75-100% of stance the left step was greater than the right step.

There was no main effect for condition on vertical impulse $F_{(1, 6)} = 0.001$, $p = 0.973$ (Table 6.3.1). However, a main effect was observed for condition for propulsive impulse $F_{(1, 6)} = 10.98$, $p = 0.016$ ($g = 0.93$ left step; 0.78 right step, Table 6.3.1), with the straight resulting in a greater propulsive impulse than the bend. There was no condition x limb interaction, $F_{(1, 6)} = 1.135$, $p = 0.328$. For braking impulse, a 27% increase with large effect size ($g = 1.29$, Table 6.3.1) was reported in the left step on the bend compared with the straight. However, the main effect for condition was not significant, $F_{(1, 6)} = 4.617$, $p = 0.075$. There was a significant condition x limb interaction for mediolateral impulse, $F_{(1, 6)} = 19.739$, $p = 0.004$ due to an increase in mediolateral impulse on the bend that was greater in the left step compared with the right. For mean ratio of force, there was a significant main effect for condition, $F_{(1, 6)} = 11.647$, $p = 0.014$ ($g = 1.72$ left step; 1.16 right step, Table 6.3.1), with the straight resulting in a higher mean ratio of force compared with the bend. There was no condition x limb interaction for mean ratio of force ($F_{(1, 6)} = 2.628$, $p = 0.156$).

For θ_{SYM}, no significant correlations were observed between mean velocity and discrete kinetic variables in both bend (vertical impulse $r = .023$, $p = 0.960$; braking impulse $r = -.649$, $p = 0.115$; propulsive impulse $r = -.006$, $p = 0.989$; mediolateral impulse $r = .164$, $p = 0.725$) and straight conditions (vertical impulse $r = .328$, $p = 0.472$; braking impulse $r = -.134$, $p = 0.775$; propulsive impulse $r = .168$, $p = 0.718$; mediolateral impulse $r = .044$, $p = 0.925$; Table 6.3.2).

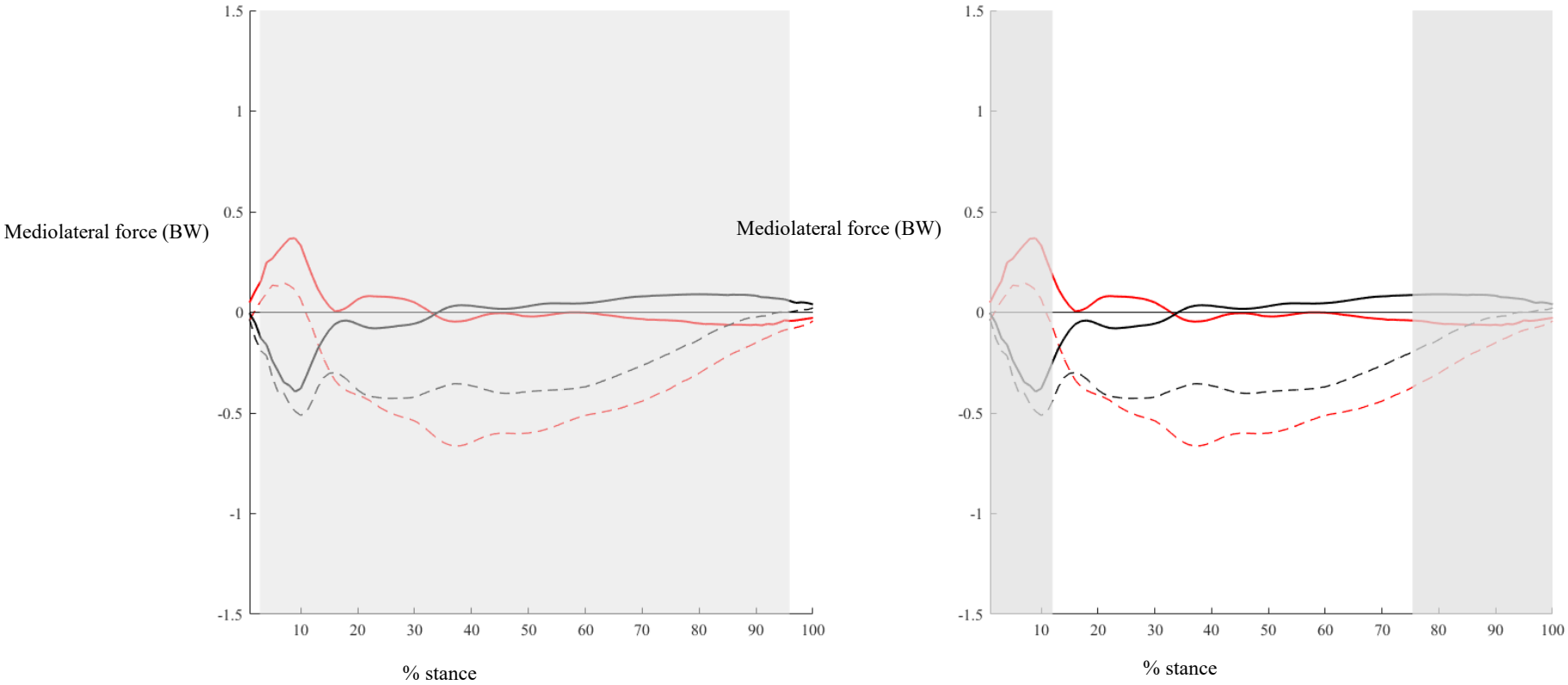

Figure 6.3.4 Group mean mediolateral force for the left (red) and right (black) steps on the bend (dashed line - - -) and straight (solid line —). Shaded areas represent supra-threshold clusters indicating a significant main effect for condition (A) and limb (B).

Table 6.3.1 Group mean values (± standard deviation), effect sizes (% difference) force variables of the left and right step. Significant main effects are marked with *. Significant interactions are marked with #.

	Straight		**Bend**		**Effect size (*g*) (% difference)**			
	Left	**Right**	**Left**	**Right**	**Left vs. right straight**	**Left vs. right bend**	**Straight vs. bend left**	**Straight vs. bend right**
Relative vertical impulse (m/s)	1.34 ± 0.41	1.08 ± 0.53	1.21 ± 0.30	1.21 ± 0.27	0.55 (24%)	0.04 (1%)	0.40 (11%)	0.31 (12%)
Relative braking impulse (m/s)	-0.08 ± 0.02	-0.09 ± 0.03	-0.11 ± 0.01	-0.10 ± 0.03	0.19 (6%)	0.24 (7%)	1.22 (27%)	0.46 (15%)
Relative propulsive impulse (m/s)	0.59 ± 0.06	0.65 ± 0.12	0.55 ± 0.06	0.58 ± 0.06	0.65 (10%)	0.60 (5%)	0.93 (7%)*	0.74 (12%)*
Relative mediolateral impulse (m/s)	0.02 ± 0.10	0.04 ± 0.05	0.42 ± 0.09	0.31 ± 0.11	0.26 (49%) #	1.16 (34%)#	4.61 (1858%)#	3.01 (660%)#
Mean ratio of force (%)	19.13 ± 1.30	23.50 ± 5.52	16.94 ± 1.12	18.44 ± 2.03	0.93 (19%)	0.51 (8%)	1.49 (11%)*	1.02 (22%)*

Table 6.3.2 Group mean values (± standard deviation) of symmetry angle (θ_{SYM}). Significant effects are marked with *.

θ_{SYM}	Straight	Bend	Pearson's *r* straight	Pearson's *r* bend
Relative vertical impulse (m/s)	4.39 ± 2.55	9.48 ± 12.06	.328	.023
Relative braking impulse (m/s)	8.47 ± 3.46	6.10 ± 3.49	-.134	-.649
Relative propulsive impulse (m/s)	2.42 ± 1.68	2.87 ± 2.71	.168	-.006
Relative mediolateral impulse (m/s)	10.97 ± 10.67	11.69 ± 12.83	.044	.164

There was a significant condition x limb interaction for CoP position, $F_{(1, 6)} = 127.878$, $p < 0.001$. The mean mediolateral CoP position was more lateral in the left step on the bend compared with the straight (Figure 6.3.5). This indicates the oblique axis was in use during the left step on the bend, while the transverse axis was used for all other conditions.

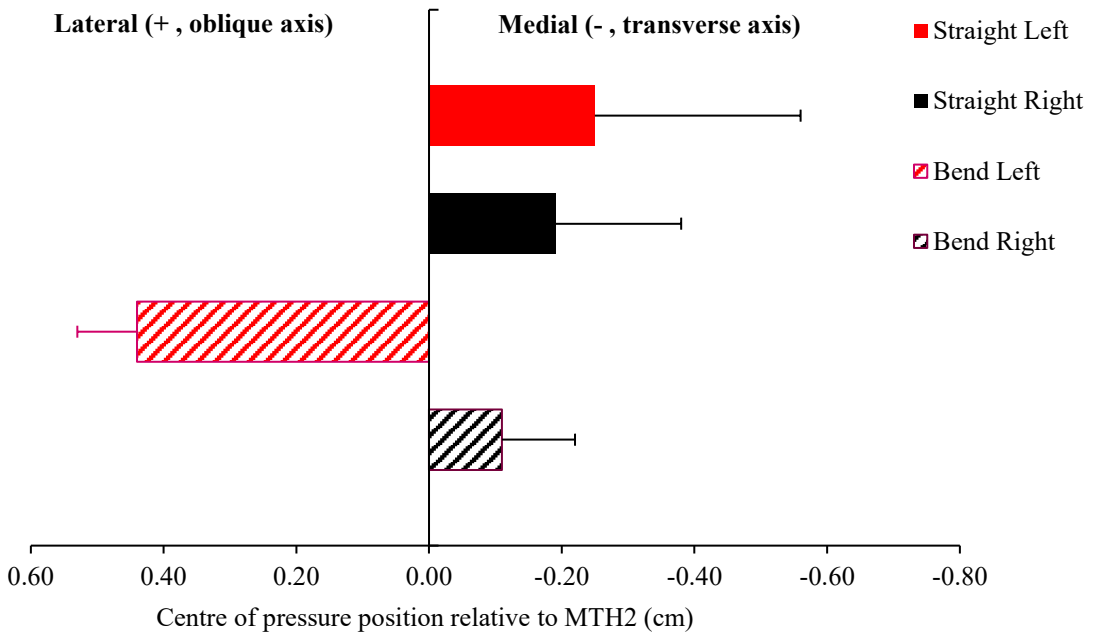

Figure 6.3.5 Mean centre of pressure mediolateral position relative to second metatarsal head during the propulsive phase.

6.4. Discussion

The aim of this study was to investigate force production and MTP joint axis use during the acceleration phase on the bend compared with the straight. The left foot was found to use the oblique axis for push-off at the MTP joint on the bend, as opposed to the transverse axis on the straight. This coincided with a decrease in anterior force and propulsive impulse on the bend.

There were no differences observed in resultant or vertical force during stance between the bend and straight conditions. These results contrast with those reported

by Churchill et al. (2016) at maximal velocity. Churchill et al. (2016) found a significant reduction in peak and mean vertical force and peak resultant force during the left step on the bend compared to the straight. The lack of differences observed in the present study might be expected when considering that, despite their importance at maximum speed (Weyand et al., 2010), vertical force and resultant force have been found not to contribute to sprint performance during the acceleration phase (Morin et al., 2011). Rabita et al. (2015) reconstructed the entire 40 m acceleration phase with several sprints and neither resultant ground reaction force, nor its vertical component, was correlated to sprint acceleration performance (Rabita et al., 2015). It was, however, found that mean anteroposterior force was strongly correlated to 40 m maximal speed and performance (Rabita et al., 2015). Thus, the results of the present study, which showed no difference between bend and straight conditions in resultant or maximal force, were as expected from the literature.

A decrease in propulsive force on the bend compared with the straight was observed, with the supra-threshold cluster occurring at 37-44% of the stance phase. Colyer et al. (2018) found better performances in straight-line sprinting were associated with the production of high amounts of propulsive force during the mid-late propulsive phase of the eighth step (55-85% of stance). As the sprint distance increased, these associations occurred earlier in the stance phase (nineteenth step: 19 - 64% of stance, Colyer et al., 2018). The present study measured in the range of the eighth to eleventh step dependent on the location of the start blocks (see Appendix C for more information). Therefore, it is reasonable to assume that the observed decrease in propulsive force observed during bend sprinting coincided with a crucial time for propulsive force production during the stance phase, which might impact upon acceleration performance.

In addition to the reduction in propulsive force, propulsive impulse was lower on the bend than straight, particularly during the left step where a large effect size was found ($g = 0.93$). Right step propulsive impulse was also reduced on the bend compared with the straight. However, the moderate effect size suggests this was not to the same extent as the left limb ($g = 0.78$). Morin et al. (2015) discussed how straight-line acceleration capability in faster sprinters was characterised by 'pushing more' but not necessarily 'braking less'. This concept suggests producing higher propulsive impulse is of greater importance than reducing braking impulse, particularly in the first twenty metres of acceleration (Morin et al., 2015). This is supported by Colyer et al. (2018) who observed a positive association between better performances and higher amounts of anterior force during the mid-late propulsion phase of stance. During bend sprinting in the present study, the ability to produce propulsive impulse was reduced, and although a significant effect was not reported for braking impulse, large effect sizes were observed when comparing left step on the bend compared with the straight ($g = 1.29$). This suggests a greater braking impulse was experienced in the left step on the bend in comparison to the straight. Unlike Morin et al. (2015), acceleration performance during bend sprinting seems to be characterised by 'pushing less' and 'braking more' in comparison to the straight, particularly with the left foot. Therefore, it seems propulsive force production of the left foot may be a limiting factor for bend sprinting performance during the acceleration phase.

However, these reductions in propulsive force observed during bend sprinting are a necessary consequence of the additional requirement to produce centripetal force. In order to achieve this requirement, and stay in the correct lane, mediolateral force was greater on the bend compared with the straight for the majority (3-96%) of the stance phase. Whilst necessary for bend sprinting, it is possible the greater mediolateral

force is a contributing factor for the decrease in ratio of force found during bend sprinting compared with straight-line sprinting. In addition, the use of SPM revealed mediolateral force during bend sprinting was greater in the right step compared to the left during 1-12% of the stance phase. Whereas later in stance (75-100%) mediolateral force was greater in the left step than right, thus further establishing the left foot as fulfilling a different role to the right foot during bend sprinting. These asymmetries demonstrate the benefit of SPM analysis, which has provided new insights that may have been lost with the analysis of discrete values.

In comparison to straight-line sprinting, bend sprinting elicited an 11% and 22% decrease in mean ratio of force for the left and right steps, respectively. A higher ratio of force has been associated with better acceleration performance (Morin et al., 2011). This reinforces the notion that athletes apply propulsive force less effectively during bend sprinting and therefore the generation and orientation of force appear a limiting factor to acceleration performance on the bend when compared with straight-line sprinting. It appears this may be due to the combination of a reduction in propulsive force and an essential increase in mediolateral force. Whilst the right step experienced a decrease in ratio of force on the bend, right step ratio of force was 8% greater than the left step on the bend ($g = 0.88$). Thus, there appear to be asymmetries in force production of the left and right limb during bend sprinting, with the right being more effective at propulsive force production. However, it is possible that ratio of force requires further evaluation during bend sprinting. For example, although reducing mediolateral force would achieve the desired outcome of increasing ratio of force, doing so would prevent the athlete from maintaining a curved path. Therefore, as mediolateral force is a necessary component of bend sprinting, rather than achieving

the highest ratio possible, it is likely there is an optimum ratio that balances the production of propulsive and mediolateral forces.

Ratio of force analysis provides an overview of force orientation and a reduction was reported in both left and right steps on the bend compared with the straight. This finding is reinforced when considering impulse, which, as the product of force and time, acts as a metric to evaluate force application. Despite longer left step contact times, reductions in the magnitude of force resulted in a decrease in propulsive impulse that was greater in the left step. Therefore, it appears the decrease in acceleration performance at approximately 12 m phase is largely due to changes in left step force orientation and application.

A mechanism behind the reported changes in force production during bend sprinting might be the use of different MTP joint push-off axes. Results showed that left step mean mediolateral CoP position was more lateral on the bend than the straight, suggesting the oblique axis is used to push-off with the left step during bend sprinting, supporting the hypothesis put forward by Churchill et al. (2016). The oblique axis is considered less effective for push-off at high speeds (Bojsen-Moller, 1979). However, during bend sprinting, the use of the oblique axis seems a necessary adaptation (dictated by the need to produce centripetal force) required to aid the change of direction. The mean mediolateral CoP position for the right step on the bend was more medial than on the straight, thus the transverse axis was in use for both bend and straight conditions. This further reinforces the notion that the right step and left steps perform different functions during bend sprinting. The left limb appears to have a controlling role, focussed upon producing the necessary rotation and centripetal force required during bend sprinting. In contrast, the right limb appears to produce

movement in the anterior direction, sharing more similar characteristics to those demonstrated during straight-line sprinting.

Although resultant and vertical forces were unaffected by the bend, the results demonstrate a reduction in the ability to produce anterior force during bend sprinting. This was combined with a lower mean ratio of force, suggesting athletes apply propulsive force less effectively during bend sprinting. There was an increase in mediolateral force on the bend, which was greater in the left step compared with the right demonstrating asymmetry between limbs. Whilst the observed mean θ_{SYM} value for mediolateral impulse was comparable on the bend (10.98 ± 10.66) and straight (11.70 ± 12.83), mediolateral force is often considered negligible during straight-line sprinting (Rabita et al., 2015). Likewise, the magnitude of mediolateral impulse generated on the straight in the current study was small (left step: 0.02 ± 0.10 m/s; right step: 0.04 ± 0.05 m/s). Therefore between-limb differences observed during straight-line sprinting are unlikely to be practically meaningful, as also suggested by the weak correlation reported (r = .044). Furthermore, in the left step, to aid with the change in direction, it was necessary for push-off to occur using the oblique axis at the MTP joint. However, similarly to straight-line sprinting, the right step maintained use of the transverse axis for push-off during bend sprinting. The asymmetries in force production and MTP joint axis suggest the left and right limb have different functional roles during bend sprinting.

There were some differences observed between the left and right limb on the straight that may not be expected (e.g., vertical impulse, g = 0.55). For vertical impulse, this resulted in a mean θ_{SYM} value of 9.48 ± 12.06 on the straight - which was twice as large as that observed on the bend (4.40 ± 2.55) and also higher than the maximum θ_{SYM} value of 6.0 reported by Exell et al. (2017) at maximal speed.

However, no significant correlations were observed relating this asymmetry to sprint performance. In addition, it was necessary to move the starting point for athletes to collect data for both the left and right step with a single force platform. The start blocks were moved a maximum of one metre forwards or backwards to facilitate a clean strike on the force platform in separate trials for the left and right steps. Consequently, athletes made contact with the force platform approximately 11 - 13 m from the start point. Therefore, asymmetry present when comparing the left and right limb may be somewhat exacerbated by the use of different steps which represent different levels of distance progressed within the acceleration phase. The number of steps taken by athletes is recorded in Appendix C. The distance run by all athletes was further in the left step, with the difference between left and right steps never greater than a single step. The step number and distance run was consistent for bend and straight comparisons by limb for all participants. However, work from Exell et al. (2017) suggested we should expect to see a certain level of asymmetry between limbs during straight-line sprinting, which is not necessarily dysfunctional or detrimental to performance. This notion is supported by Haugen, Danielsen, McGhie, Sandbakk, and Ettema (2018) who concluded that asymmetry within the sprint stride cycle is more likely the norm rather than the exception. This is likely pertinent when considering bend sprinters who perform sprints on the bend consistently in the same direction, and so asymmetry in muscle strength is expected. Moreover, kinematic lower limb asymmetries were not associated with maximal sprint running performance or the prevalence of injury among high-level athletic sprinters (Haugen et al., 2018).

6.5. Conclusion

The present study has identified differing functions in the force production of the left and right limb during bend sprinting. The need to produce centripetal force is

fulfilled primarily by the left leg, whilst the right limb serves to produce force in the anteroposterior direction. Therefore, training should be developed to fully reflect this, ensuring acceleration training takes place on the bend, and non-sagittal plane exercises are included in strength and conditioning programmes.

Chapter Seven: JOINT MOMENTS, POWER AND ENERGY IN BEND SPRINTING

THE WORK IN THIS CHAPTER FORMED THE BASIS OF THE FOLLOWING CONFERENCE PRESENTATION:

Judson, L. J., Churchill, S. M., Barnes, A., Stone, J. A. & Wheat, J. (2019). Lower extremity joint moments during the acceleration phase of bend sprinting. *Presented at the European College of Sports Science (ECSS) Congress,* Prague 2019.

AND PEER-REVIEWED JOURNAL ARTICLE:

Judson, L. J., Churchill, S. M., Barnes, A., Stone, J. A. & Wheat, J. (in press). Joint moments, power and energy in the acceleration phase of bend sprinting. *Journal of Biomechanics.*

7. Joint moments, power and energy in bend sprinting

7.1. Introduction

In comparison to straight-line sprinting, bend sprinting at maximal and sub-maximal speed induces several lower limb kinematic changes which occur predominantly in the frontal and transverse planes (Alt et al., 2015; Churchill et al., 2015, Chapter 5). These kinematic adaptations result in changes in spatio-temporal parameters such as contact time, step length and step frequency (Alt et al., 2015; Churchill et al., 2015; Churchill et al., 2016, Chapter 5). Furthermore, asymmetrical changes in force production are evident during bend sprinting, with Churchill et al. (2016) reporting a reduction in mean vertical force and peak resultant force in the left step but not the right step. In addition, mediolateral forces are greater during bend sprinting relative to the straight (Churchill et al., 2016). This increase in mediolateral force was also demonstrated in the acceleration phase (Chapter 6), where the use of SPM revealed greater mediolateral force during 3-96% of stance. The combination of these kinematic and kinetic adaptations result in a decrease in velocity on the bend compared to the straight (Churchill et al., 2015; Churchill et al., 2016, Chapter 5). Thus, furthering our understanding of bend sprinting and its associated limits may aid overall race performance in events such as the 200 and 400 m and the 4 x 100 m relay.

Chang and Kram (2007) hypothesised that muscles operating in the non-sagittal plane are at a critical threshold during bend sprinting at small radii (1-6 m). It was suggested the ability to sustain muscle forces in the frontal and transverse planes prevents the generation of necessary sagittal plane moments and consequently inhibits the production of ground reaction force in the direction of travel (Chang & Kram, 2007). This hypothesis has generally been accepted as a

plausible explanation within the bend sprinting literature (e.g., Alt et al., 2015; Churchill et al., 2015), however, has yet to be confirmed empirically in conditions representative of a competitive athletics environment.

There is some evidence at smaller radii which appears to refute the hypothesis of Chang and Kram (2007). For example, Luo and Stefanyshyn (2012a) introduced a wedged footwear condition during bend sprinting with a 2.5 m radius. In the wedged footwear condition, the midsole structure was modified with the aim of aligning the foot more neutrally and decreasing eversion during anti-clockwise bend sprinting. In the left step, a decrease in ankle eversion angle was observed, which coincided with an increase in plantar flexion moment and a 4.3% increase in speed compared with the control condition with no wedge. Whilst a decrease in non-sagittal plane moments was also observed at the ankle, an increase in non-sagittal plane moments was observed at the knee, suggesting the load was distributed elsewhere. If, as Chang and Kram (2007) suggested, the non-sagittal plane moments were operating at their critical limits and therefore preventing further generation of limb extension force, it would be expected that the participants continue to operate at the same threshold, regardless of experimental condition. However, the results from Luo and Stefanyshyn (2012a) demonstrate this not to be the case, although the right limb was not investigated. Moreover, in a further study from Luo and Stefanyshyn (2012b) which compared bend sprinting with and without an additional mass (achieved through a weighted vest), an increase in left limb non-sagittal plane moments was observed in the additional mass condition. Therefore, it appears the left limb possesses the ability to generate larger moments than demonstrated in the control 'without mass' condition but is prevented from doing so in some way. This provides further evidence against the hypothesis of Chang and Kram (2007) since the

increasing moments in the weighted condition demonstrate the limb was able to endure a greater external load.

At present, only Viellehner et al. (2016) have investigated joint moments with a radius representative of athletic bend sprinting competitions (36.5 m). An increase in left step ankle plantar flexion moment was observed during bend sprinting relative to the straight, although the sub-maximal effort is not representative of performance in a competitive environment. It is possible similar adaptations are present during the acceleration phase of bend sprinting. Therefore, there is a direct contradiction between what has been empirically evaluated within the literature (Luo & Stefanyshyn, 2012a, 2012b; Viellehner et al., 2016), and what has been hypothesised as possible within the bend sprinting community (Alt et al., 2015; Chang & Kram, 2007; Churchill et al., 2015). Thus, analysis of 3D joint moments at maximal effort and at radii representative of competitive athletics would provide insight into the function of each leg and the mechanisms of performance.

Whilst analysis of joint moments provides an indication of the magnitude of muscular force generation, calculation of joint powers and energies would provide further in-depth insight into joint function during bend sprinting. For example, during straight-line sprinting, the production of high propulsive ground reaction force is often associated with high hip extension angular velocity (Hunter et al., 2004a). When analysing the mid-acceleration phase of straight-line sprinting, Johnson and Buckley (2001) noted this forceful production of hip extension was possible due to a large power at the hip (3242 W). Furthermore, a proximal-distal sequencing of peak joint extension powers was observed during the stance phase (Johnson & Buckley, 2001). It is thought this sequential pattern is necessary to allow the transfer of power from proximal to distal joints and enable greater power generation by the smaller

muscles of the foot and ankle (Jacobs et al., 1996). Kinematic adaptations, such as a high peak hip adduction angles (e.g., 13.8°, Alt et al., 2015; 10.6 °, Churchill et al., 2015) and high peak ankle eversion (e.g., 12.7°, Alt et al., 2015) found during bend sprinting could not only impact upon the muscles' ability to produce forces in the sagittal plane, but also disrupt this sequencing, resulting in a decrease in sprint performance. Furthermore, it is possible the complex arrangement of the lower limb and associated non-sagittal plane adaptations are a risk factor for injury during bend sprinting. Analysis of joint kinetics would establish the net demand of the joint and surrounding musculature, thus being influential in developing strength and conditioning and injury prevention programmes. Therefore, investigation of joint kinetics during bend sprinting is required. These findings would enable strength and condition programmes to target the strengthening of specific muscles to improve bend sprinting performance and also decrease the risk of injury.

The aim of this study was to investigate joint moments, power and energies of the lower limb during sprinting on the bend compared with the straight. In line with the empirical evidence presented, it was hypothesised that increased frontal and transverse plane moments would be greater on the bend compared with the straight.

7.2. Methods

7.2.1. Participants

Following ethical approval from Sheffield Hallam University, seven male sprinters (mean age 22 ± 4 years; body mass 68.32 ± 6.98 kg; stature 1.79 ± 0.06 m) volunteered to participate in the study. The inclusion criteria required a 200 m personal best of 23.5 s or faster, consequently, all athletes were experienced bend sprinters (personal bests: 21.8 - 23.43 s) in full training and with no history of injury in the six

months before testing. Participants provided written informed consent having had the study procedures fully explained and the opportunity to ask any questions.

7.2.2. Experimental set-up

The experimental set-up is demonstrated in section 0. A 15-camera optoelectronic motion capture system (13 x Raptor model and 2 x Eagle model, Motion Analysis Corporation, Santa Rosa, CA, USA) sampling at 200 Hz was used to collect kinematic data. A rigid L-frame with four markers at known locations was used to define a right-handed laboratory coordinate system. The direction of progression was most closely aligned with the positive *x*-axis, where the positive *y*-axis was directed vertically upwards, and the positive *z*-axis was mediolateral, pointing to the athletes' right. Individual intrinsic and extrinsic parameters of the 15 optoelectronic cameras were scaled using a three-marker wand (length: 500 mm) within the calibration volume (7 m long, 3 m wide and 1.5 m high), located tangentially to the apex of the curve to record data through the 10 - 17 m section of the 30 m sprints (see Chapter 5, Figure 5.2.1.1). Torso, pelvis, thighs, shanks and feet segments (toebox, forefoot, rearfoot) were modelled using a modified Vicon Plug-in Gait (PiG) marker set (lower limb and trunk, 4.2.2).

A Kistler force plate (Model: 9287BA, 900 x 600 mm) embedded into the track surface at approximately 12 m was used to collect kinetic data (1000 Hz). Kinetic and kinematic data were synchronised using a rising edge 5 V signal from the force plate at the onset of data collection.

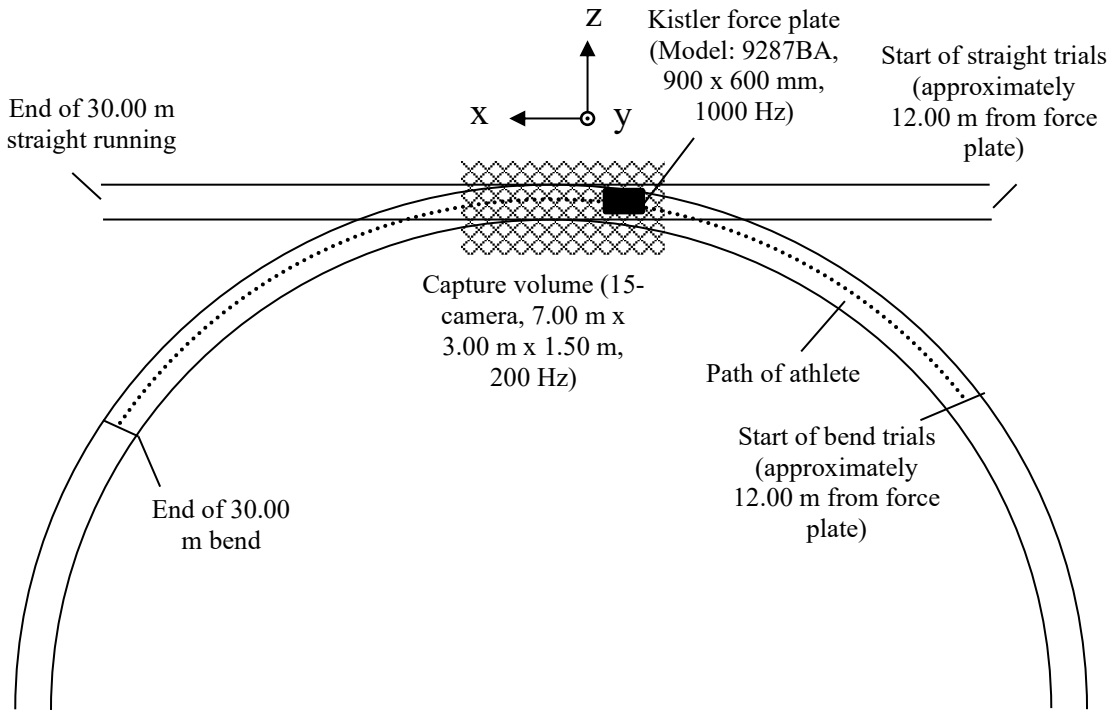

Figure 7.2.1.1 Plan view of experimental set-up (not to scale).

7.2.3. Protocol

Data were collected on a 30 m section of straight track for straight-line trials. A bend replicating lane 1 (radius 36.5 m) of a standard 400 m running track (IAAF, 2008) was reconstructed on a flat section of indoor track for bend trials. The order of experimental conditions was randomised to minimise order effects.

Participants completed their typical competition warm-up before performing a maximum of six 30 m sprints at maximal effort in each condition (bend and straight). To maintain the representativeness of the protocol, starting blocks and an '*on your marks, set, go*' signal was used. A successful trial was defined as contact being made with the force plate without changes to their running gait caused by 'targeting'. To reduce the risk of targeting, athletes were not informed of the location of the force plate. Instead, one researcher modified the start location of the athletes to aid the athlete in making contact with the force plate. Approximately eight minutes were

allowed between trials to allow full recovery and avoid the onset of fatigue (Churchill et al., 2015). Participants wore their own sprint spikes for the testing session.

7.2.4. Data processing

Raw 3D marker coordinate data were analysed using Cortex software (version 5.3, Motion Analysis Corporation, Santa Rosa, CA, USA). Automatic gap filling using a cubic spline was performed with all gaps <10 frames. Visual 3D (version 6, C-Motion, Rockville, MD, USA) was used to define and construct segments, LCS and joint centres in line with ISB guidelines (Wu et al., 2002; Wu et al., 2005) for the majority of segments. However, the joint coordinate system for the multi-segment foot was defined in accordance with Cappozzo et al. (1995).

A lower limb and trunk model was used, having been previously established as appropriate for whole-body CoM calculations (Chapter 3). Previous work from Bezodis et al. (2012) established that, when excluding the MTP joint from moment and power analyses of the lower limb, peak moments at the ankle were artificially high. Due to the linked segment nature of inverse dynamics, this consequently affected the accuracy of knee and hip joint kinetics (Bezodis et al., 2012). Thus, Bezodis et al. (2012) advocated the use of a multi-segment foot in sprint analyses of the lower limb. This was supported by Zelik and Honert (2018) who suggest a single segment foot is inappropriate for calculations of ankle power, which should instead be computed about the shank-calcaneus joint. Therefore, a multi-segment foot model (toebox, forefoot and rearfoot) was used.

Body segment parameters were estimated from (de Leva, 1996), recommended by Rao et al. (2006) as the most accurate regression equations for use in the assessment of joint kinetics. Owing to the small mass of the foot, it is unlikely that body segment parameters have a significant influence over the calculation of inverse dynamics

(Bruening & Takahashi, 2018). Therefore, body segment parameter estimates for a single segment foot were applied to each segment of the multi-segment, foot based upon individual segment length, as is the case with previous gait research (Deschamps et al., 2017; Dixon et al., 2012). Adapting methods of Hunter et al. (2004b), multi-segment foot values were adjusted by 0.150 to 0.189 kg (according to manufacturer specification) representing the mass of individual participants' spiked shoe. Owing to the use of a multi-segment foot, this additional mass required redistribution amongst each segment. A number of methods have been implemented within previous literature such as CT scans (Saraswat et al., 2010; Saraswat et al., 2014); distribution based on the relative forefoot:rearfoot length (Bezodis et al., 2012; Bruening et al., 2012) and arbitrary use of 50:50 for forefoot:rearfoot (Dixon et al., 2012) For the purpose of the present study, the distribution based on relative segment length was considered the most feasible and appropriate.

Kinetic data were analysed using Matlab (v2017a, Mathworks, Natick, USA). Large fluctuations in knee joint moments during sprinting have been observed when filtering kinematic and kinetic data at different cut-off frequencies (Bezodis et al., 2013). Therefore, both kinetic and kinematic force data were filtered with a low-pass, fourth-order recursive Butterworth filter 18 Hz cut-off frequency, chosen with the use of residual analysis.

One successful trial per condition and participant was analysed. CV was calculated for a sample of key variables where additional trials were available (Appendix D). CV was ≤ 10 % for peak MTP moment (1.80 - 9.26 %) and peak hip adductor moment (2.98 - 10.28 %), whilst one participant demonstrated a CV of 16.22 % for peak hip flexor moment, the remaining values were ≤ 10 % (1.88 - 9.45). Atkinson and Nevill (1998) suggest a CV of 10 % or less indicates very good

reliability, thus the CV results presented support the use of a single trial for further analysis. This is further supported by Johnson and Buckley (2001) who demonstrated high intra-individual consistency in sprint trials (alpha coefficients of 0.95 to 0.99 for hip, knee and ankle angles and vertical and horizontal ground reaction forces), establishing one trial was sufficient for analysis of joint kinetics. Where more than one successful trial was available, the first successful trial was selected for analysis. *Touchdown* and *take-off events* were identified from vertical ground reaction force using the mean plus two standard deviations of the last three seconds of data (where there was zero load on the force plate) as a threshold (Bezodis et al., 2007). All variables were calculated separately for the left and right step. Steps were defined by the foot that initiated the step.

Joint moments were calculated in Visual 3D (version 6, C-Motion, Rockville, MD, USA) and expressed in the joint coordinate system, discussed in section 2.8.2. In previous sprint research, this issue of force redistribution amongst foot segments has not needed addressing, since sprinters tend to remain on their toes throughout early acceleration (Bezodis, Salo, & Trewartha, 2010; Bezodis et al., 2012). Therefore, the entire ground reaction force can be allocated to the MTP joint. However, qualitative analysis of the trials within the current body of work established a small number of frames where the heel came into contact with the ground, resulting in the centre of pressure passing proximally to the MTP joint and therefore requiring the redistribution of force (see section 2.8.2. for discussion). Consequently, joint moment data were cropped to the propulsive phase of stance (identified using the corresponding anteroposterior force), at which point the centre of pressure was distal to the MTP joint. Joint moment data were normalised to body weight and height (Hof, 1996,

adapted from leg length to maintain consistency with previous sprint literature such as Charalambous et al., 2012).

As Schache and Baker (2007) noted, expression of joint moments in the joint coordinate system is purely for representation purposes, and thus, any further calculations should be completed in an orthogonal reference frame. Therefore, *joint powers* were calculated in Matlab (v2017a, Mathworks, Natick, USA) using the following equations and non-normalised joint moments expressed in the proximal segment reference frame:

$$Power = \vec{F} \cdot \vec{\omega} \qquad \textit{Equation 20}$$

where $\vec{F}$ represents force (moment) and $\vec{\omega}$ represents angular velocity. As the dot product of two vectors, power is a scalar quantity. As such, it is mathematically incorrect to split power into its components; since a one-dimensional calculation of power might not represent the actual rate work is performed in three-dimensions. However, as Vigotsky, Zelik, Lake, and Hinrichs (2019) noted, there may be circumstances where directional components of power remain of interest, and therefore it should not necessarily be disregarded. Bend sprinting has been shown as multi-dimensional, with kinematic adaptations occurring predominantly in the frontal and transverse planes (Alt et al., 2015; Churchill et al., 2015). Consequently, the analysis of directional powers is necessary for gaining an in-depth understanding of the mechanisms required for sprinting on the bend. Therefore, power data were calculated in each direction and normalised using the following equation (Hof, 1996, modified by Bezodis et al., 2010):

$$\frac{\vec{P}}{m \cdot g^{3/2} \cdot h^{1/2}}$$ *Equation 21*

where $\vec{P}$ is power, m is the mass of the sprinter, g is gravitational acceleration and h is the height of the sprinter.

Energy was calculated as the integral of the non-normalised power-time curve, and cumulative positive and negative phases represent energy generation and absorption, respectively. Energy data were normalised to body weight and height (Hof, 1996).

7.2.5. Statistical analysis

Descriptive statistics (mean and standard deviation) were calculated for all variables. The Shapiro-Wilk normality test ($p > 0.05$) was used to assess the normal distribution of the data for each variable. Two-way repeated measures ANOVAs were performed where condition (bend vs. straight) x limb (left vs. right) were analysed. It is acknowledged that the sample size in this study was small and that this inflates the type II familywise error rate. As such, effect size (Hedges' *g,* Equation 16) was used to give an indication of the magnitude of the effect, interpreted with reference to Cohen (1988) guidelines where $g < 0.20$ represents a trivial difference, $0.20 \geq 0.50$ indicating a small difference, $0.50 \geq 0.80$ a moderate difference and ≥ 0.80 a large difference between means.

7.3. Results

Joint angle, moment and power across the propulsive phase of stance are shown in Figures 7.3.1.1-4.

7.3.1. Joint moments

For peak hip flexor moment, there was no significant condition x limb interaction ($F_{(1, 6)} = 0.57$, $p = 0.48$). Although the main effect for condition was non-significant ($F_{(1, 6)} = 4.47$, $p = 0.08$, Table 7.3.2.1), a large and moderate effect size

(g = 1.10, 0.70) suggest a trend towards a decrease in peak hip flexor moment for the left and right steps on the bend compared with the straight, respectively. This was also the case for peak knee flexor moment, where a large effect size (g = 1.06) suggests a decrease in peak knee flexor moment was observed during the left step of bend sprinting compared with the straight. However, the condition x limb interaction was non-significant ($F_{(1, 6)} = 4.66$, $p = 0.07$). There was no significant condition x limb interaction for hip adduction ($F_{(1, 6)} = 2.84$, $p = 0.14$). However, there was a trend towards a large ($g = 0.85$) increase in peak left step hip adductor moment during sprinting on the bend relative to the straight.

A trend towards a large ($g = 1.07$) increase in peak left step ankle plantar flexion moment was also observed on the bend compared with the straight, although a significant interaction was not found ($F_{(1, 6)} = 2.33$, $p = 0.18$, Table 7.3.2.2). For peak MTP joint plantar flexor moment, the condition x limb interaction was non-significant ($F_{(1, 6)} = 0.06$, $p = 0.81$). However, there was a main effect for limb due to a larger plantar flexor moment in the right MTP joint than left ($F_{(1, 6)} = 8.46$, $p = 0.03$, $g = 0.53$). Moderate and large effect sizes ($g = 0.50$, 1.90) suggest a trend towards a greater plantar flexor moment on the bend than straight in the right and left MTP joints, respectively.

For peak ankle eversion moment, there was no significant condition x limb interaction ($F_{(1, 6)} = 0.70$, $p = 0.43$). However, a main effect for limb was observed, $F_{(1, 6)} = 26.00$, $p < 0.01$, due to an increase in left step peak ankle eversion moment on the bend compared with and the right step on the bend ($g = 1.23$). There was also a large effect size suggesting a greater left step peak ankle eversion moment on the bend than straight ($g = 0.82$). There was no significant condition x limb interaction for midfoot eversion ($F_{(1, 6)} = 3.20$ $p = 0.12$). However, a moderate increase in left step

peak midfoot eversion moment was observed during bend sprinting compared with the straight (g = 0.65) and also when compared with the right step on the bend (g = 1.31).

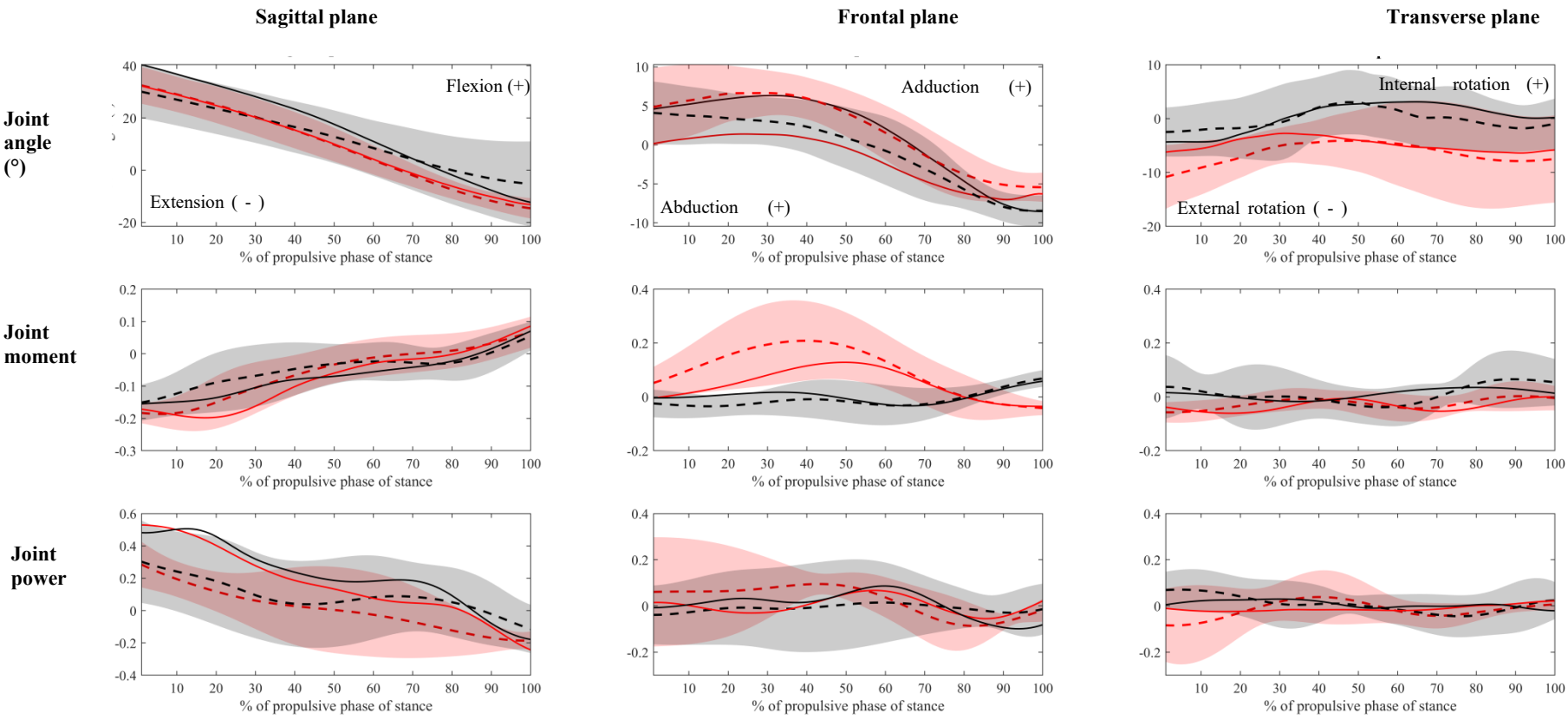

Figure 7.3.1.1 Hip joint angle, joint moment and joint power for the left (red) and right (black) steps on the bend (dashed line - - -) and straight (solid line —).

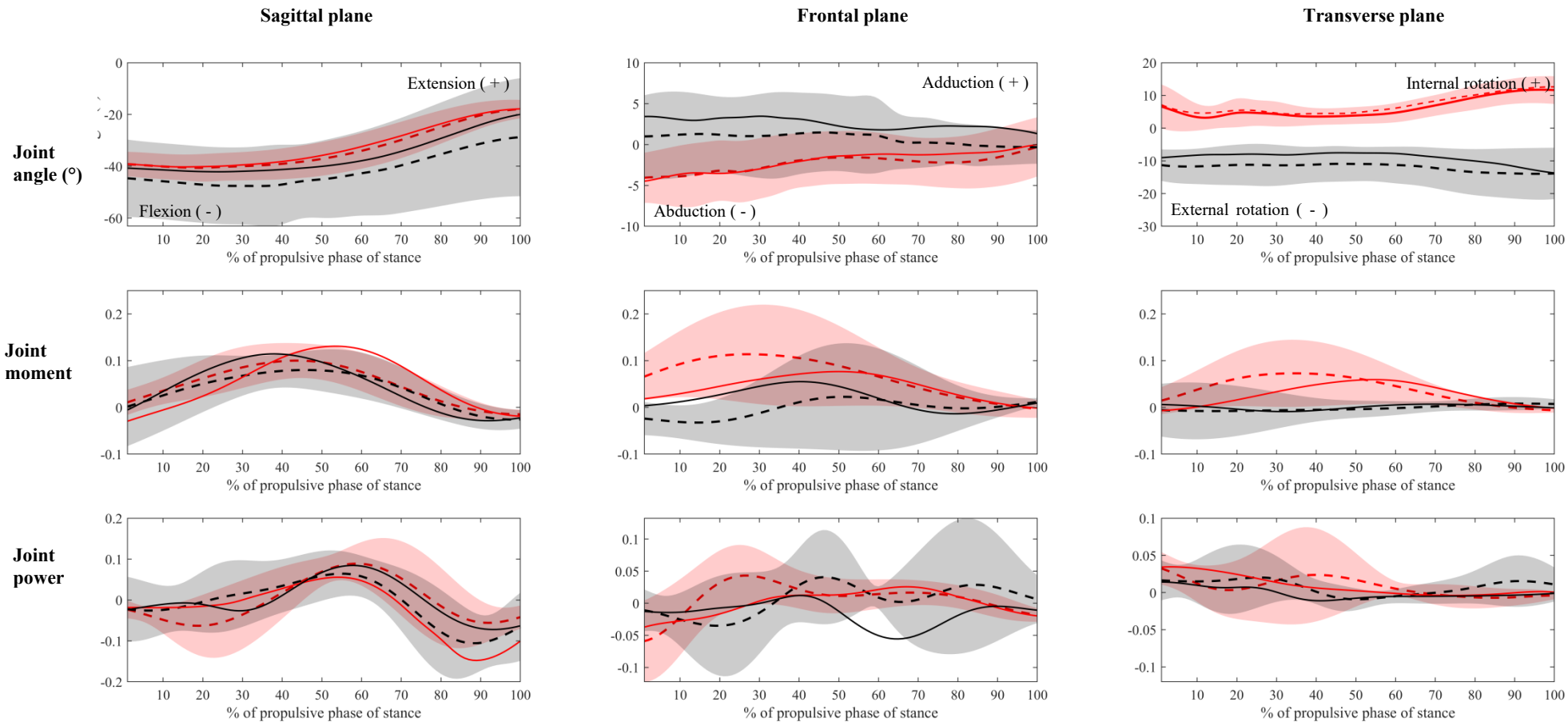

Figure 7.3.1.2 Knee joint angle, joint moment and joint power for the left (red) and right (black) steps on the bend (dashed line - - -) and straight (solid line —).

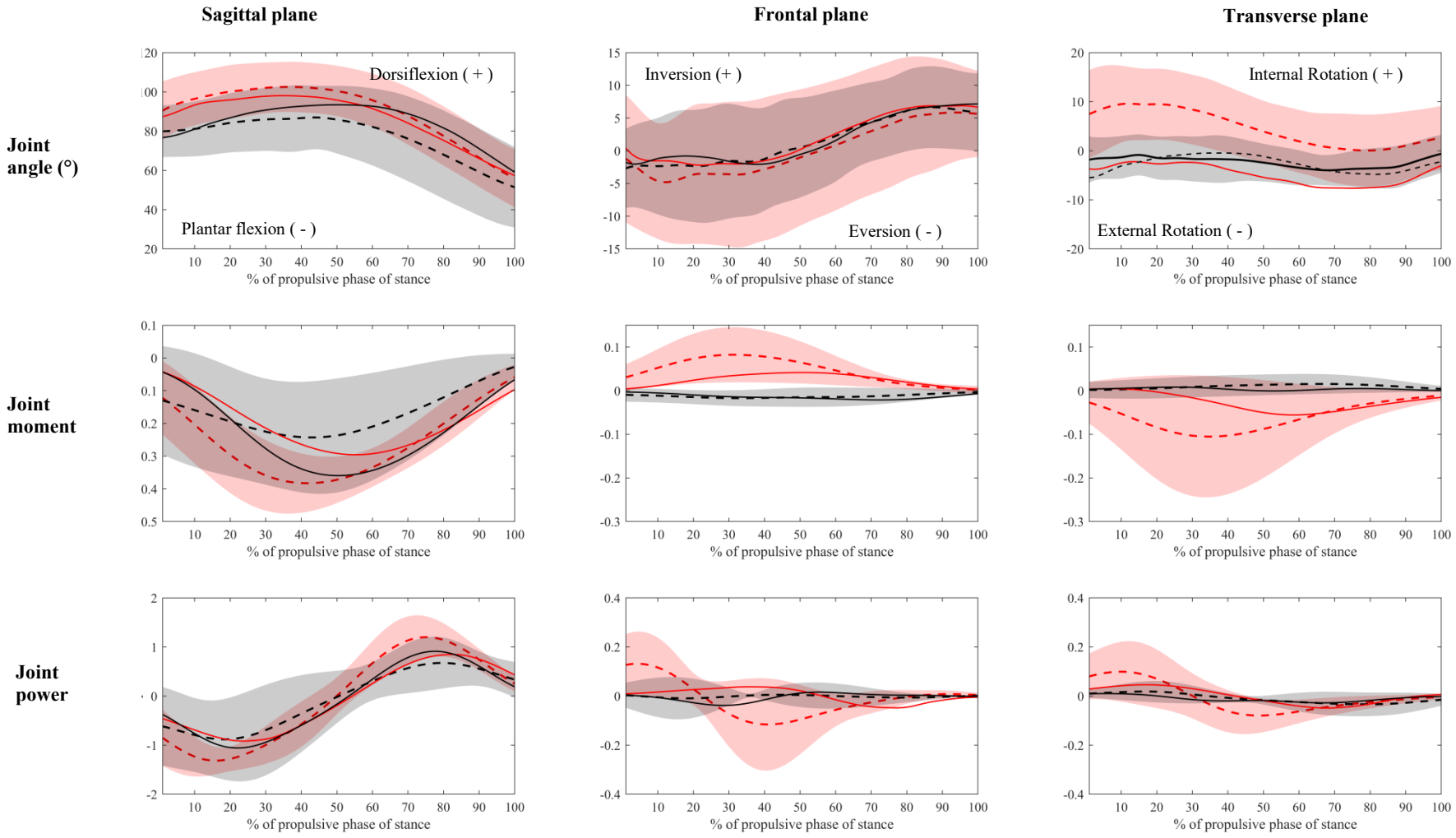

Figure 7.3.1.3 Ankle joint angle, joint moment and joint power for the left (red) and right (black) steps on the bend (dashed line - - -) and straight (solid line ——).

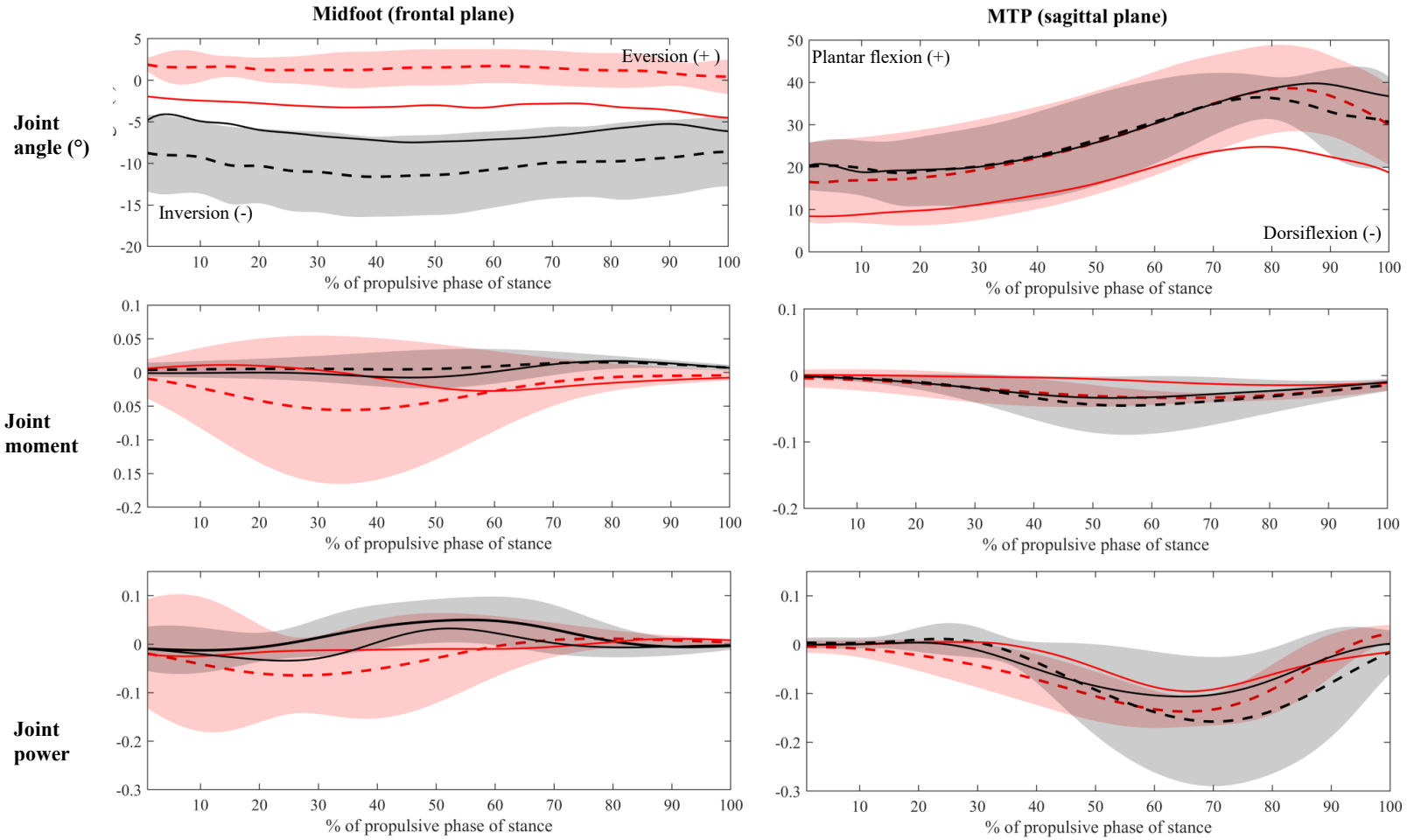

Figure 7.3.1.4 Midfoot and MTP joint angle, joint moment and joint power for the left (red) and right (black) steps on the bend (dashed line - - -) and straight (solid line ——).

7.3.2. Joint power and energy

At the hip joint, no significant condition x limb interactions for peak power in the sagittal plane (positive: $F_{(1, 6)} = 0.06$, $p = 0.82$, negative: $F_{(1, 6)} = 0.23$, $p = 0.65$, Table 7.3.2.3) or sagittal plane energy (generated: $F_{(1, 6)} = 0.02$, $p = 0.88$, absorbed: $F_{(1, 6)} = 0.97$, $p = 0.36$) were observed. Although there was no significant condition x limb interaction ($F_{(1, 6)} = 1.59$, $p = 0.25$), there was a large effect size ($g = 0.82$), suggesting a trend towards an increase in left step peak positive hip power in the frontal plane during bend sprinting compared with the straight (main effect, limb: $F_{(1, 6)} = 6.29$, $p = 0.05$). There was also a moderate ($g = 0.63$) increase in left step peak negative hip power in the transverse plane during bend sprinting relative to the straight. However, no significant condition x limb interaction was reported ($F_{(1, 6)} = 2.88$, $p = 0.14$). Although there was no significant condition x limb interaction for hip joint energy absorption in the frontal plane ($F_{(1, 6)} = 0.31$, $p = 0.60$), there was a main effect for condition ($F_{(1, 6)} = 17.29$, $p = 0.01$) due to increased energy absorption during sprinting on the bend compared with the straight (left step, $g = 1.12$, right step $g = 0.89$, Table 7.3.2.5).

At the ankle, there was no significant condition x limb interaction for peak negative sagittal plane joint power ($F_{(1, 6)} = 0.05$, $p = 0.841$. Table 7.3.2.4), although a moderate increase ($g = 0.61$) in left step peak sagittal plane negative joint power was observed in the (main effect limb: $F_{(1, 6)} = 3.174$, $p = 0.15$). This was combined with a large, but non-significant, increase in left step sagittal plane ankle energy absorption on the bend compared with the straight (main effect limb: $F_{(1, 6)} = 3.287$, $p = 0.13$, $g = 0.80$). The condition x limb interaction was non-significant for peak positive transverse plane ankle power ($F_{(1, 6)} = 1.13$, $p = 0.34$). However, there was a moderate

increase in peak positive left step ankle power in the transverse plane during bend sprinting relative to the straight (main effect limb: $F_{(1, 6)} = 4.800$, $p = 0.08$, $g = 0.76$). There was no significant condition x interaction for transverse plane ankle energy absorption ($F_{(1, 6)} = 3.87$, $p = 0.10$, Table 7.3.2.6). However, the effect size ($g = 1.08$) suggests an increase in left step transverse plane ankle energy absorption during sprinting on the bend relative to the straight.

At the MTP joint, no significant condition x limb interaction was found ($F_{(1, 6)} = 0.261$, $p = 0.627$). However, there were large and moderate effect sizes ($d = 0.95, 0.52$) suggesting increases in peak negative joint power for the left and right step, respectively (main effect condition: $F_{(1, 6)} = 6.27$, $p = 0.05$). This was related to an increase in MTP joint energy absorption (main effect condition: $F_{(1, 6)} = 7.14$, $p = 0.04$) on the bend compared with the straight (left step, $d = 1.68$, right step, $d = 0.30$). For midfoot peak positive power, there was a main effect for condition, $F_{(1, 6)} = 48.04$, $p < 0.01$, due to an increase in peak positive midfoot power in both the left ($g = 1.20$) and right ($g = 0.74$) step on the bend compared with the straight. For peak negative midfoot power, there was a main effect for limb ($F_{(1, 6)} = 19.683$, $p < 0.01$, due to an increase in peak negative midfoot power in the left step compared with the straight ($g = 1.45$).

Table 7.3.2.1 Peak joint moments for hip and knee joints Group mean values (± standard deviation), effect sizes (% difference) of the left and right step. Significant main effects are marked with *. Significant interactions are marked with #.

Peak moment during the propulsive phase of stance (dimensionless)	Straight		Bend		Effect size (*g*)			
	Left	Right	Left	Right	Left vs. right straight	Left vs. right bend	Straight vs. bend left	Straight vs. bend right
Hip extension	-0.238 ± 0.138	-0.179 ± 0.047	-0.204 ± 0.066	-0.179 ± 0.061	0.39 (34%)	0.29 (14%)	0.34 (15%)	0.00 (0%)
Hip flexion	0.138 ± 0.074	0.104 ± 0.053	0.070 ± 0.046	0.068 ± 0.034	0.24 (27%)	0.00 (3%)	1.10 (49%)	0.70 (44%)
Hip adduction	0.130 ± 0.057	0.122 ± 0.093	0.217 ± 0.133	0.079 ± 0.036	0.13 (12%)	1.39 (173%)	0.85 (67%)	0.55 (35%)
Hip abduction	-0.062 ± 0.034	-0.067 ± 0.055	-0.059 ± 0.058	-0.063 ± 0.057	0.00 (3%)	0.00 (7%)	0.00 (5%)	0.00 (0%)
Hip internal rotation	0.050 ± 0.033	0.090 ± 0.036	0.040 ± 0.025	0.118 ± 0.074	1.07 (44%)	1.48 (65%)	0.37 (20%)	0.50 (31%)
Hip external rotation	-0.098 ± 0.017	-0.054 ± 0.049	-0.088 ± 0.028	-0.086 ± 0.060	1.21 (82%)	0.00 (3%)	0.37 (9%)	0.69 (60%)
Knee flexion	-0.058 ± 0.048	-0.040 ± 0.023	-0.019 ± 0.012	-0.041 ± 0.023	0.50 (42%)	1.20 (53%)	1.06 (67%)	0.01 (1%)
Knee extension	0.157 ± 0.129	0.127 ± 0.064	0.108 ± 0.032	0.105 ± 0.033	0.30 (24%)	0.00 (3%)	0.50 (32%)	0.40 (17%)
Knee abduction	0.187 ± 0.154	0.094 ± 0.117	0.143 ± 0.099	0.060 ± 0.077	0.70 (107%)	0.84 (140%)	0.37 (36%)	0.28 (36%)
Knee adduction	-0.002 ± 0.020	-0.047 ± 0.041	0.009 ± 0.017	-0.036 ± 0.031	1.12 (76%)	1.50 (95%)	0.48 (73%)	0.27 (31%)
Knee internal rotation	-0.012 ± 0.007	-0.024 ± 0.032	-0.010 ± 0.008	-0.026 ± 0.050	0.43 (48%)	0.53 (61%)	0.00 (18%)	0.23 (10%)
Knee external rotation	0.061 ± 0.058	0.021 ± 0.010	0.077 ± 0.063	0.019 ± 0.009	0.88 (191%)	1.33 (308%)	0.32 (26%)	0.00 (10%)

Table 7.3.2.2 Peak joint moments for ankle, midfoot and MTP joints**.** Group mean values (± standard deviation), effect sizes (% difference) of the left and right step. Significant main effects are marked with *. Significant interactions are marked with #.

Peak moment during the propulsive phase of stance (dimensionless)	**Straight**		**Bend**		**Effect size (*g*)**			
	Left	**Right**	**Left**	**Right**	**Left vs. right straight**	**Left vs. right bend**	**Straight vs. bend left**	**Straight vs. bend right**
Ankle dorsiflexion	-0.017 ± 0.026	0.001 ± 0.009	-0.034 ± 0.026	0.003 ± 0.018	0.85 (1328%)	1.12 (1077%)	0.32 (98%)	0.05 (307%)
Ankle plantar flexion	0.309 ± 0.061	0.358 ± 0.077	0.391 ± 0.081	0.378 ± 0.054	0.67 (14%)	0.14 (3%)	1.07 (36%)	0.29 (5%)
Ankle inversion	0.001 ± 0.010	-0.023 ± 0.021	0.001 ± 0.010	-0.024 ± 0.019	1.49 (105%)	1.67 (105%)	0.01 (9%)	0.05 (5%)
Ankle eversion	0.047 ± 0.047	0.009 ± 0.012	0.098 ± 0.063	0.025 ± 0.038	1.34 (409%)	1.23 (259%)*	0.82 (91%)	0.55 (172%)
Ankle internal rotation	0.004 ± 0.011	0.020 ± 0.020	0.003 ± 0.011	0.020 ± 0.022	0.95 (84%)	1.03 (82%)	0.04 (15%)	0.03 (3%)
Ankle external rotation	-0.063 ± 0.059	-0.016 ± 0.022	-0.117 ± 0.123	-0.034 ± 0.050	0.85 (291%)	0.93(246%)	0.60 (85%)	0.25 (110%)
Midfoot inversion	0.003 ± 0.015	0.019 ± 0.009	0.005 ± 0.010	0.021 ± 0.008	1.33 (84%)	1.70 (76%)	0.16 (64%)	0.23 (10%)
Midfoot eversion	-0.054 ± 0.046	-0.056 ± 0.075	-0.097 ± 0.088	-0.011 ± 0.016	0.16 (2%)	1.31 (798%)	0.65 (78%)	0.93 (81%)
MTP dorsiflexion	0.013 ± 0.025	0.008 ± 0.007	0.003 ± 0.006	0.002 ± 0.002	0.30 (70%)	0.63 (55)	0.06 (11%)	1.05 (72%)
MTP plantar flexion	-0.020 ± 0.014	-0.040 ± 0.018	-0.039 ± 0.012	-0.064± 0.056	1.20 (51%)	0.53 (40%)	1.90 (98%)*	0.50 (62%)*

Table 7.3.2.3 Peak power values for the hip and knee joints. Group mean values (± standard deviation), effect sizes (% difference) of the left and right step. Significant main effects are marked with *. Significant interactions are marked with #.

Peak power during the propulsive phase of stance (dimensionless)	Straight		Bend		Effect size (*g*)			
	Left	Right	Left	Right	Left vs. right straight	Left vs. right bend	Straight vs. bend left	Straight vs. bend right
Hip sagittal (concentric)	0.519 ± 0.217	0.557 ± 0.219	0.515 ± 0.092	0.525 ± 0.171	0.17 (7%)	0.07 (2%)	0.03 (15%)	0.02 (0%)
Hip sagittal (eccentric)	-0.261 ± 0.104	-0.270 ± 0.094	-0.231 ± 0.072	-0.273 ± 0.090	0.10 (4%)	0.47 (16%)	0.33 (11%)	0.04 (1%)
Hip frontal (concentric)	0.119 ± 0.064	0.104 ± 0.048	0.232 ± 0.171	0.099 ± 0.085	0.34 (15%)	0.93 (135%)	0.82 (94%)	0.08 (5%)
Hip frontal (eccentric)	-0.104 ± 0.065	-0.159 ± 0.138	-0.145 ± 0.083	-0.141 ± 0.119	0.51 (35%)	0.10 (3%)	0.78 (39%)	0.14 (11%)
Hip transverse (concentric)	0.064 ± 0.054	0.115 ± 0.054	0.073 ± 0.090	0.139 ± 0.05	0.94 (44%)	0.92 (48%)	0.13 (13%)	0.57 (21%)
Hip transverse (eccentric)	-0.092 ± 0.062	-0.087 ± 0.050	-0.172 ± 0.157	-0.087 ± 0.080	0.09 (6%)	0.60 (99%)	0.63 (87%)	0.00 (0%)
Knee sagittal (concentric)	0.095 ± 0.042	0.122 ± 0.109	0.107 ± 0.037	0.104 ± 0.045	0.34 (22%)	0.24 (3%)	0.47 (13%)	0.23 (15%)
Knee sagittal (eccentric)	-0.161 ± 0.058	-0.151 ± 0.071	-0.115 ± 0.042	-0.151 ± 0.044	0.15 (6%)	0.71 (24%)	0.75 (28%)	0.00 (0%)
Knee frontal (concentric)	0.050 ± 0.041	0.046 ± 0.037	0.061 ± 0.037	0.098 ± 0.066	0.00 (8%)	0.50 (30%)	0.24 (22%)	0.67 (89%)
Knee frontal (eccentric)	-0.062 ± 0.038	-0.107 ± 0.146	-0.082 ± 0.070	-0.059 ± 0.052	0.43 (42%)	0.33 (40%)	0.31 (33%)	0.43 (45%)
Knee transverse (concentric)	0.055 ± 0.037	0.028 ± 0.014	0.030 ± 0.017	0.051 ± 0.033	0.65 (94%)	0.75 (42%)	0.60 (46%)	0.85 (81%)
Knee transverse (eccentric)	-0.014 ± 0.008	-0.021 ± 0.012	-0.019 ± 0.020	-0.025 ± 0.016	0.95 (30%)	0.00 (21%)	0.60 (34%)	0.00 (19%)

Table 7.3.2.4 Peak power for the ankle, midfoot and MTP joints. Group mean values (± standard deviation), effect sizes (% difference) of the left and right step. Significant main effects are marked with *. Significant interactions are marked with #.

Peak power during the propulsive phase of stance (dimensionless)	Straight		Bend		Effect size (*g*)			
	Left	Right	Left	Right	Left vs. right straight	Left vs. right bend	Straight vs. bend left	Straight vs. bend right
Ankle sagittal (concentric)	1.103 ± 0.161	0.965 ± 0.070	1.244 ± 0.380	0.993 ± 0.086	1.00 (48%)	0.86 (25%)	0.46 (13%)	0.24 (3%)
Ankle sagittal (eccentric)	-1.303 ± 0.383	-1.103 ± 0.251	-1.532 ± 0.338	-1.401 ± 0.391	0.59 (18%)	0.34 (9%)	0.61 (18%)	0.87 (27%)
Ankle frontal (concentric)	0.062 ± 0.043	0.052 ± 0.050	0.143 ± 0.118	0.042 ± 0.038	0.21 (19%)	1.06 (237%)	0.85 (134%)	0.21 (18%)
Ankle frontal (eccentric)	-0.074 ± 0.048	-0.044 ± 0.044	-0.153 ± 0.155	-0.044 ± 0.057	0.63 (66%)	0.87 (252%)	0.64 (108%)	0.02 (2%)
Ankle transverse (concentric)	0.042 ± 0.035	0.021 ± 0.019	0.111 ± 0.119	0.027 ± 0.030	0.74 (97%)	0.87 (311%)	0.76 (163%)	0.37 (26%)
Ankle transverse (eccentric)	-0.063 ± 0.041	-0.045 ± 0.044	-0.099 ± 0.070	-0.047 ± 0.045	0.24 (39%)	0.78 (109%)	0.67 (57%)	0.05 (4%)
Midfoot (concentric)	0.026 ± 0.016	0.040 ± 0.035	0.053 ± 0.012	0.063 ± 0.045	0.37 (35%)	0.60 (16%)	1.20 (100%)*	0.74 (56%)*
Midfoot (eccentric)	-0.063 ± 0.037	-0.050 ± 0.032	-0.142 ± 0.066	-0.041 ± 0.020	0.37 (25%)#	1.85 (243%)#	1.34 (124%)#	0.37 (18%)#
MTP sagittal (concentric)	0.015 ± 0.016	0.019 ± 0.018	0.028 ± 0.016	0.025 ± 0.022	0.22 (20%)	0.20 (14%)	0.83 (85%)	0.28 (31%)
MTP sagittal (eccentric)	-0.104 ± 0.084	-0.116 ± 0.046	-0.158 ± 0.035	-0.199 ± 0.133	0.28 (10%)	0.11 (6%)	0.95 (52%)	0.52 (44%)

Table 7.3.2.5 Energy generation and absorption at the hip and knee joints. Group mean values (± standard deviation), effect sizes (% difference) of the left and right step. Significant main effects are marked with *. Significant interactions are marked with #.

Energy during the propulsive phase of stance (dimensionless)	Straight		Bend		Effect size (*g*)			
	Left	Right	Left	Right	Left vs. right straight	Left vs. right bend	Straight vs. bend left	Straight vs. bend right
Hip sagittal (generated)	0.052 ± 0.045	0.061 ± 0.037	0.034 ± 0.018	0.047 ± 0.031	0.20 (13%)	0.48 (29%)	0.50 (36%)	0.39 (22%)
Hip sagittal (absorbed)	-0.011 ± 0.007	-0.011 ± 0.010	-0.016 ± 0.015	-0.010 ± 0.008	0.05 (4%)	0.51 (62%)	0.41 (40%)	0.12 (10%)
Hip frontal (generated)	0.006 ± 0.002	0.007 ± 0.005	0.017 ± 0.016	0.008 ± 0.007	0.25 (20%)	0.69 (109%)	0.92 (197%)	0.16 (13%)
Hip frontal (absorbed)	-0.005 ± 0.004	-0.003 ± 0.001	-0.011 ± 0.006	-0.007 ± 0.006	0.65 (74%)	0.64 (62%)	1.12 (101%)*	0.89 (117%)*
Hip transverse (generated)	0.003 ± 0.004	0.001 ± 0.008	0.004 ± 0.005	0.019 ± 0.027	0.30 (433%)	0.74 (79%)	0.21 (22%)	0.86 (2940%)
Hip transverse (absorbed)	-0.006 ± 0.004	-0.006 ± 0.006	-0.013 ± 0.013	-0.019 ± 0.031	0.10 (8%)	0.24 (32%)	0.69 (121%)	0.55 (202%)
Knee sagittal (generated)	0.006 ± 0.003	0.009 ± 0.009	0.007 ± 0.004	0.006 ± 0.003	0.43 (71%)	0.27 (4%)	0.27 (14%)	0.42 (31%)
Knee sagittal (absorbed)	-0.011 ± 0.004	-0.009 ± 0.008	-0.008 ± 0.004	-0.009 ± 0.004	0.30 (15%)	0.24 (10%)	0.71 (27%)	0.09 (6%)
Knee frontal (generated)	0.003 ± 0.003	0.002 ± 0.002	0.004 ± 0.003	0.005 ± 0.004	0.37 (42%)	0.27 (15%)	0.32 (37%)	0.90 (128%)
Knee frontal (absorbed)	-0.003 ± 0.002	-0.003 ± 0.001	-0.003 ± 0.002	-0.004 ± 0.003	0.29 (15%)	0.35 (25%)	0.29 (17%)	0.34 (28%)
Knee transverse (generated)	0.002 ± 0.003	0.001 ± 0.001	0.002 ± 0.001	0.003 ± 0.002	0.43 (95%)	0.79 (42%)	0.47 (38%)	1.20 (107%)
Knee transverse (absorbed)	-0.001 ± 0.001	-0.001 ± 0.001	-0.001 ± 0.001	-0.001 ± 0.000	0.21 (16%)	0.18 (18%)	0.24 (32%)	0.12 (6%)

Table 7.3.2.6 Energy generation and absorption at the ankle, midfoot and MTP joints. Group mean values (± standard deviation), effect sizes (% difference) of the left and right step. Significant main effects are marked with *. Significant interactions are marked with #.

Energy during the propulsive phase of stance (dimensionless)	Straight		Bend		Effect size (*g*)			
	Left	Right	Left	Right	Left vs. right straight	Left vs. right bend	Straight vs. bend left	Straight vs. bend right
Ankle sagittal (generated)	0.076 ± 0.021	0.056 ± 0.027	0.087 ± 0.018	0.055 ± 0.029	0.28 (12%)	1.31 (58%)	0.56 (14%)	0.04 (2%)
Ankle sagittal (absorbed)	-0.085 ± 0.036	-0.070 ± 0.038	-0.110 ± 0.022	-0.070 ± 0.052	0.39 (22%)	0.95 (57%)	0.80 (29%)	0.01 (1%)
Ankle frontal (generated)	0.003 ± 0.002	0.002 ± 0.002	0.005 ± 0.004	0.002 ± 0.003	0.48 (48%)	0.81 (126%)	0.61 (85%)	0.19 (21%)
Ankle frontal (absorbed)	-0.004 ± 0.002	-0.003 ± 0.003	-0.008 ± 0.008	-0.003 ± 0.004	0.30 (40%)	0.75 (208%)	0.65 (87%)	0.15 (15%)
Ankle transverse (generated)	0.003 ± 0.002	0.002 ± 0.003	0.005 ± 0.007	0.002 ± 0.002	0.37 (48%)	0.56 (245%)	0.37 (83%)	0.16 (21%)
Ankle transverse (absorbed)	-0.003 ± 0.003	-0.003 ± 0.003	-0.007 ± 0.004	-0.003 ± 0.004	0.23 (20%)	0.95 (29%)	1.08 (136%)	0.01 (1%)
Midfoot (generated)	0.002 ± 0.002	0.003 ± 0.003	0.005 ± 0.003	0.006 ± 0.006	0.37 (29%)	0.20 (21%)	1.12 (151%)	0.60 (82%)
Midfoot (absorbed)	-0.005 ± 0.003	-0.005 ± 0.003	-0.009 ± 0.004	-0.002 ± 0.001	0.16 (9%)	2.29 (308%)	1.07 (91%)*	1.28 (58%)*
MTP sagittal (generated)	0.001 ± 0.001	0.001 ± 0.001	0.000 ± 0.000	0.001 ± 0.001	0.25 (2%)	0.92(46%)	0.50 (37%)	0.05 (5%)
MTP sagittal (absorbed)	-0.006 ± 0.005	-0.011 ± 0.004	-0.014 ± 0.004	-0.013 ± 0.008	1.05 (42%)	0.15 (8%)	1.68 (133%)*	0.30 (26%)*

7.4. Discussion

This study aimed to compare joint kinetics during the acceleration phase of bend sprinting with straight-line sprinting. During bend sprinting, there was a large, but non-significant, decrease in peak flexor moment of the left hip (g = 1.10) and knee (g = 1.06) compared with straight-line sprinting. There was also a moderate decrease in peak flexor moment of the right hip (g = 0.70), although no change was observed at the right knee (g = 0.01). Changes in non-sagittal plane moments were also observed, with a large (g = 0.85) increase in peak left hip adduction moment.

During both straight-line and bend sprinting, sagittal plane hip moment was extensor for the majority of the propulsive phase of stance, becoming flexor dominant towards latter stages of ground contact. This pattern is similar to that found in previous research in early (Bezodis et al., 2014) to mid-acceleration (Johnson & Buckley, 2001) and maximal speed (Bezodis et al., 2008) during straight-line sprinting. A large effect size suggests a trend towards a lower hip flexor moment during sprinting on the bend compared with the straight. The need for a hip flexor moment towards the end of the stance phase has previously been attributed to the requirements of the hip flexors in driving the limb forward during the swing phase (Charalambous et al., 2012). Consequently, it is possible that athletes' experience difficulties repositioning the left leg on the bend due to the kinematic alterations such as greater hip adduction and external rotation observed in Chapter 5. Consequently, swing phase mechanics might also be of interest in understanding the mechanisms of bend sprinting performance.

Furthermore, there were moderate effect sizes suggesting a trend towards a greater left step peak negative frontal (g = 0.78) and transverse (g = 0.63) plane power at the hip on the bend than on the straight. This negative power indicates an eccentric contraction of the muscles surrounding the hip joint, which could be required to

stabilise the pelvis during sprinting on the bend since Segal, Yack, Brubaker, Torner, and Wallace (2009) suggested negative hip power in the frontal plane is likely associated with pelvic control. In walking gait, Shultz, Hills, Sitler, and Hillstrom (2010) noted the negative frontal plane hip power is due to the need to control for pelvic drop, whilst negative hip power in the transverse plane facilitates deceleration of forward rotation of the pelvis. Since the pelvis is mutually influenced by each limb, and the left and right limb have been shown to behave differently during bend sprinting (Chapter 5), a greater level of pelvic control is likely required to overcome these adaptations. Consequently, bend sprinting athletes and coaches should consider introducing muscle strengthening exercises targeted at reducing the amplitude of motions such as increased hip adduction. Research suggests this can be achieved through improving the strength of hip abductors to increase the mechanical resistance against adduction and strengthening the rotators and lateral flexors of the trunk to increase eccentric resistance against pelvic drop (Cruz et al., 2019).

Results observed at the ankle joint suggest the limiting factor to sprint performance on the bend is more complex than supposed by Chang and Kram (2007). A large (g = 1.07), but non-significant, increase in left step peak plantar flexor moment was observed on the bend compared with the straight, supporting results of sub-maximal effort bend sprinting (Heinrich et al., 2015). The greater plantar flexor moment at the ankle joint contradict the hypothesis that moment production at the ankle joint is constrained by moments in the non-sagittal planes (although a large [g = 0.82] increase in peak ankle eversion moment and a moderate [g = 0.60] increase in peak ankle external rotation moment were observed). In previous straight-line sprinting studies, plantar flexor moment of the ankle has been attributed to acting against the anterior rotation of the shank to prevent the collapse of the shank due to

the effect of ground reaction force (Hunter, Marshall, & McNair, 2004c; Johnson & Buckley, 2001). It is possible the increase in left step peak ankle plantar flexor moment is due to the need to further stabilise the shank as a consequence of the non-sagittal plane adaptations of the lower limb. Whilst an increase in plantar flexor moment was observed during bend sprinting, this might be insufficient to overcome the combination of greater non-sagittal plane moments and the greater need for stabilisation. Therefore, strategies aimed at improving the ability to produce plantar flexion from an internally rotated position may be beneficial in improving sprint performance.

Furthermore, an increase in peak MTP plantar flexor moment was also observed during bend sprinting compared with the straight, thus providing further support against the hypothesis of Chang and Kram (2007). MTP moment in the sagittal plane was plantar flexor for the duration of the propulsive phase of stance. These results are similar to previous research in the acceleration phase of straight-line sprinting, demonstrating no dorsiflexor moment (Bezodis et al., 2014; Smith et al., 2014; Stefanyshyn & Nigg, 1997). In Chapter 6, use of the oblique axis for push-off at the MTP joint was observed in the left step. Therefore, future research examining MTP moment about the oblique axis may be beneficial in further advancing knowledge in this area.

Orendurff et al. (2009) calculated the differential between the peak pressure value at the base and the head of the fifth metatarsal. This measure was proposed as a proxy for bending moments applied to the fifth metatarsal, where a high pressure differential was said to indicate more load at the head than the base and thus, application of a greater bending moment (Orendurff et al., 2009). It was found that acceleration elicited the highest bending moments when compared with a range of athletic movements, including straight-line running, cutting left and right and jumping

(Orendurff et al., 2009). These bending moments, attributed to high moments at the forefoot (or toebox) during push-off, have been identified as a possible risk factor for fifth-metatarsal stress fractures (Orendurff et al., 2009). Moreover, it is likely that bend sprinting also increases the torsional load experienced by the long bones of the foot. Therefore, the increase in ankle and MTP plantar flexor moments observed in the present study is possibly a risk factor for injury. To minimise the injury risk, Orendurff et al. (2009) recommended careful consideration of the rate at which training volume increases and the number of sprint accelerations performed within a session. In addition, sufficient rest between training sessions should also be prioritised (Orendurff et al., 2009). With the results of the present study in mind, it seems these recommendations may have particular importance in preparation for bend sprinting.

The ankle joint generated the most power in the sagittal plane (normalised power: 0.97 - 1.24) compared with the hip (0.52 - 0.56) and knee joints (0.09 - 0.12). These findings are in agreement with previous literature demonstrating the dominant role of the ankle joint in sprinting (Brazil et al., 2017; Debaere et al., 2015; Dorn et al., 2012; Johnson & Buckley, 2001). Thus, the results of the present study reinforce the importance of the ankle joint during sprinting. During bend sprinting, both large and moderate increases in left step peak positive power were observed at the ankle in the frontal ($g = 0.85$) and transverse ($g = 0.76$) planes. However, this did not affect positive power production in the sagittal plane, where no differences were observed. In line with the ankle joint moment results, strength and conditioning programmes aiming to ensure the ankle joint is capable of withstanding these additional loads observed in the non-sagittal plane, whilst also improving the capacity to generate sufficient power in the sagittal plane, might be beneficial for sprint performance on the bend.

Compared with the hip and ankle joints, power generation at the knee joint was relatively low. These results suggest a supporting role at the knee and agree with previous literature such as Heinrich et al. (2015), who proposed the knee may only have a sub-unit function. As suggested by Bezodis et al. (2008), it is likely the knee plays an enabling role, facilitating the transfer of power from the hip through to the ankle. In both conditions (bend and straight), a proximal to distal sequence of peak extensor power generation was observed. However, during bend sprinting with the left step, the timing of peak extensor power at the knee was later than that of the straight. This sequential transfer of power, occurring distally from the hip joint, is thought necessary to allow joints, such as the ankle, to achieve a higher power output despite having relatively smaller muscles (Jacobs et al., 1996). Kinematic adaptations, such as increased left hip adduction (Churchill et al., 2015; Churchill et al., 2018), which in the present study resulted in a large (g = 0.82) increase in peak hip power in the frontal plane, might delay the transfer of power from the hip to the knee. At maximum speed, the left limb has been found to achieve 1.6° more turning of the CoM than the right limb during ground contact (Churchill et al., 2016), which suggests more turning is achieved during left step ground contact. Therefore, this increase in peak left hip frontal plane power is likely a necessary consequence of the need to generate centripetal force and stay in the correct lane.

Large amounts of energy were absorbed in the ankle (0.070 - 0.110) and MTP joints (0.006 - 0.014) in the sagittal plane in both the bend and straight conditions. Energy absorption was greater in the left step on the bend compared with the straight at the MTP joint (g = 1.68), with a trend towards greater absorption at the ankle (g = 0.80). During bend sprinting, the left step also demonstrated greater energy absorption than the straight in the frontal plane at the midfoot (g = 1.07) and ankle

(g = 0.65), and the transverse plane at the ankle (g = 1.08). Therefore, it appears the absorption and generation of energy in the foot and ankle may be a key consideration in improving bend sprinting performance. Stefanyshyn and Nigg (1997) previously demonstrated the MTP joint to be a large absorber of energy during stance, with the energy absorbed being dissipated into the shoe and foot complex. With this in mind, Stefanyshyn and Nigg (1997) proposed that reducing energy loss at the MTP joint should result in performance improvements. Smith et al. (2014) demonstrated that, although there was no change in energy absorption at the MTP joint, energy generated at the MTP joint during push-off increased in a shod condition, compared with the barefoot condition. An increase in sprint velocity was also observed during the shod condition (Smith et al., 2014) suggesting sprint spikes are capable of enabling changes in MTP joint function, resulting in improved sprint performance. Strength training targeted at the extrinsic muscles of the foot and ankle such as tibialis anterior and posterior, in addition to the intrinsic foot muscles such as abductor hallucis and flexor digitorum brevis, might provide a further opportunity to influence sprint performance, particularly on the bend (Smith et al., 2014).

7.5. Conclusion

The results of the present study demonstrate that bend sprinting results in substantial changes to the function of the joints of the lower limb and loading of the surrounding musculoskeletal structures compared with straight-line sprinting. Whilst peak flexor moments at the hip and knee were lower during sprinting on the bend than straight, increased plantar flexor moment at the ankle and MTP suggest the limiting factor to sprint performance on the bend is more complex than previously thought. Compared with straight-line sprinting, there was also an increase in non-sagittal plane joint moments during bend sprinting, particularly at the hip and ankle joints. To

improve bend sprinting performance, athletes should consider developing the ability to produce plantar flexion from an internally rotated position specific to bend sprinting.

Chapter Eight: OVERALL DISCUSSION

8. Overall discussion

8.1. Review of previous chapters

The aim of this thesis was to further understanding of the biomechanical aspects of technique and performance in the acceleration phase of sprinting on the bend compared with the straight. To date, this thesis represents the first collection of empirical research to evaluate the kinematic and kinetic adaptations of bend sprinting, specifically in the acceleration phase (Chapters 5 - 7). In addition, the reliability and minimal detectable difference of a lower limb and trunk marker set have been presented for use in analysing bend sprinting with 3D motion capture (Chapter 4). It is hoped these methods will be adopted by other researchers to advance the field further. Therefore, the experimental studies presented within this thesis represent a significant contribution to the theoretical understanding of bend sprinting performance, whilst also providing methodological recommendations for further research and practical guidance for programmes aimed at improving performance and reducing the risk of injury.

The majority of key alterations occurred during ground contact with the left step. For example, a 2% reduction in absolute speed was observed compared with the straight for the left step during bend sprinting ($g = 0.56$, Chapter 5). Whilst the associated effect size suggests this change is moderate in magnitude, this difference is likely to be meaningful in terms of race performance. For example, the difference between first and second place in the women's 200 m final at the 2017 International Association of Athletic Federations (IAAF) World Championships was 0.03 s. Therefore, achieving even a small improvement in bend sprinting performance could have a large impact on the outcome of a competitive race.

This decrease in left step absolute speed coincided with a reduction in left step frequency (Chapter 5), supporting results from Churchill et al. (2015). The reduction in left step frequency is a consequence of the longer left step contact time observed on the bend compared with the straight since left flight time remained constant between bend and straight conditions (Chapter 5). With an increased contact time and flight time remaining constant during bend sprinting, Usherwood and Wilson (2006) proposed a consequential decrease in step frequency would ultimately reduce velocity on the bend. The results of this thesis have empirically confirmed this to be the case for the left step during the acceleration phase.

Furthermore, a lower hip flexor moment (present towards the end of the stance phase) was observed during sprinting on the bend than the straight for both the left and right steps (Chapter 7). This hip flexor moment is needed to drive the hip forward during the swing phase (Charalambous et al., 2012). In addition, Dorn et al. (2012) demonstrated with the use of musculoskeletal modelling that, at speeds above 7 m/s, increases in running speed are achieved through an increased step frequency. Increased muscle forces (primarily iliopsoas, gluteus maximus, and the hamstrings) at the hip joint enable the rapid acceleration of the hip and knee joints during the swing phase and were therefore considered responsible for increasing step frequency (Dorn et al., 2012). Therefore, training to increase hip flexor moment might also have the consequential benefit of increasing step frequency, and thus velocity on the bend.

An increase in left step touchdown distance was apparent on the bend compared with the straight (Chapter 5). A longer touchdown distance is related to a decrease in ratio of force (Bezodis et al., 2015) which was also observed during bend sprinting in Chapter 6, suggesting reducing touchdown distance may be a key consideration for improving performance on the bend. The reduction in ratio of force

can in part be attributed to an increase in mediolateral force (Chapter 6). However, the increase in mediolateral force is an essential component of bend sprinting, required to enable the athlete to follow the curve of the track and stay in lane. The analysis of ratio of force makes one of the first attempts to holistically understand force application and orientation during bend sprinting. These results provide some initial evidence that athletes are applying propulsive force 'less effectively' on the bend than the straight. However, the left limb could be considered to be applying force effectively when taking into consideration the demands required to achieve the task of sprinting around the bend, which are different to what is considered effective for straight-line sprinting. Moreover, ratio of force may require further evaluation during bend sprinting, as unlike straight-line sprinting, where the aim is to maximise the ratio of force (Morin et al., 2011), it is likely an optimum ratio exists, taking into consideration both propulsive and mediolateral forces. Furthermore, the novel application of SPM is an important step in better understanding force production without the need to reduce data to discrete form (Chapter 6). A reduction in propulsive force at 38-44% of stance coincided with greater mediolateral force for the majority of the stance phase (3-96%) during sprinting on the bend compared with the straight.

Bend sprinting also induced several kinematic adaptations at the foot when compared with straight-line sprinting. In particular, there was an increased left step peak midfoot eversion combined with increased left step peak internal ankle rotation on the bend compared with the straight. Although there was no significant main effect, a large effect size suggests a trend towards an increase in left step peak ankle eversion angle (g = 0.88). These results provide unique insight since the function of the multi-segment foot during bend sprinting has yet to be presented within the literature. Furthermore, evaluation of MTP axis use during push-off provides the first empirical

evidence to demonstrate use of the oblique axis with the left step during bend sprinting (Chapter 6). This finding identifies a significant constraint to performance on the bend and can, therefore, be considered a critical advance for the research area, providing experimental evidence to confirm the hypothesis originally proposed by Churchill et al. (2016).

In the foot and ankle complex, energy absorption was greater during the left step on the bend than the straight (Chapter 7), providing further insight into of multi-segment foot function during bend sprinting. Kelly, Cresswell, and Farris (2018) observed a foot-energy dissipation ratio greater than zero when evaluating the energetic function of the foot at different running speeds on the straight (2.2 m/s - 4.4 m/s). The authors suggested energy absorption within the foot may result in a slowing of the CoM progression and prolonged contact time to maximise the time required to generate a propulsive impulse (Kelly et al., 2018). A longer left step contact time was demonstrated on the bend compared with the straight (Chapter 5) and is supported during sub-maximal (Alt et al., 2015), and maximal velocity (Churchill et al., 2015; Churchill et al., 2016) bend sprinting. Therefore, the increased energy absorption observed at the foot and ankle (Chapter 7) might be a contributing factor to the longer contact time observed during bend sprinting (Chapter 5). These results have significant implications for practice since energy loss at the foot might be offset by force produced at larger, more proximal muscles (Kelly et al., 2018). Therefore, whilst decreasing energy absorption at the foot might be a key area for improvement, increasing energy generation at the hip might also be beneficial.

8.2. Implications for performance

There are a number of practical applications from the findings of this thesis which have specific relevance to informing practice and improving sprint

performance. Results from this thesis suggest athletes are restricted due to a complex interaction of adaptations at the joints of the ankle and foot and the need to produce force in the non-sagittal planes (Chapters 5 - 7). This is an important and necessary addition to our understanding of bend sprinting and can be used to inform strength and conditioning programmes with the aim of improving performance. Improving the strength of extrinsic and intrinsic muscles of the foot has been suggested as being beneficial to sprint performance (Smith et al., 2014). Although there is no direct evidence in sprinting to confirm this hypothesis, results from Farris, Kelly, Cresswell, and Lichtwark (2019) showed that, alongside the longitudinal arch, the plantar intrinsic muscles contributed to a stiffer forefoot during late stance of treadmill running, which may have particular importance during bend sprinting where the oblique axis is in use. Therefore, strength training, targeted at both the extrinsic and intrinsic muscles of the foot, may have a positive influence on sprint performance. Ridge et al. (2019) demonstrated an increase in muscular strength of both extrinsic and intrinsic foot muscles with an eight-week intervention where participants used minimalist footwear for walking, gradually increasing the number of steps each week up to a maximum of 7000 steps for at least five days a week. The increase in strength observed was similar to that of the control group who undertook a strength training programme (Ridge et al., 2019). The habitual wearing of minimalist shoes has also been associated with a stiffer longitudinal arch (Holowka, Wallace, & Lieberman, 2018), thus possibly having implications for the production of propulsive force at push-off. Therefore, it is possible that walking with minimalist shoes is a plausible alternative to strength training, with the additional benefit of being easy to implement.

To ensure the transfer of strength training to sports performance, the principle of training specificity is of paramount importance (Young, 2006). Therefore,

practitioners should seek to strengthen lower limb muscles in frontal and transverse planes, which may aid in improving performance. Plyometric bounding exercises have similar contact times to those found in the acceleration phase of sprinting (Young, 1992) and consequently aid the transfer of strength training to performance through comparable contraction velocity specificity (Young, 2006). Therefore, the inclusion of bounding exercises with a change of direction might be an area worth consideration by coaches and practitioners. Burnie et al. (2017) noted that coaches tend to prefer that the specificity of training is addressed by adding resistance to sporting movements rather than attempting to make gym exercises more sports specific. Therefore, training interventions such as the use of ropes or harnesses in training to provide resistance in a leaning position might be beneficial to performance (Churchill et al., 2016). In addition, frontal and transverse moment data at the hip (Chapter 7) suggest interventions aimed at improving pelvic control to prevent inwards collapse of the hip and provide a stable base for the athlete may be warranted. Finally, as previously suggested by Churchill et al. (2015) and Churchill et al. (2018), undertaking maximal speed training on the bend to further promote specificity, is essential. The current programme of research has affirmed that this should include acceleration training on the bend.

8.3. Implications for injury

It is possible that repeated stress in the frontal and transverse planes may be a precursor to injury. Thus, strengthening muscles has implications for injury prevention as well as performance improvements. Hamill et al. (1987) theorised the left limb would most likely suffer injuries such as plantar fasciitis or post-tibialis tendonitis as a consequence of bend running and repeated exposure to stress in the frontal and transverse planes. The results of the research presented throughout Chapters 5-7

support these possible injury aetiologies and advance current knowledge in this area. Repetitive loading and excessive eversion are considered a risk factor for plantar fasciitis (Beeson, 2014). The increased eversion of the left midfoot and ankle that occurs during the first 15% of stance during bend sprinting may place additional stress on tibialis anterior which provides a 'stirrup' for the arch under the foot (Palastanga et al., 2006) and may, therefore be a contributing factor in the onset of plantar fasciitis.

An increase in body lateral lean has been reported in Chapter 5 in both the left and right steps during bend sprinting compared with the straight. Tibialis posterior helps maintain the balance of the tibia on the foot, particularly when the bodyweight is moving laterally (Palastanga et al., 2006). This, along with the observed greater mediolateral force in the left and right steps on the bend than straight (Chapter 6), suggests the weight is likely moving laterally. Maharaj, Cresswell, and Lichtwark (2016) showed that, during walking, the tibialis posterior muscle actively lengthens at touchdown to resist pronation then shortens later in stance to contribute towards supination. This stretch and recoil mechanism results in the storage and return of energy at the rearfoot unit (Maharaj et al., 2016). However, during bend sprinting with the left step, a large positive power was observed in the frontal plane in the ankle and midfoot at the beginning of the propulsive phase of stance (Chapter 7). Therefore, it is possible this stretch-shortening cycle was disrupted. Moreover, it has been suggested the excessive eversion (Chapter 5) results in muscular fatigue occurring earlier in the stance phase, thus resulting in abnormal loading of the tibia (Pohl, Mullineaux, Milner, Hamill, & Davis, 2008), which leads to injuries such as medial tibial stress syndrome (Chuter & Janse de Jonge, 2012). Medial tibial stress syndrome was amongst the most frequently reported injuries in indoor bend sprinters (Beukeboom et al., 2000),

therefore strengthening of the tibialis posterior to minimise fatigue related adaptations may be a key area in reducing the risk of injury.

Both iliotibial band syndrome and patellofemoral pain were also recorded by Beukeboom et al. (2000) in a season-long evaluation of injuries indoor track athletes. Therefore, the high peak hip adduction angle observed in Chapter 5 may also be a mechanism for injury since it is associated with both these conditions (Li et al., 2015). Thus, in addition to the foot and ankle, it appears that ensuring the hip is not neglected through strength and conditioning programmes may also be beneficial for reducing injury risk.

8.4. Limitations

There are several limitations to this programme of research that are worthy of discussion. It should be noted that Chapters 3 and 4 which established the accuracy and repeatability of a reduced marker set were conducted under different experimental conditions than Chapters 5-7. For instance, data for Chapters 3 and 4 were collected at maximal speed, compared with the acceleration phase that was used in Chapters 5-7. Moreover, two additional cameras were introduced into the experimental set-up which, alongside the use of the LLT marker set, allowed the width of the capture volume to be extended from 1.5 m (Chapters 3 and 4) to 3 m (Chapters 5-7). Sprinting at maximal speed is likely to result in greater error than lower speeds due to increased soft tissue artefact and larger ranges of joint motion. Therefore, it is appropriate to assume that MDDs determined from maximal speed sprinting are applicable to sprinting at slower speeds during the acceleration phase and we can assume the data represent an upper bound on the MDD. However, it is possible some MDDs may be overestimated when applied to the acceleration phase. In addition, the greater number of cameras would lead to increased resolution within the capture volume. Thus, the risk of marker

dropout is further reduced which likely has a positive influence on the reliability of the protocol. Therefore, the additional cameras in the experimental set-up could also be indicative of inflated MDDs for Chapters 5-7. However, it is likely the influence of the additional cameras was negated by the increased capture volume.

The use of shoe-mounted markers to represent the movement of the underlying bones of the foot could be associated with some inaccuracies of joint kinematics, as observed by Sinclair, Taylor and Chockalingam (2014) during running. However, the use of sprint spikes, which tend to have a tight fit, helped minimise this risk. Furthermore, this approach ensured a more representative experimental design (see Pinder, Davids, Renshaw, & Araujo, 2011) in comparison to other options, such as bone-mounted markers. Also, whilst cutting holes in the shoes to enable skin-mounted markers would be a feasible alternative, this would compromise the integrity of the shoe and prevent athletes from wearing their own spikes. Furthermore, qualitative analysis of the dataset determined a small number of frames where the heel came in contact with the ground. Thus, distribution of ground reaction force amongst each segment of the multi-segment foot is required for the accurate analysis of joint moments. However, methods such as pressure insoles that enable the redistribution force were not available for use in the current body of work. Therefore, analysis of joint kinetics were restricted to the propulsive phase of stance where the ground reaction force could be allocated in its entirety to the toebox segment. Whilst necessary, restricting analysis to the propulsive phase is acknowledged as a limitation of this thesis which could have particular implications in understanding adaptations such as increased eversion, which is said to typically occur in the first 15% of stance (Chan & Rudins, 1994). Therefore, to enable analysis of the entire stance phase, future

work should seek to establish methods of accurately redistributing force amongst the multi-segment foot during bend sprinting.

In addition, although in line with previous bend sprinting literature evaluating in the range of six to nine participants (Alt et al., 2015; Churchill et al., 2015; Churchill et al., 2016), the sample size of the studies within this thesis is small. Although an increased sample size would be desirable in terms of statistical power, the inclusion criteria (200 m PB: 23.5 s) meant this was not possible. Expanding the inclusion criteria in order to increase the number of eligible athletes was not considered appropriate for the present body of work. The findings from Alt et al. (2015) imply that velocity specific modulations may be apparent during bend sprinting. Consequently, extending the inclusion criteria to include less-skilled sprinters may introduce variability into the sample and consequently conceal adaptations. Therefore, the evaluation of a smaller but more homogenous sample size was thought more appropriate. However, doing so did rule out the inclusion of female participants, which is noted as a further limitation of this thesis.

A smaller sample size is associated with a loss of statistical power which inflates the risk of a type II error, reducing the chance of a statistically significant result being found. To overcome this risk, effect size (Hedges' *g*) was also used to aid in the interpretation of the results, which includes a correction for smaller sample sizes (Lakens, 2013). Furthermore, as Knudson (2017) suggested, replication studies are encouraged to further advance the findings of this thesis. Despite the small sample size, it was felt a group design was the most appropriate approach for the statistical analyses and interpretation of the data. Whilst it could be argued that a group design might mask individual differences in the data, this is only problematic when the participants are expected to respond differently to the change in experimental

condition. In bend sprinting, it was expected that there are a number of key adaptations that are required to maintain a curved path. Therefore, identifying the kinematic and kinetic variables necessary to sprint on the bend was thought of greater importance to provide a starting point for coaches and athletes to start to consider where improvements can be made.

In some instances, there are non-significant but non-trivial differences between the left and right limb on the straight. For example, small effect sizes of $g = 0.26$, 0.34 and 0.41 were reported for directional step length, ankle inversion and hip internal rotation, respectively (Chapter 5). However, existing sprint literature offers some plausible explanations for these slight differences. Exell, et al. (2017) reported asymmetry in all kinetic and kinematic variables analysed during maximal velocity straight-line sprinting, possibly due to muscular strength imbalances and resulting compensatory mechanisms. It was concluded that asymmetry was athlete-specific and not necessarily detrimental to performance (Exell et al., 2017). Furthermore, asymmetrical differences in the strength of invertor and evertor muscle groups of indoor bend sprinters have been observed (Beukeboom et al., 2000). The differences observed between the left and right limbs on the straight may be a result of muscular changes due to expertise in the discipline of bend sprinting. Therefore, it is crucial that researchers evaluate the left and right limb separately for both straight-line and bend sprinting. However, asymmetry between left and right limbs may be exaggerated by the collection of different steps which represent different amounts of progress in the acceleration phase. The distance run by all athletes was further in the left step, with the difference between left and right steps limited to a single step (Appendix C). Where possible, future work should use multiple force plates to avoid this limitation and the potential overestimation of asymmetry.

Finally, the evaluation of one lane is a limitation, since Churchill et al. (2018) demonstrated differences in kinematic modifications across lanes. It is possible that adaptations demonstrated throughout this thesis during the acceleration phase would become less prominent as the radius of the lane increased. However, Chapter 4 demonstrated that the reliability of kinematic variables decreases when sessions take place across two days. Therefore, the collection of data in one session was prioritised, which constrained the number of trials available due to the risk of fatigue induced injury or changes in technique. Due to the limited number of trials available, lane one was chosen for evaluation since it has the tightest radius, and consequently, adaptations were expected to be more prominent in this lane. The limited number of trials available for data collection was also problematic with regard to the collection of force plate data. Since only a single force platform was available for data collection, this limited the analysis to a single step and a single trial. Whilst the collection of multiple steps and trials is preferable, access to and availability of equipment prevented this. It was the intention to gain a minimum of two trials for each foot and condition for analysis; however throughout data collection this proved not to be possible for all participants.

8.5. Future work

The body of work presented within this thesis has important implications for future work. It has been demonstrated that the demands of sprinting on the bend are substantially different from straight-line sprinting during the acceleration phase. Therefore, future work comparing the two may not be warranted, but rather investigations should focus upon identification of factors related to sprint performance on the bend. For example, research using correlations between the identified adaptations (such as hip adduction) and performance to determine which aspects of bend sprinting are beneficial would be insightful for coaches and athletes in better

understanding technique. In addition, future research conducted with the use of electromyography to investigate the intermuscular coordination of the muscles involved in bend sprinting might be beneficial in further enhancing the specificity of training. In addition, an intervention study aimed at evaluating the effectiveness of strength training targeting the hip, ankle and foot in the frontal and transverse planes would also be insightful.

Moreover, there are a number of methodological limitations identified within the present thesis that could be addressed by future research. More specifically, evaluating acceleration performance during bend sprinting across several lanes, which could influence strategies and team allocation in races such as the 4 x 100 m relay would be beneficial. In addition, whilst increasing the number of steps analysed would typically require a higher number of force plates, or collection of data across multiple days, these may not be available or desirable options. A possible option would be to explore the use of multiple inertial measurement units as a method of predicting ground reaction force. However, development of more accurate algorithms and validation during bend sprinting is required before this is possible. Furthermore, future research should consider evaluating phases that have not yet currently been considered within the literature, such as the mechanics of the swing phase and transition from bend to straight, to better understand sprint performance on the bend.

8.6. Conclusion

In conclusion, lower limb adaptations to bend sprinting have been shown to occur in acceleration which occurs during the early phases of the race. Whilst the adaptations, such as increased hip adduction, ankle eversion and lower propulsive force, appear to be more prominent in the left leg, this is due to the different functional requirements of the left and right legs. For instance, whilst both limbs produced greater

mediolateral force on the bend than straight, mediolateral impulse was 34% greater in the left leg on the bend compared with the right. Combined with the use of the oblique axis for push-off at the MTP joint, this suggests the left limb achieves a greater change in direction compared with the right. These findings have practical implications from a strength and conditioning perspective, which have been suggested throughout this thesis, to reduce injury and improve performance.

9. References

Alenezi, F., Herrington, L., Jones, P., & Jones, R. (2016). How reliable are lower limb biomechanical variables during running and cutting tasks. *Journal of Electromyography and Kinesiology, 30*, 137-142. doi:10.1016/j.jelekin.2016.07.001

Alt, T., Heinrich, K., Funken, J., & Potthast, W. (2015). Lower extremity kinematics of athletics curve sprinting. *Journal of Sports Sciences, 33*(6), 552-560. doi:10.1080/02640414.2014.960881

Aristotle, & Barnes, J. (1984). *The complete works of Aristotle: the revised Oxford translation*. Princeton, N.J.: Princeton University Press.

Atkinson, G., & Nevill, A. M. (1998). Statistical methods for assessing measurement error (reliability) in variables relevant to sports medicine. *Sports Medicine, 26*(4), 217-238. doi:0112-1642/98/0010-0217

Baker, R. (2006). Gait analysis methods in rehabilitation. *Journal of NeuroEngineering and Rehabilitation, 3* , 4. doi:10.1186/1743-0003-3-4

Barnes, A., Wheat, J., & Milner, C. E. (2010). Use of gait sandals for measuring rearfoot and shank motion during running. *Gait & Posture, 32*(1), 133-135. doi:10.1016/j.gaitpost.2010.01.015

Beeson, P. (2014). Plantar fasciopathy: revisiting the risk factors. *Foot and Ankle Surgery, 20*(3), 160-165. doi:10.1016/j.fas.2014.03.003

Benedetti, M. G., Catani, F., Leardini, A., Pignotti, E., & Giannini, S. (1998). Data management in gait analysis for clinical applications. *Clinical Biomechanics, 13*(3), 204-215. doi:10.1016/S0268-0033(97)00041-7

Beukeboom, C., Birmingham, T. B., Forwell, L., & Ohrling, D. (2000). Asymmetrical strength changes and injuries in athletes training on a small radius curve indoor track. *Clinical Journal of Sport Medicine, 10*(4), 245-250. doi:10.1097/00042752-200010000-00004

Bezodis, I. N., Thomson, A., Gittoes, M., & Kerwin, D. (2007). *Identification of instants of touchdown and take-off in sprint running using an automatic motion analysis system.* Paper presented at the 25th Conference of the International Society of Biomechanics in Sport. Ouro Preto, Brazil.

Bezodis, I. N., Kerwin, D. G., & Salo, A. I. (2008). Lower-limb mechanics during the support phase of maximum-velocity sprint running. *Medicine & Science in Sports & Exercise, 40*(4), 707-715. doi:10.1249/MSS.0b013e318162d162

Bezodis, N. E., Salo, A. I., & Trewartha, G. (2010). Choice of sprint start performance measure affects the performance-based ranking within a group of sprinters: which is the most appropriate measure? *Sports Biomechanics, 9*(4), 258-269. doi:10.1080/14763141.2010.538713

Bezodis, N. E., Salo, A. I., & Trewartha, G. (2012). Modelling the stance leg in two-dimensional analyses of sprinting: inclusion of the MTP joint affects joint kinetics. *Journal of Applied Biomechanics, 28*(2), 222-227. doi:10.1123/jab.28.2.222

Bezodis, N. E., Salo, A. I., & Trewartha, G. (2013). Excessive fluctuations in knee joint moments during early stance in sprinting are caused by digital filtering procedures. *Gait & Posture, 38*(4), 653-657. doi:10.1016/j.gaitpost.2013.02.015

Bezodis, N. E., Salo, A. I., & Trewartha, G. (2014). Lower limb joint kinetics during the first stance phase in athletics sprinting: three elite athlete case studies. *Journal of Sports Sciences, 32*(8), 738-746. doi: 10.1080/02640414.2013.849000

Bezodis, N. E., Trewartha, G., & Salo, A. I. (2015). Understanding the effect of touchdown distance and ankle joint kinematics on sprint acceleration performance through computer simulation. *Sports Biomechanics, 14*(2), 232-245. doi:10.1080/14763141.2015.1052748

Bini, R., Hume, P., Croft, J. L., Cowan, E., & Kilding, A. (2013). Pedal force effectiveness in cycling: A review of constraints and training effects. *Journal of Science and Cycling, 2*(1), 426-450. doi:10.28985/jsc.v2i1.32

Bishop, C., Paul, G., & Thewlis, D. (2012). Recommendations for the reporting of foot and ankle models. *Journal of Biomechanics, 45*(13), 2185-2194. doi:10.1016/j.jbiomech.2012.06.019

Bishop, C., Paul, G., & Thewlis, D. (2013). The reliability, accuracy and minimal detectable difference of a multi-segment kinematic model of the foot-shoe complex. *Gait & Posture, 37*(4), 552-557. doi:10.1016/j.gaitpost.2012.09.020

Bojsen-Moller, F. (1979). Calcaneocuboid joint and stability of the longitudinal arch of the foot at high and low gear push off. *Journal of Anatomy, 129*(1), 165-176.

Brazil, A., Exell, T., Wilson, C., Willwacher, S., Bezodis, I., & Irwin, G. (2017). Lower limb joint kinetics in the starting blocks and first stance in athletic sprinting. *Journal of Sports Sciences, 35*(16), 1629-1635. doi:10.1080/02640414.2016.1227465

Bruening, D. A., Cooney, K. M., & Buczek, F. L. (2012). Analysis of a kinetic multi-segment foot model. Part I: Model repeatability and kinematic validity. *Gait & Posture, 35*(4), 529-534. doi:10.1016/j.gaitpost.2011.10.363

Bruening, D. A., & Takahashi, K. Z. (2018). Partitioning ground reaction forces for multi-segment foot joint kinetics. *Gait & Posture, 62*, 111-116. doi:10.1016/j.gaitpost.2018.03.001

Burnie, L., Barratt, P., Davids, K., Stone, J. A., Worsfold, P., & Wheat, J. (2017). Coaches' philosophies on the transfer of strength training to elite sports performance. *International Journal of Sports Science & Coaching, 13*(5), 729-736. doi:10.1177_1747954117747131

Camomilla, V., Cereatti, A., Cutti, A. G., Fantozzi, S., Stagni, R., & Vannozzi, G. (2017). Methodological factors affecting joint moments estimation in clinical gait analysis: a systematic review. *BioMedical Engineering OnLine, 16*(1), 106. doi:10.1186/s12938-017-0396-x

Cappozzo, A., Catani, F., Della Croce, U., & Leardini, A. (1995). Position and orientation in space of bones during movement: anatomical frame definition and determination. *Clinical Biomechanics, 10*(4), 171-178. doi:10.1016/0268-0033(95)91394-T

Chan, C. W., & Rudins, A. (1994). Foot biomechanics during walking and running. *Mayo Clinic Proceedings, 69*(5), 448-461. doi:10.1016/S0025-6196(12)61642-5

Chang, Y. H., & Kram, R. (2007). Limitations to maximum running speed on flat curves. *The Journal of Experimental Biology, 210*(6), 971-982. doi: 10.1242/jeb.02728 8

Charalambous, L., Irwin, G., Bezodis, I. N., & Kerwin, D. (2012). Lower limb joint kinetics and ankle joint stiffness in the sprint start push-off. *Journal of Sports Sciences, 30*(1), 1-9. doi:10.1080/02640414.2011.616948

Choppin, S., & Wheat, J. (2013). The potential of the Microsoft Kinect in sports analysis and biomechanics. *Sports Technology, 6*(2), 78-85. doi:10.1080/19346182.2013.819008

Churchill, S. M., Salo, A. I., & Trewartha, G. (2015). The effect of the bend on technique and performance during maximal effort sprinting. *Sports Biomechanics, 14*(1), 106-121. doi:10.1080/14763141.2015.1024717

Churchill, S. M., Trewartha, G., Bezodis, I. N., & Salo, A. I. (2016). Force production during maximal effort bend sprinting: Theory vs reality. *Scandinavian Journal of Medicine & Science in Sports, 26*(10), 1171-1179. doi:10.1111/sms.12559

Churchill, S. M., Trewartha, G., & Salo, A. I. (2018). Bend sprinting performance: new insights into the effect of running lane. *Sports Biomechanics*, *18*(4), 437-447. doi:10.1080/14763141.2018.1427279

Chuter, V. H., & Janse de Jonge, X. A. K. (2012). Proximal and distal contributions to lower extremity injury: A review of the literature. *Gait & Posture, 36*(1), 7-15. doi:10.1016/j.gaitpost.2012.02.001

Cicchetti, D. (1994). Guidelines, criteria, and rules of thumb for evaluating normed and standardized assessment instruments in psychology. - PsycNET. *Psychological Assessment, 4*(6), 284-290. doi:10.1037/1040-3590.6.4.284

Clark, K. P., & Weyand, P. G. (2015). Sprint running research speeds up: A first look at the mechanics of elite acceleration. *Scandinavian Journal of Medicine & Science in Sports, 25*(5), 581-582. doi:10.1111/sms.12520

Clarke, T. E., Frederick, E. C., & Hamill, J. (1984). The study of rearfoot movement in running. In E. C. Frederick (Ed.), *Sport shoes and playing surfaces* (pp. 166-189). Champaign, IL: Human Kinetics.

Coe, R. (2002). *It's the effect size, stupid: what effect size is and why it is important.* Paper presented at the Annual Conference of the British Educational Research Association, University of Exeter, England.

Cohen, J. (1988). *Statistical power analysis for the behavioural sciences*. Hillsdale, NJ: Lawrence Erlbaum Associates.

Collins, T. D., Ghoussayni, S. N., Ewins, D. J., & Kent, J. A. (2009). A six degrees-of-freedom marker set for gait analysis: Repeatability and comparison with a modified Helen Hayes set. *Gait & Posture, 30*(2), 173-180. doi:10.1016/j.gaitpost.2009.04.004

Colyer, S. L., Nagahara, R., & Salo, A. I. (2018). Kinetic demands of sprinting shift across the acceleration phase: novel analysis of entire force waveforms. *Scandinavian Journal of Medicine & Science in Sports, 28*(7), 1874-1792. doi:10.1111/sms.13093

Cruz, A., Fonseca, S., Araújo, V., Carvalho, D., Barsante, D., Pinto, V. & Souza, T. (2019). Pelvic Drop Changes due to Proximal Muscle Strengthening Depend on Foot-Ankle Varus Alignment. *Applied Bionics and Biomechanics*, vol. 2019. doi: 10.1155/2019/2018059.

Cureton Jr, T. K. (1939). Elementary principles and techniques of cinematographic analysis as aids in athletic research. *Research Quarterly.American Association for Health, Physical Education and Recreation, 10*(2), 3-24.

Davis, R., Õunpuu, S., Tyburski, D., & Gage, J. R. (1991). A gait analysis data collection and reduction technique. *Human Movement Science, 10*(5), 575-587. doi:10.1016/0167-9457(91)90046-Z

de Leva, P. (1996). Adjustments to Zatsiorsky-Seluyanov's segment inertia parameters. *Journal of Biomechanics, 29*(9), 1223-1230. doi:10.1016/0021-9290(95)00178-6

Debaere, S., Delecluse, C. H., Aerenhouts, D., Hagman, F., & Jonkers, I. (2015). Control of propulsion and body lift during the first two stances of sprint running: a simulation study. *Journal of Sports Science, 33*(19), 2016-2024. doi:10.1080/02640414.2015.1026375

Delecluse, C. H., Coppenolle, H. v., Willems, E., Diels, R., Goris, M., Leemputte, M. v., & Vuylsteke, M. (1995). Analysis of 100 meter sprint performance as a multidimensional skill. *Journal of Human Movement Studies, 28*(2), 87-101.

Dempster, W. T., & Gaughran, G. R. L. (1967). Properties of body segments based on size and weight. *American Journal of Anatomy, 120*(1), 33-54.

Deschamps, K., Staes, F., Bruyninckx, H., Busschots, E., Jaspers, E., Atre, A., & Desloovere, K. (2012). Repeatability in the assessment of multi-segment foot kinematics. *Gait & Posture, 35*(2), 255-260. doi:10.1016/j.gaitpost.2011.09.016

Deschamps, K., Eerdekens, M., Desmet, D., Matricali, G. A., Wuite, S., & Staes, F. (2017). Estimation of foot joint kinetics in three and four segment foot models using an existing proportionality scheme: Application in paediatric barefoot

walking. *Journal of Biomechanics, 61*, 168-175. doi:10.1016/j.jbiomech.2017.07.017

Desroches, G., Cheze, L., & Dumas, R. (2010). Expression of joint moment in the joint coordinate system. *Journal of Biomechanical Engineering, 132*(11), 114503. doi:10.1115/1.4002537

Dixon, P. C., Böhm, H., & Döderlein, L. (2012). Ankle and midfoot kinetics during normal gait: A multi-segment approach. *Journal of Biomechanics, 45*(6), 1011-1016. doi:http10.1016/j.jbiomech.2012.01.001

Dorn, T. W., Schache, A. G., & Pandy, M. G. (2012). Muscular strategy shift in human running: dependence of running speed on hip and ankle muscle performance. *Journal of Experimental Biology, 215*, 1944-1956. doi:10.1242/jeb.064527

Durlak, J. A. (2009). How to select, calculate, and interpret effect sizes. *Journal of Pediatric Psychology, 34*(9), 917-928. doi:10.1093/jpepsy/jsp004

Exell, T., Irwin, G., Gittoes, M., & Kerwin, D. (2017). Strength and performance asymmetry during maximal velocity sprint running. *Scandinavian Journal of Medicine & Science in Sports, 27*(11), 1273-1282. doi:10.1111/sms.12759

Farris, D. J., Kelly, L. A., Cresswell, A. G., & Lichtwark, G. A. (2019). The functional importance of human foot muscles for bipedal locomotion. *Proceedings of the National Academy of Sciences, 116*(5), 1645-1650. doi:10.1073/pnas.1812820116

Fenn, W. O. (1931). A Cinematographic Study of Sprinters. *The Scientific Monthly, 32*(4), 346-354.

Ferber, R., McClay Davis, I., Williams, D. S., & Laughton, C. (2002). A comparison of within- and between-day reliability of discrete 3D lower extremity variables in runners. *Journal of Orthopaedic Research, 20*(6), 1139-1145. doi:10.1016/S0736-0266(02)00077-3

Ferrari, A., Benedetti, M. G., Pavan, E., Frigo, C., Bettinelli, D., Rabuffetti, M., . . . Leardini, A. (2008). Quantitative comparison of five current protocols in gait analysis. *Gait & Posture, 28*(2), 207-216. doi:10.1016/j.gaitpost.2007.11.009

Friston, K. J., Ashburner, J. T., Kiebel, S. J., Nichols, T. E., & Penny, W. D. (2007). *Statistical Parametric Mapping: The Analysis of Functional Brain Images*. Amsterdam, Netherlands: Elsevier/Academic Press.

Girard, O., Brocherie, F., Tomazin, K., Farooq, A., & Morin, J.B. (2016). Changes in running mechanics over 100-m, 200-m and 400-m treadmill sprints. *Journal of Biomechanics, 49*(9), 1490-1497. doi:10.1016/j.jbiomech.2016.03.020

Glaister, B. C., Orendurff, M. S., Schoen, J. A., & Klute, G. K. (2007). Rotating horizontal ground reaction forces to the body path of progression. *Journal of Biomechanics, 40*(15), 3527-3532. doi:10.1016/j.jbiomech.2007.05.014

Grant, J., & Chester, V. (2015). The Effects of Walking Speed on Adult Multi-segment Foot Kinematics. *Journal of Bioengineering & Biomedical Science, 5*(2), 1. doi:10.4172/2155- 9538.1000156

Greene, P. R. (1985). Running on flat turns: experiments, theory, and applications. *Journal of Biomechanical Engineering, 107*(2), 96-103.

Hamill, J., Murphy, M., & Sussman, D. (1987). The effects of track turns on lower extremity function. *International Journal of Sport Biomechanics, 3*(3), 276-286. doi: 10.1123/ijsb.3.3.276

Hanavan, E. P., Jr. (1964). A mathematical model of the human body. *American Aerospace Research Laboratories*, 1-149.

Hay, J. G. (1993). *The Biomechanics of Sports Techniques*. New Jersey, Prentice Hall: Pearson.

Heinrich, K., Alt, T., Funken, J., Brueggemann, G.P., & Potthast, W. (2015). *Contribution of the lower extremity joints to mechanical energy in athletics curve sprinting.* Paper presented at the 33rd Conference of the International Society of Biomechanics in Sports (ISBS), Pottiers, France.

Hof, A. L. (1996). Scaling gait data to body size. *Gait & Posture, 4*(3), 222-223. doi:10.1016/0966-6362(95)01057-2

Holowka, N. B., Wallace, I. J., & Lieberman, D. E. (2018). Foot strength and stiffness are related to footwear use in a comparison of minimally- vs. conventionally-shod populations. *Scientific Reports, 8*(1), 3679. doi:10.1038/s41598-018-21916-7

Hood, S., McBain, T., Portas, M., & Spears, I. (2012). Measurement in sports biomechanics. *Measurement and Control, 45*(6), 182-186. doi: 10.1177/002029401204500604

Hopkins, W. G. (2000). Measures of reliability in sports medicine and science. *Sports Medicine, 30*(1), 1-15. doi:10.2165/00007256-200030010-00001

Hreljac, A. (2004). Impact and Overuse Injuries in Runners. *Medicine & Science in Sports & Exercise, 36*(5), 845-849. doi:10.1249/01.mss.0000126803.66636.dd

Hunter, J. P., Marshall, R. N., & McNair, P. J. (2004a). Reliability of biomechanical variables of sprint running. *Medicine & Science in Sports & Exercise, 36*(5), 850-861. doi: 10.1249/01.mss.0000126467.58091.38

Hunter, J. P., Marshall, R. N., & McNair, P. J. (2004b). Interaction of step length and step rate during sprint running. *Medicine & Science in Sport & Exercise, 36*(2), 261-271. doi:10.1249/01.MSS.0000113664.15777.53

Hunter, J. P., Marshall, R. N., & McNair, P. J. (2004c). Segment-interaction analysis of the stance limb in sprint running. *Journal of Biomechanics, 37*(9), 1439-1446. doi:10.1016/j.jbiomech.2003.12.018

Hunter, J. P., Marshall, R. N., & McNair, P. J. (2005). Relationships between ground reaction force impulse and kinematics of sprint-running acceleration. *Journal of Applied Biomechanics, 21*(1), 31-43.

Ishimura, K., & Sakurai, S. (2010). *Comparison of inside contact phase and outside contact phase in curved sprinting.* Paper presented at the 28th Conference of the International Society of Biomechanics in Sports (ISBS), Marquette, Michigan, USA.

Ishimura, K., & Sakurai, S. (2016). Asymmetry in Determinants of Running Speed During Curved Sprinting. *Journal of Applied Biomechanics, 32*(4), 394-400. doi:10.1123/jab.2015-0127

Ishimura, K., Tsukada, T., & Sakurai, S. (2013). *Relationship between sprint performance and stride parameters in curved sprinting.* Paper presented at the 31st Conference of the International Society of Biomechanics in Sports (ISBS), Taipei, Taiwan.

Jacobs, R., & van Ingen Schenau, G. J. (1992). Intermuscular coordination in a sprint push-off. *Journal of Biomechanics, 25*(9), 953-965. doi: 10.1016/0021-9290(92)90031-u

Jacobs, R., Bobbert, M. F., & van Ingen Schenau, G. J. (1996). Mechanical output from individual muscles during explosive leg extensions: the role of biarticular muscles. *Journal of Biomechanics, 29*(4), 513-523. doi: 10.1016/0021-9290(95)00067-4

Johnson, M. D., & Buckley, J. G. (2001). Muscle power patterns in the mid-acceleration phase of sprinting. *Journal of Sports Science, 19*(4), 263-272. doi:10.1080/026404101750158330

Kadaba, M. P., Ramakrishnan, H. K., & Wootten, M. E. (1990). Measurement of lower extremity kinematics during level walking. *Journal of Orthopaedic Research, 8*(3), 383-392. doi:10.1002/jor.1100080310

Kelly, L. A., Cresswell, A. G., & Farris, D. J. (2018). The energetic behaviour of the human foot across a range of running speeds. *Scientific Reports, 8*(1), 10576. doi:10.1038/s41598-018-28946-1

Knudson, D. (2017). Confidence crisis of results in biomechanics research. *Sports Biomechanics, 16*(4), 425-433. doi:10.1080/14763141.2016.1246603

Koo, T. K., & Li, M. Y. (2016). A Guideline of Selecting and Reporting Intraclass Correlation Coefficients for Reliability Research. *Journal of Chiropractic Medicine, 15*(2), 155-163. doi:10.1016/j.jcm.2016.02.012

Krell, J. B., & Stefanyshyn, D. (2006). The relationship between extension of the metatarsophalangeal joint and sprint time for 100 m Olympic athletes. *Journal of Sports Sciences, 24*(2), 175-180. doi:10.1080/02640410500131621

Kristianslund, E., Krosshaug, T., Mok, K. M., McLean, S., & van den Bogert, A. J. (2014). Expressing the joint moments of drop jumps and sidestep cutting in different reference frames--does it matter? *Journal of Biomechanics, 47*(1), 193-199. doi:10.1016/j.jbiomech.2013.09.016

Krzysztof, M., & Mero, A. (2013). A kinematic analysis of three best 100 m performances ever. *Journal of Human Kinetics, 36*(1), 149-160. doi:10.2478/hukin-2013-0015

Kulmala, J. P., Korhonen, M. T., Kuitunen, S., Suominen, H., Heinonen, A., Mikkola, A., & Avela, J. (2017). Whole-body frontal plane mechanics across walking, running, and sprinting in young and older adults. *Scandinavian Journal of Medicine & Science in Sports, 27*(9), 956-963. doi:10.1111/sms.12709

Lakens, D. (2013). Calculating and reporting effect sizes to facilitate cumulative science: a practical primer for t-tests and ANOVAs. *Frontiers in Psychology,* 863-863. doi:10.3389/fpsyg.2013.00863

Lees, A., & Lake, M. (2008) Chapter Four: Force and pressure measurement. In C. Payton & R. Bartlett (Eds.), *Biomechanical evaluation of movement in sport*

and exercise science: The British Association of Sport and Exercise Guidelines. Oxon: Routledge.

Li, X., Ma, R., Zhou, H., Thompson, M., Dawson, C., Nguyen, J., & Coleman, S. (2015). Evaluation of hip internal and external rotation range of motion as an injury risk factor for hip, abdominal and groin injuries in professional baseball players. *Orthopedic reviews, 7*(4).

Luo, G., & Stefanyshyn, D. (2012a). Ankle moment generation and maximum-effort curved sprinting performance. *Journal of Biomechanics, 45*(16), 2763-2768. doi:10.1016/j.jbiomech.2012.09.010

Luo, G., & Stefanyshyn, D. (2012b). Limb force and non-sagittal plane joint moments during maximum-effort curve sprint running in humans. *The Journal of Experimental Biology, 215*(24), 4314-4321. doi: 10.1242/jeb.073833

MacWilliams, B. A., Cowley, M., & Nicholson, D. E. (2003). Foot kinematics and kinetics during adolescent gait. *Gait & Posture, 17*(3), 214-224. doi:10.1016/S0966-6362(02)00103-0

Maharaj, J. N., Cresswell, A. G., & Lichtwark, G. A. (2016). The mechanical function of the tibialis posterior muscle and its tendon during locomotion. *Journal of Biomechanics, 49*(14), 3238-3243. doi:10.1016/j.jbiomech.2016.08.006

Manal, K., McClay, I., Stanhope, S., Richards, J., & Galinat, B. (2000). Comparison of surface mounted markers and attachment methods in estimating tibial rotations during walking: an in vivo study. *Gait & Posture, 11*(1), 38-45. doi:10.1016/S0966-6362(99)00042-9

Mann, R., & Herman, J. (1985). Kinematic analysis of Olympic sprint performance: men's 200 meters. *International Journal of Sport Biomechanics, 1*(15), 151-162. doi:10.1123/ijsb.1.2.151

McDonald, K. A., Honert, E. C., Cook, O. S., & Zelik, K. E. (2019). Unholey shoes: Experimental considerations when estimating ankle joint complex power during walking and running. *Journal of Biomechanics, 92*, 61-66. doi:10.1016/j.jbiomech.2019.05.031

McGinley, J. L., Baker, R., Wolfe, R., & Morris, M. E. (2009). The reliability of three-dimensional kinematic gait measurements: a systematic review. *Gait & Posture, 29*(3), 360-369. doi:10.1016/j.gaitpost.2008.09.003

Meinel, K. (2008). Competition area. In International Association of Athletics

Federations (Ed.), IAAF track and field facilities manual 31–54. Monaco: Multiprint

Mero, A. (1988). Force-time characteristics and running velocity of male sprinters during the acceleration phase of sprinting. *Research Quarterly for Exercise and Sport, 59*(2), 94-98. doi:10.1080/02701367.1988.10605484

Milner, C. E. (2008). Chapter Three: Motion Analysis Using On-Line Systems. In C. Payton & R. Bartlett (Eds.), *Biomechanical evaluation of movement in sport and exercise science: The British Association of Sport and Exercise Guidelines*. London: Routledge.

Milner, C. E., & Brindle, R. A. (2016). Reliability and minimal detectable difference in multisegment foot kinematics during shod walking and running. *Gait & Posture, 43*, 192-197. doi:10.1016/j.gaitpost.2015.09.022

Morin, J. B., Bourdin, M., Edouard, P., Peyrot, N., Samozino, P., & Lacour, J. R. (2012). Mechanical determinants of 100-m sprint running performance. *European Journal of Applied Physiology, 112*(11), 3921-3930. doi:10.1007/s00421-012-2379-8

Morin, J. B., Edouard, P., & Samozino, P. (2011). Technical ability of force application as a determinant factor of sprint performance. *Medicine & Science in Sport & Exercise, 43*(9), 1680-1688. doi:10.1249/MSS.0b013e318216ea37

Morin, J. B., Slawinski, J., Dorel, S., de Villareal, E. S., Couturier, A., Samozino, P., . . . Rabita, G. (2015). Acceleration capability in elite sprinters and ground impulse: Push more, brake less? *Journal of Biomechanics, 48*(12), 3149-3154. doi:10.1016/j.jbiomech.2015.07.009

Mündermann, L., Corazza, S., & Andriacchi, T. P. (2006). The evolution of methods for the capture of human movement leading to markerless motion capture for biomechanical applications. *Journal of NeuroEngineering and Rehabilitation, 3*, 6. doi:10.1186/1743-0003-3-6

Muybridge, E. (1887). *Animal Locomotion* Philadelphia: Photo-Gravure Co.

Nair, S. P., Gibbs, S., Arnold, G., Abboud, R., & Wang, W. (2010). A method to calculate the centre of the ankle joint: A comparison with the Vicon® Plug-in-Gait model. *Clinical Biomechanics, 25*(6), 582-587. doi:10.1016/j.clinbiomech.2010.03.004

Neal, B.S., Barton, C.J., Birn-Jeffery, A., and Morrissey, D. (2019). Increased hip adduction during running is associated with patellofemoral pain and differs between males and females: A case-control study. *Journal of Biomechanics, 91,* 133-139. 10.1016/j.jbiomech.2019.05.014

Akbarshahi, M., Schache, A. G., Fernandez, J. W., Baker, R., Banks, S., & Pandy, M. G. (2010). Non-invasive assessment of soft-tissue artifact and its effect on knee joint kinematics during functional activity. *Journal of Biomechanics, 43*(7), 1292-1301. doi:https://doi.org/10.1016/j.jbiomech.2010.01.002

Exell, T., Irwin, G., Gittoes, M., & Kerwin, D. (2017). Strength and performance asymmetry during maximal velocity sprint running. *Scandinavian Journal of Medicine & Science in Sports, 27*(11), 1273-1282. doi:10.1111/sms.12759

Haugen, T., Danielsen, J., McGhie, D., Sandbakk, Ø., & Ettema, G. (2018). Kinematic stride cycle asymmetry is not associated with sprint performance and injury prevalence in athletic sprinters. *Scandinavian Journal of Medicine & Science in Sports, 28*(3), 1001-1008. doi:10.1111/sms.12953

Krzysztof, M., & Mero, A. (2013). A kinematics analysis of three best 100 m performances ever. *Journal of human kinetics, 36*(1), 149-160. doi:10.2478/hukin-2013-0015

Leardini, A., Chiari, L., Croce, U. D., & Cappozzo, A. (2005). Human movement analysis using stereophotogrammetry: Part 3. Soft tissue artifact assessment and compensation. *Gait & posture, 21*(2), 212-225. doi:https://doi.org/10.1016/j.gaitpost.2004.05.002

Orendurff, M. S., Rohr, E. S., Segal, A. D., Medley, J. W., Green, J. R., 3rd, & Kadel, N. J. (2009). Biomechanical analysis of stresses to the fifth metatarsal bone during sports manoeuvres: implications for fifth metatarsal fractures. *The Physician and Sports Medicine, 37*(2), 87-92. doi:10.3810/psm.2009.06.1714

Paik, A. M. H., Stebbins, J., Kothari, A., & Zavatsky, A. B. (2014). Effect of marker placement on Oxford Foot Model hindfoot segment axes. *Journal of Foot and Ankle Research, 7*(Suppl 1), A62. doi:10.1186/1757-1146-7-S1-A62

Palastanga, N., Field, D., & Soames, R. (2006). *Anatomy and human movement: Structure and function*. Philadelphia, PA: Elsevier.

Pinder, R. A., Davids, K., Renshaw, I., & Araujo, D. (2011). Representative learning design and functionality of research and practice in sport. *Journal of Sport & Exercise Psychology, 33*(1), 146-155.doi: 10.1123/jsep.33.1.146

Pohl, M. B., Mullineaux, D. R., Milner, C. E., Hamill, J., & Davis, I. S. (2008). Biomechanical predictors of retrospective tibial stress fractures in runners. *Journal of Biomechanics, 41*(6), 1160-1165. doi: 10.1016/j.jbiomech.2008.02.001

Pollock, N., Dijkstra, P., Calder, J., & Chakraverty, R. (2016). Plantaris injuries in elite UK track and field athletes over a 4-year period: a retrospective cohort study. *Knee Surgery, Sports Traumatology, Arthroscopy, 24*(7), 2287-2292. doi:10.1007/s00167-014-3409-3

Powers, C. M. (2010). The influence of abnormal hip mechanics on knee injury: a biomechanical perspective. *Journal of Orthopaedic & Sports Physical Therapy, 40*(2), 42-51. doi: 10.2519/jospt.2010.3337.

Queen, R. M., Gross, M. T., & Liu, H.-Y. (2006). Repeatability of lower extremity kinetics and kinematics for standardized and self-selected running speeds. *Gait & Posture, 23*(3), 282-287. doi:10.1016/j.gaitpost.2005.03.007

Rabita, G., Dorel, S., Slawinski, J., Saez-de-Villarreal, E., Couturier, A., Samozino, P., & Morin, J. B. (2015). Sprint mechanics in world-class athletes: a new insight into the limits of human locomotion. *Scandinavian Journal of Medicine & Science in Sports, 25*(5), 583-594. doi:10.1111/sms.12389

Radzak, K. N., Putnam, A. M., Tamura, K., Hetzler, R. K., & Stickley, C. D. (2017). Asymmetry between lower limbs during rested and fatigued state running gait in healthy individuals. *Gait & Posture, 51*, 268-274. doi:10.1016/j.gaitpost.2016.11.005

Rand, M. K., & Ohtsuki, T. (2000). EMG analysis of lower limb muscles in humans during quick change in running directions. *Gait & Posture, 12*(2), 169-183. doi:10.1016/S0966-6362(00)00073-4

Rankine, L., Long, J. T., Canseco, K., & Harris, G. F. (2008). Multisegmental foot modelling: a review. *Critical Reviews™ in Biomedical Engineering, 36*(2-3), 127-181.

Rao, G., Amarantini, D., Berton, E., & Favier, D. (2006). Influence of body segments' parameters estimation models on inverse dynamics solutions during gait. *Journal of Biomechanics, 39*(8), 1531-1536. doi:10.1016/j.jbiomech.2005.04.014

Ridge, S. T., Olsen, M. T., Bruening, D. A., Jurgensmeier, K., Griffin, D., Davis, I. S., & Johnson, A. W. (2019). Walking in Minimalist Shoes Is Effective for Strengthening Foot Muscles. *Medicine and Science in Sports and Exercise, 51*(1), 104-113. doi:10.1249/mss.0000000000001751

Robertson, G., Caldwell, G., Hamill, J., Kamen, G., & Whittlesey, S. (2013). *Research Methods in Biomechanics*. Champaign, IL: Human Kinetics.

Ryan, G. J., & Harrison, A. J. (2003). Technical adaptations of competitive sprinters induced by bend running. *New Studies in Athletics, 18*(4), 57-70.

Salo, A. I., & Grimshaw, P. (1998). An Examination of Kinematic Variability of Motion Analysis in Sprint Hurdles. *Journal of Applied Biomechanics, 14*, 211-222. doi:10.1123/jab.14.2.211

Salo, A. I., Bezodis, I. N., Batterham, A. M., & Kerwin, D. G. (2011). Elite sprinting: are athletes individually step-frequency or step-length reliant? *Medicine and Science in Sports and Exercise, 43*(6), 1055-1062. doi:10.1249/MSS.0b013e318201f6f8

Sanderson, D.J., Franks, I, M., & Elliot, D. (1993). The effects of targeting on the ground reaction forces during level walking. *Human Movement Science, 12*(3), 327-337. doi: 10.1016/0167-9457(93)90022-H

Saraswat, P., Andersen, M. S., & MacWilliams, B. A. (2010). A musculoskeletal foot model for clinical gait analysis. *Journal of Biomechanics, 43*(9), 1645-1652. doi: 10.1016/j.jbiomech.2010.03.005

Saraswat, P., MacWilliams, B. A., Davis, R. B., & D'Astous, J. L. (2014). Kinematics and kinetics of normal and planovalgus feet during walking. *Gait & Posture, 39*(1), 339-345. doi: 10.1016/j.gaitpost.2013.08.003

Schache, A. G., & Baker, R. (2007). On the expression of joint moments during gait. *Gait & Posture, 25*(3), 440-452. doi:10.1016/j.gaitpost.2006.05.018

Schweizer, G., & Furley, P. (2016). Reproducible research in sport and exercise psychology: The role of sample sizes. *Psychology of Sport and Exercise, 23*, 114-122. doi: 10.1016/j.psychsport.2015.11.005

Segal, N. A., Yack, H. J., Brubaker, M., Torner, J. C., & Wallace, R. (2009). Association of Dynamic Joint Power With Functional Limitations in Older Adults With Symptomatic Knee Osteoarthritis. *Archives of Physical Medicine and Rehabilitation, 90*(11), 1821-1828. doi: 10.1016/j.apmr.2009.07.009

Shultz, S. P., Hills, A. P., Sitler, M. R., & Hillstrom, H. J. (2010). Body size and walking cadence affect lower extremity joint power in children's gait. *Gait & Posture, 32*(2), 248-252. doi: 10.1016/j.gaitpost.2010.05.001

Sinclair, J., Taylor, P., Hebron, J., Chockalingam, N. (2014). Differences in multi-segment foot kinematics measured using skin and shoe mounted markers. *The Foot and Ankle Online Journal, 7*(2). doi: 10.3827/faoj.2014.0701.0001

Smith, G. (1989). Padding point extrapolation techniques for the Butterworth digital filter. *Journal of Biomechanics, 22*(8-9), 967-971. doi:10.1016/0021-9290(89)90082-1

Smith, G., Lake, M., & Lees, A. (2014). Metatarsophalangeal joint function during sprinting: a comparison of barefoot and sprint spike shod foot conditions. *Journal of Applied Biomechanics, 30*(2), 206-212. doi:10.1123/jab.2013-0072

Smith, G., Lake, M., Lees, A., & Worsfold, P. (2012). Measurement procedures affect the interpretation of metatarsophalangeal joint function during accelerated sprinting. *Journal of Sports Sciences, 30*(14), 1521-1527. doi:10.1080/02640414.2012.713501

Smith, N., Dyson, R., Hale, T., & Janaway, L. (2006). Contributions of the inside and outside leg to maintenance of curvilinear motion on a natural turf surface. *Gait & Posture, 24*(4), 453-458. doi:10.1016/j.gaitpost.2005.11.007

Stacoff, A., Reinschmidt, C., & Stüssi, E. (1992). The movement of the heel within a running shoe. *Medicine and Science in Sports and Exercise*, *24*(6), 695-701.

Standing, R. J., & Maulder, P. S. (2017). The biomechanics of standing start and initial acceleration: reliability of the key determining kinematics. *Journal of Sports Science and Medicine, 16*(1), 154-162.

Stebbins, J., Harrington, M., Thompson, N., Zavatsky, A., & Theologis, T. (2006). Repeatability of a model for measuring multi-segment foot kinematics in children. *Gait & Posture, 23*(4), 401-410. doi:10.1016/j.gaitpost.2005.03.002

Stefanyshyn, D., & Nigg, B. M. (1997). Mechanical energy contribution of the metatarsophalangeal joint to running and sprinting. *Journal of Biomechanics, 30*(11-12), 1081-1085. doi:10.1016/S0021-9290(97)00081-X

Stoner, L., & Ben-Sira, D. (1979). Sprinting on the curve. *Science in Athletics*, 167-173.

Usherwood, J. R., & Wilson, A. M. (2006). Accounting for elite indoor 200 m sprint results. *Biology Letters, 2*(1), 47-50. doi:10.1098/rsbl.2005.0399

van Ingen Schenau, G. J., Bobbert, M. F., & Rozendal, R. H. (1987). The unique action of bi-articular muscles in complex movements. *Journal of Anatomy, 155*, 1-5.

Vanrenterghem, J., Gormley, D., Robinson, M., & Lees, A. (2010). Solutions for representing the whole-body centre of mass in side cutting manoeuvres based on data that is typically available for lower limb kinematics. *Gait & Posture, 31*(4), 517-521. doi:10.1016/j.gaitpost.2010.02.014

Viellehner, J., Heinrich, K., Funken, J., Alt, T., & Potthast, W. (2016). *Lower extremity joint moments in athletics curve sprinting.* Paper presented at the 34th Conference of the International Society of Biomechanics in Sport. Tsukuba, Japan.

Vigotsky, A., Zelik, K., Lake, J., & Hinrichs, R. N. (2019). Mechanical Misconceptions: Have we lost the "mechanics" in "sports biomechanics"? *Journal of Biomechanics 93*, 1-5. doi: 10.1016/j.jbiomech.2019.07.005

Ward-Smith, A. J., & Radford, P. F. (2002). A mathematical analysis of the 4× 100 m relay. *Journal of Sports Sciences, 20*(5), 369-381. doi:10.1080/026404102317366627

Weber, W. E. (1836). *Mechanik der menschlichen Gehwerkzeuge: eine anatomisch-physiologische Untersuchung*: Dieterich.

Weir, J. P. (2005). Quantifying test-retest reliability using the intraclass correlation coefficient and the SEM. *Journal of Strength & Conditioning Research, 19*(1), 231-240. doi:10.1519/15184.1

Weyand, P., Sternlight, D. B., Bellizzi, M. J., & Wright, S. (2000). Faster top running speeds are achieved with greater ground forces not more rapid leg movements. *Journal of Applied Physiology, 89*(5), 1991-1999. doi:10.1152/jappl.2000.89.5.1991

Weyand, P., Sandell, R., Prime, D., & Bundle, M. (2010). The biological limits to running speed are imposed from the ground up. *Journal of Applied Physiology, 108*(4), 950-961. doi:10.1152/japplphysiol.00947.2009

Winter, D. (2009). *Biomechanics and Motor Control of Human Movement* (Fourth ed.). Hoboken, New Jersey: John Wiley & Sons.

Wu, G., Siegler, S., Allard, P., Kirtley, C., Leardini, A., Rosenbaum, D., . . . Witte, H. (2002). ISB recommendation on definitions of joint coordinate system of various joints for the reporting of human joint motion—part I: ankle, hip, and spine. *Journal of Biomechanics, 35*(4), 543-548. doi:10.1016/S0021-9290(01)00222-6

Wu, G., Van der Helm, F. C., Veeger, H. D., Makhsous, M., Van Roy, P., Anglin, C., . . . Wang, X. (2005). ISB recommendation on definitions of joint coordinate systems of various joints for the reporting of human joint motion—Part II: shoulder, elbow, wrist and hand. *Journal of Biomechanics, 38*(5), 981-992. doi:10.1016/j.jbiomech.2004.05.042

Yeadon, M. R. (1990). The simulation of aerial movement--I. The determination of orientation angles from film data. *Journal of Biomechanics, 23*(1), 59-66. doi:10.1016/0021-9290(90)90369-E

Young, W. (1992). Sprint bounding and the sprint bound index. *Strength & Conditioning Journal, 14*(4), 18-22.

Young, W. B. (2006). Transfer of strength and power training to sports performance. *International Journal of Sports Physiology and Performance, 1*(2), 74-83.

Yu, B., Gabriel, D., Noble, L., & An, K.-N. (1999). Estimate of the Optimum Cutoff Frequency for the Butterworth Low-Pass Digital Filter. *Journal of Applied Biomechanics, 15*(3), 318-329. doi:10.1123/jab.15.3.318

Yu, J., Sun, Y., Yang, C., Wang, D., Yin, K., Herzog, W., & Liu, Y. (2016). Biomechanical Insights Into Differences Between the Mid-Acceleration and Maximum Velocity Phases of Sprinting. *Journal of Strength & Conditioning Research, 30*(7), 1906-1916. doi:10.1519/jsc.0000000000001278

Zajac, F. E., Neptune, R. R., & Kautz, S. A. (2002). Biomechanics and muscle coordination of human walking. Part I: Introduction to concepts, power transfer, dynamics and simulations. *Gait & Posture, 16*(3), 215-232. doi:10.1016/S0966-6362(02)00068-1

Zatsiorsky, V. (1983). The Mass and Inertia Characteristics of the Main Segments of the Human Body. *Biomechanics*, 1152-1159.

Zatsiorsky, V., Seluyanov, V., & Chugunova, L. (1990). *Methods of Determining Mass-Inertial Characteristics of Human Body Segments* Boston: CRC Press.

Zelik, K. E., & Honert, E. C. (2018). Ankle and foot power in gait analysis: Implications for science, technology and clinical assessment. *Journal of Biomechanics, 75*, 1-12. doi:10.1016/j.jbiomech.2018.04.017

Zifchock RA, Davis I, Higginson J, Royer, T. The symmetry angle: a novel, robust method of quantifying asymmetry. Gait Posture. 2008; 27; 622–627. doi:10.1016/j.gaitpost.2007.08.006.

Żuk, M., & Pezowicz, C. (2015). Kinematic Analysis of a Six-Degrees-of-Freedom Model Based on ISB Recommendation: A Repeatability Analysis and Comparison with Conventional Gait Model. *Applied Bionics and Biomechanics*, 1-9. doi:10.1155/2015/503713

Appendix A. Comparison of key kinematic variables calculated from force plate and marker identification of touch down.

Variable	Value when touchdown identified with force plate data	Value when touchdown identified from marker data	Difference	CV
Bend Left				
Contact time	0.124 s	0.125 s	0.001 s	0.005 %
Hip adduction	7.02°	7.45°	0.43°	0.04 %
Ankle eversion	-7.84°	-6.93°	0.91°	0.09 %
Straight Left				
Contact time	0.120 s	0.115 s	0.005 s	0.03 %
Hip adduction	3.41°	3.75°	0.34°	0.07 %
Ankle eversion	4.39°	5.43°	1.04°	0.14 %

*CV = coefficient of variance

Appendix B. Additional force trials to demonstrate repeatability.

	Trial one	Trial two	Trial three	CV
Peak propulsive force (BW; bend left)				
Participant a	0.877	0.868		0.52 %
Participant b	0.736	0.761		1.67 %
Participant c	0.822	0.829		0.42 %
Peak braking impulse (Ns; bend left)				
Participant a	-11.19	-11.83		2.78 %
Participant b	-10.15	-9.87		1.40 %
Participant c	-13.13	-12.04		4.33 %
Peak propulsive force (BW; straight right)				
Participant d	0.893	0.909	0.886	1.07 %
Participant e	0.784	0.799	0.789	0.79 %
Participant f	0.694	0.715		1.49 %
Peak braking impulse (Ns; straight right)				
Participant d	-7.16	-6.22	-6.68	5.74 %
Participant e	-6.93	-6.29	-7.00	4.74 %
Participant f	-7.68	-8.47		4.89 %

*** CV = coefficient of variance**

Appendix C. Recorded step numbers for force trials.

Bend / Straight Left step	Step Number	Number of Participants
	11	2
	10	4
	9	1
Bend / Straight Right step	**Step Number**	**Number of Participants**
	10	2
	9	4
	8	1

Appendix D. Additional joint moment trials to demonstrate repeatability.

	Trial one	Trial two	Trial three	CV
Peak MTP moment (bend left)				
Participant a	-0.051	-0.042		9.26 %
Participant b	-0.034	-0.036		3.51 %
Participant c	-0.026	-0.028		5.27 %
Peak hip flexor moment (bend left)				
Participant a	0.026	0.024		4.21 %
Participant b	0.091	0.088		1.88 %
Participant c	0.095	0.083		6.87 %
Peak hip adductor moment (bend left)				
Participant a	0.090	0.075		9.16 %
Participant b	0.253	0.294		7.46 %
Participant c	0.134	0.109		10.28 %
Peak MTP moment (straight right)				
Participant d	-0.064	-0.056	-0.055	7.10 %
Participant e	-0.037	-0.035	-0.037	1.80 %
Participant f	-0.053	-0.045		8.16 %
Peak hip flexor moment (straight right)				
Participant d	0.071	0.062	0.070	6.49 %
Participant e	0.050	0.075	0.065	16.22 %
Participant f	0.121	0.146		9.45 %
Peak hip adductor moment (straight right)				
Participant d	0.103	0.096	0.100	2.98 %
Participant e	0.042	0.045	0.046	3.24 %
Participant f	0.081	0.092		6.16 %

*** CV = coefficient of variance**

Appendix E. Example consent form.

THE EFFECT OF BEND SPRINTING ON KINEMATIC AND KINETIC TECHNIQUE DURING THE ACCELERATION PHASE

Please answer the following questions by ticking the response that applies

		YES	NO
1.	I have read the Information Sheet for this study and have had details of the study explained to me.	☐	☐
2.	My questions about the study have been answered to my satisfaction and I understand that I may ask further questions at any point.	☐	☐
3.	I understand that I am free to withdraw from the study within the time limits outlined in the Information Sheet, without giving a reason for my withdrawal or to decline to answer any particular questions in the study without any consequences to my future treatment by the researcher.	☐	☐
4.	I agree to provide information to the researchers under the conditions of confidentiality set out in the Information Sheet.	☐	☐
5.	I wish to participate in the study under the conditions set out in the Information Sheet.	☐	☐
6.	I consent to the information collected for the purposes of this research study, once anonymised (so that I cannot be identified), to be used for any other research purposes.	☐	☐

Participant's Signature: _____ Date: _____

Participant's Name (Printed): _____

Contact details:

_____

_____

Researcher's Name (Printed): _____

Researcher's Signature: _____

Laura Judson
Email: l.judson@shu.ac.uk
Tel. +44(0)7875 930 025
Sheffield Hallam University
Sheffield, South Yorkshire, S10 2BP, UK

I have listened to Bruce Springsteen almost daily throughout my PhD. His music has provided me with comfort and companionship on the days that I needed it most. Therefore, it is only fitting that my thesis ends with his words, a reminder to us all to keep moving forwards:

We busted out of class had to get away from those fools
We learned more from a three minute record than we ever learned in school
Tonight I hear the neighborhood drummer sound
I can feel my heart begin to pound
You say you're tired and you just want to close your eyes and follow your dreams down

We made a promise we swore we'd always remember
No retreat, baby, no surrender
Like soldiers in the winter's night with a vow to defend
No retreat, baby, no surrender

Now young faces grow sad and old and hearts of fire grow cold
We swore blood brothers against the wind
I'm ready to grow young again
And hear your sister's voice calling us home across the open yards
Well maybe we could cut someplace of our own
With these drums and these guitars

Cause we made a promise we swore we'd always remember
No retreat, baby, no surrender
Blood brothers in the stormy night with a vow to defend
No retreat, baby, no surrender

Now on the street tonight the lights grow dim
The walls of my room are closing in
There's a war outside still raging
You say it ain't ours anymore to win
I want to sleep beneath peaceful skies in my lover's bed
With a wide open country in my eyes
And these romantic dreams in my head

Cause we made a promise we swore we'd always remember
No retreat, baby, no surrender
Blood brothers in the stormy night with a vow to defend
No retreat, baby, no surrender

No retreat, baby, no surrender